Title
Regulation of neural circuits for oxygen-dependent behaviors in Caenorhabditis elegans

Author
Chang, Andy J

Publication Date
2006

Peer reviewed|Thesis/dissertation

Regulation of Neural Circuits for Oxygen-Dependent Behaviors in C. elegans

by

Andy J. Chang

DISSERTATION

Submitted in partial satisfaction of the requirements for the degree of

DOCTOR OF PHILOSOPHY

in

Cell Biology

in the

GRADUATE DIVISION

of the

UNIVERSITY OF CALIFORNIA, SAN FRANCISCO

Acknowledgements

Graduate school has been simultaneously the most exciting and challenging time in my life. Unlike my schooling to this point, I was now discovering and synthesizing something new from the unknown. Faced with this daunting endeavor, I feel fortunate to have had the support and mentorship of people what have already tread this path. First, I would like to acknowledge my undergraduate thesis advisor, Donald Morisato, for peaking my interest in research and steering me down this path. Next, I would like to thank my qualifying exam and thesis committee (Herwig Baier, Grae Davis, and Cynthia Kenyon) for their continued encouragement and enthusiasm in my work. I enjoyed interacting with Herwig from my coursework and appreciated his calm coolness. As chair of my qualifying exam committee, he made the experience enjoyable. I want to thank for Grae for a fun rotation in *Drosophila* neurobiology and making me learn about electrophysiology, which has come in very handy. Cynthia has been a motivating force, finding interesting aspects of projects even as I was ready to abandon them.

My advisor, Cori Bargmann, has been a wonderful advisor and mentor. Her intellectual thirst and energy continues to amaze me and has helped me think more broadly about my work. Cori is always full of new ideas, drawn from her tremendous knowledge of the scientific literature and constant pursuit of new learning. Besides being a professional mentor, Cori has been a good psychological coach. The most difficult challenges I faced in graduate school were not technical, but personal, and she was instrumental in motivating and guiding me through trying times. I will always value our friendship and my growth in her lab.

What has made graduate school so much fun for me has been the great people I have had the fortune to meet and know. Cori has cultivated a fun, collaborative work environment full of bright and curious people. In particular, I would like to thank the Annex (Jesse Gray, Sarah Bauer Huang, Joe Hill, Sreekanth Chalasani, Jon Watanabe, Mo Silver, et al.) for stimulating discussions from giant squid to Civil War history to baseball. Sheltered behind a curtain of pink beads, there was never a boring moment in the Annex and always a side to take, except maybe for the 9-9:30 A.M. time slot when Joe was the only person in. Sarah was a patient benchmate who was also the voice of reason in our raucous debates. I appreciate the advice from senior graduate students Jesse, Carrie Adler, and Amanda Kahn-Kirby, as well as the comaraderie of my class/labmates Sarah, Makoto Tsunozaki, and Jason Kennerdell. I would also like to acknowledge several postdocs for all their advice and help. Manuel Zimmer has been a fun Chinese language student and imaging expert. Hang Lu is a wonderful musician who taught me the oxygen gradient experiments. Massimo Hilliard is a good friend and fitness coach; his balance of professional and personal life sets an example for me. Sreekanth is a good friend with admirable interests in public service and unwavering patriotism for his native India.

Outside of the lab, I have made wonderful friends in San Francisco. Foremost, I would to acknowledge the many housemates at 2017 Judah over the years, especially Kaiwen Kam, Ammon Corl, Mark Bates, and Muluye Liku. Another special group of people are the Bridge Players: Richard Morreale, Laura Goodwin, Eric Slivka, Rachel Tompa, and Jason Kennerdell. Thanks for all the booze and rubbers. I would also like to

thank other PIBS friends Mike Verzi and Charles Lo and non-PIBS friends Heather Finlay-Morreale and Evan Levine. I enjoyed all our outdoor excursions and gatherings.

Most importantly, I would like to acknowledge my family for all their support throughout the years. They continue to serve as a pillar of strength for me. My aunt Joyce and her family in Fremont always reminded me that family was near when I lived in San Francisco. My grandmother Yu-Yin has always encouraged me in my studies; she remains undoubtedly the smartest and most academic person in our family. My brother Jimmy has been instrumental is getting me out of the lab during the past two years. I feel that we have gotten closer because of my time in New York City. Finally, my parents David and Susan have put in much effort over many years to shape me into the person I am today. I am grateful to them for their love and encouragement. They are always there for me unconditionally, and I could not have completed graduate school without them. This thesis is dedicated to my parents.

Regulation of Neural Circuits for Oxygen-Dependent Behaviors in *Caenorhabditis elegans*

by

Andy J. Chang

Abstract

Behavior, an organism's ability to sense and respond to its environment, is paramount to its survival in nature. In multicellular animals, behavior is generated by the nervous system. Innate genetic programs form neural circuits that are sensitive to the environment and experience.

To understand the function of the nervous system at a systems level, I have chosen the soil nematode *Caenorhabditis elegans* as a model animal. In this dissertation, I describe neural circuits underlying *C. elegans* behaviors towards an important sensory cue, oxygen, using a genetic and neuroanatomical approach.

In the absence of bacterial food, wild-type adult hermaphrodites of the N2 strain prefer 7-14% oxygen in a linear 0-21% oxygen gradient, avoiding higher and lower oxygen levels. In Chapter 2, I define a chemosensory circuit for hyperoxia avoidance (>14% oxygen) and its regulation by food. In N2 animals, hyperoxia avoidance is mediated by two groups of neurons that express soluble guanylate cyclase homologs and two groups of neurons that express TRPV channels. The presence of bacterial food suppresses hyperoxia avoidance of N2 animals. This modulation is regulated by NPR-1 neuropeptide signaling, the DAF-7 (TGF-ß) transcriptional pathway, and serotonin in

distinct groups of neurons. The distributed nature of this chemosensory circuit resembles dynamic modulated networks from more complex nervous systems.

In Chapter 3, I describe effects of a transcriptional oxygen-sensing pathway on hyperoxia avoidance behavior of *C. elegans*. The hypoxia-inducible factor-1 (HIF-1) pathway is a conserved transcriptional pathway for oxygen homeostasis in metazoa. Upregulation of HIF-1 signaling alters the chemosensory circuit for hyperoxia avoidance in *C. elegans* and suppresses food regulation.

In Chapter 4, I show that hypoxia avoidance (avoidance of <4% oxgyen) requires signaling through the TAX-4/TAX-2 cyclic nucleotide-gated channel in sensory neurons and normal regulation of the HIF-1 pathway, and appears genetically distinct from hyperoxia avoidance. These preliminary results suggest that *C. elegans* behaviors can be used to identify additional acute sensors of oxygen.

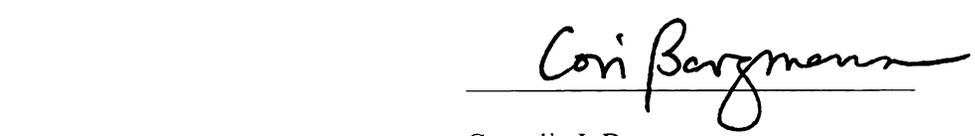

Cornelia I. Bargmann

Chair, Thesis Commitee

Table of Contents

List of Tables

List of Figures

Chapter 1:

Introduction

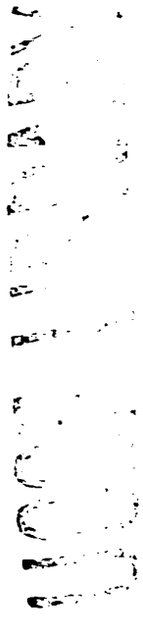

Living organisms must be able to receive sensory cues and generate appropriate responses to find food and mates and avoid harmful stimuli and predators. From bacteria to mammals, behavior, defined as a rapid physical response to external and internal stimuli, is critical for organisms to thrive in their natural environment. Behavior allows organisms to respond effectively to changes in their physical and chemical environment and to interact with conspecific and heterospecific organisms.

Behavior is studied at many levels. In single-celled bacteria, the focus has been on molecular and theoretical aspects of sensory transduction in chemotaxis as well as the role of chemical communication in group behavior (Bassler and Losick, 2006; Berg, 1988). In multicellular organisms, the nervous system generates behavior, and studies of behavior span many overlapping fields of study. At the finest level, molecular and cellular neuroscience is interested in molecular components that regulate cellular activity in the nervous system; these studies often use a combination of techniques, including genetics, molecular biology, biochemistry, and cell biology. Systems neuroscience studies the function of neural circuits, often in intact, behaving animals by directly measuring neural activity. Behavioral and cognitive neuroscience focuses on high-level processes, such as language, memory, and consciousness. At a whole-animal level, ethology is interested in evolutionary aspects of innate animal behaviors, and psychology has traditionally been concerned with human behavior.

In my graduate studies, I have been interested in systems-level analysis of behavior. My goal is to understand how external cues are processed by the nervous system to generate behavioral outputs. In vertebrate models, systems neuroscience relies heavily on electrophysiology or imaging techniques, such as calcium imaging or fMRI, to

collect data on neural activity, and correlate these results with behavior; nervous system function is sometimes perturbed by lesion or pharmacology. These experiments usually take place in the laboratory with well-controlled stimulus presentation, which is especially useful for studies of sensory processing. Although individual brain areas have been successfully studied using these approaches, the sheer number of cells and complexity of vertebrate nervous systems makes complete circuit analysis difficult at technical and conceptual levels.

The simpler nervous systems of invertebrate animals make them more tractable for circuit analysis. One complete neural circuit described in invertebrates is the lobster *Homarus americanus* somatogastric system. The relatively small number of easily distinguishable neurons allowed this circuit for a rhythmic motor pattern to be characterized electrophysiologically and pharmacologically, contributing to our understanding of central pattern generators (Marder et al., 2005). Central pattern generators are studied in similar ways in the crab *Cancer borealis*, the sea slug *Aplysia*, the mollusk *Tritonia diomedea*, and the leech *Hirudo medicinalis* (Marder et al., 2005). In insects like the fruit fly *Drosophila melanogaster* and honeybee *Apis mellifera*, calcium imaging experiments have shed light on how learning changes neural activity in the olfactory circuit (Menzel, 2001; Yu et al., 2006)

One great advantage of fast-growing invertebrates is their genetic versatility. The fruit fly *Drosophila melanogaster* and the nematode *Caenorhabditis elegans* are two genetic model organisms that have been used to study behavior (Bargmann, 1993; Benzer, 1973; Brenner, 1974). In both invertebrates, their short generation times and well-developed genetic tools facilitate a forward genetic approach to find genes involved

in behavior. This unbiased approach has allowed *Drosophila* and *C. elegans* researchers to identify many molecular components of sensory signal transduction as well as modulatory players in behavior (Bargmann, 2006; de Bono and Maricq, 2005; Zuker, 1996). Mutagenesis screens can also be used to isolate mutants in genes of interest by a reverse genetics approach.

Forward genetics has more recently been applied to behavioral studies in vertebrate model organisms, such as zebrafish and mouse (Muto et al., 2005; Neuhauss, 2003; Takahashi et al., 1994), but these models remain more challenging experimentally due to their long generation time. In mouse, the preferred strategy is targeted genetic manipulation of animals, with efforts placed on precise anatomical and temporal control of gene expression. This important approach is increasingly used in the invertebrate model animals as well.

Genetic analysis of behavior is not restricted to classical forward or reverse genetics. Genome-wide gene expression studies are being applied to model behavioral systems without classical genetics, such as honeybee and rat (Cavallaro et al., 2002; Whitfield et al., 2003). In addition, quantitative trait locus (QTL) analysis of recombinant inbred lines can be used to find genes that contribute to natural variation in *Drosophila*, zebrafish, and rat behavior (Flint, 2003; Jordan et al., 2006; Wright et al., 2006).

Identifying genes involved in a behavior is only the first step in a genetic approach to circuit analysis. Because many genes are expressed in multiple cells, determining where a gene acts to affect the behavior of interest is critical. This is where *C. elegans* is a particularly attractive system. The *C. elegans* adult hermaphrodite has a

simple nervous system composed of exactly 302 neurons with reproducible neuroanatomy from animal to animal (White et al., 1986). Because of its small numbers of neurons, transgenic expression experiments can readily identify in which cells a gene's activity is sufficient to rescue a mutant behavior. As a complement to this approach, cell ablation by laser microsurgery or genetics can determine if those cells are necessary for a behavior in wild-type and mutant backgrounds. Finally, these data can be mapped onto the wiring diagram of *C. elegans* neural connections, derived from EM reconstructions, to model the circuit for a behavior and generate hypotheses about its function and regulation (White et al., 1986). These hypotheses can then be tested with functional assays by targeted manipulations. In other genetic systems like *Drosophila*, zebrafish, and mouse, molecular and cellular components of behavior can be identified by genetics; however, complete circuit analysis is currently limited by incomplete knowledge of the neuroanatomy from sensory input to motor output in these complex nervous systems.

To date, a genetic approach to circuit analysis has been applied to many *C. elegans* behaviors (de Bono and Maricq, 2005). Simple behaviors, such as acute avoidance of noxious stimuli and touch or rhythmic cycles in defecation and egg-laying, have been studied in great molecular and cellular detail due to the simplicity of these circuits (Bargmann et al., 1990; Chalfie et al., 1985; Culotti and Russell, 1978; Hilliard et al., 2002; Hilliard et al., 2004; Liu and Thomas, 1994; Thomas, 1990; Trent et al., 1983; Weinshenker et al., 1995). More complicated locomotory behaviors, such as area-restricted search, chemotaxis, and thermotaxis, are now being studied beyond the sensory level, focusing on quantitative analyses of behavior and functional imaging techniques in downstream interneurons (Gray et al., 2005; Hills et al., 2004; Kodama et al., 2006;

Pierce-Shimomura et al., 1999; Zariwala et al., 2003). *C. elegans* researchers are also beginning to dissect circuits for complex feeding and learning behaviors that involve interactions of individuals with bacterial food and other animals (Chao et al., 2004; de Bono and Bargmann, 1998; Gray et al., 2004; Rogers et al., 2006; Sawin et al., 2000; Zhang et al., 2005).

In this dissertation, I will describe *C. elegans* behaviors in response to an important sensory cue, oxygen, from a molecular to systems level. Oxygen is an important molecule for the life of most organisms, and most animals can respond to changes in oxygen levels physiologically and behaviorally. From bacterial to mammals, a number of oxygen sensors have been identified. Sensors that bind oxygen through a heme domain have been found in bacteria and *Drosophila*; these molecules couple oxygen binding to enzymatic activity (Delgado-Nixon et al., 2000; Gilles-Gonzalez et al., 1991; Langlais et al., 2004; Morton, 2004; Morton et al., 2005). A transcriptional pathway for oxygen homeostasis found in metazoa is the hypoxia-inducible factor-1 (HIF-1) pathway. HIF-1 activity is negatively regulated by an oxygen-dependent enzyme under normoxia and induced only in hypoxic conditions (Kaelin, 2005). Chapter 3 will delve more into known oxygen sensors and explore the role of the HIF-1 pathway in *C. elegans* behavior.

In *C. elegans*, wild-type N2 animals accumulate at 7-14% oxygen in a linear oxygen gradient. The soluble guanylate cyclase GCY-35 binds oxygen and regulates this aerotaxis behavior (Gray et al., 2004). A second soluble guanylate cyclase, *gcy-36*, is also implicated in aerotaxis (Cheung et al., 2005). GCY-35 and GCY-36 are proposed to

regulate the activity of the cyclic nucleotide-gated channel TAX-4/TAX-2 in URX, AQR, and PQR chemosensory neurons to promote hyperoxia avoidance (Gray et al., 2004).

The hyperoxia avoidance behavior of wild-type N2 animals is suppressed in the presence of bacterial food (Gray et al., 2004). Hyperoxia avoidance on food is regulated by a natural polymorphism in a neuropeptide receptor gene, *npr-1*, which was first described in the context of social feeding behavior, in which animals feed in groups on bacterial lawns (Cheung et al., 2004; de Bono and Bargmann, 1998). Animals carrying the N2 *npr-1* 215V allele, which has high activity, are solitary feeders while animals carrying the *npr-1* 215F allele, which has low activity, or a *npr-1(lf)* allele are social feeders (Coates and de Bono, 2002; de Bono and Bargmann, 1998; Rogers et al., 2003). Unlike N2 solitary feeders, *npr-1(215F)* and *npr-1(lf)* social feeders exhibit strong hyperoxia avoidance in the presence of food (Gray et al., 2004). Mutations in *gcy-35* and *gcy-36* have hyperoxia avoidance defects and suppress social feeding behavior of *npr-1(lf)* mutants; social feeding can be restored to these double mutants by expression of *gcy-35* or *gcy-36* in URX, AQR, and PQR neurons (Cheung et al., 2004; Cheung et al., 2005; Gray et al., 2004). Besides *gcy-35* and *gcy-36*, other suppressors of *npr-1* social feeding have been identified (de Bono et al., 2002). Starting with this knowledge, I took a candidate approach to find other regulators of hyperoxia avoidance both in the absence and presence of food in Chapter 2.

Two interesting sets of neurons that mediate *npr-1* social feeding are ASH and ADL (de Bono et al., 2002). Ablation of these neurons in *npr-1* mutants abolishes social feeding (de Bono et al., 2002). Activity of the TRPV channels *osm-9* and *ocr-2* and the receptor chaperone *odr-4* in ASH and ADL regulate *npr-1* social feeding and aerotaxis

(de Bono et al., 2002; Rogers et al., 2006). The ASH neurons are polymodal nociceptors that sense a variety of noxious stimuli, such as high osmolarity, heavy metal ions, low pH, quinine, detergents, and nose touch (Bargmann et al., 1990; Culotti and Russell, 1978; Hilliard et al., 2004; Kaplan and Horvitz, 1993; Sambongi et al., 1999; Sambongi et al., 2000). These stimuli elicit a rapid reversal behavior, followed by a change in direction in forward locomotion. Similarly, ADL neurons mediate repulsion from 1-octanol (Chao et al., 2004; Troemel et al., 1997). These acute reversals may allow *npr-1* mutants to maintain tight aggregates on food (Rogers et al., 2006). The role of TRPV channels in aerotaxis will be examined in more detail in this dissertation.

The role of neuromodulators in regulation of *C. elegans* behavior by food has been studied. Similar to their effects in other organisms, the biogenic amines serotonin and octopamine have antagonistic effects on behaviors in *C. elegans*. Locomotion, egg-laying, and pharyngeal pumping are all behaviors regulated by food. Serotonin suppresses locomotion and enhances egg-laying and pharyngeal pumping, mimicking the effect of ample food. Conversely, octopamine stimulates locomotion and suppresses egg-laying and pharyngeal pumping (Avery and Horvitz, 1990; Horvitz et al., 1982; Segalat et al., 1995). Feeding state also modulates locomotory rates via distinct pathways. Well-fed animals move more slowly on bacterial food than off food. This basal slowing response is regulated by a dopamine circuit that senses mechanical stimulation from bacterial lawns. When animals are starved, a serotonin mediated pathway causes animals to slow down even more dramatically in an enhanced slowing response (Sawin et al., 2000).

Serotonin and feeding state also modulate the chemosensory circuit for acute repulsion from 1-octanol. Low serotonin levels and the starved state decrease sensitivity to 1-octanol while high serotonin levels and the well-fed state increase sensitivity. Food and serotonin alter the complement of sensory neurons that participate in 1-octanol repulsion, acting through G protein signaling in at least one pair of neurons (Chao et al., 2004). In Chapter 2 and 3, I will investigate the role of serotonin in modulation of aerotaxis.

Wild-type N2 animals prefer 7-14% oxygen, avoiding higher and lower oxygen levels. In this dissertation, I will study these two distinct behaviors independently. In Chapter 2, I will describe a chemosensory circuit for hyperoxia avoidance and its regulation by food in N2 and *npr-1(lf)* backgrounds. In Chapter 3, I will examine how changes in the canonical HIF-1 oxygen-sensing pathway affect this circuit. In Chapter 4, I will show analysis of hypoxia avoidance. My results demonstrate that *C. elegans* assembles a flexible, distributed circuit for hyperoxia avoidance akin to dynamic circuits from more complex nervous systems. This circuit can be dramatically altered by upregulation of the HIF-1 pathway. Furthermore, I present preliminary results that suggest *C. elegans* behaviors can be used to identify more acute sensors for oxygen.

References

Avery, L., and Horvitz, H. R. (1990). Effects of starvation and neuroactive drugs on feeding in Caenorhabditis elegans. J Exp Zool *253*, 263-270.

Bargmann, C. I. (1993). Genetic and cellular analysis of behavior in C. elegans. Annu Rev Neurosci *16*, 47-71.

Bargmann, C. I. (2006). Comparative chemosensation from receptors to ecology. Nature *444*, 295-301.

Bargmann, C. I., Thomas, J. H., and Horvitz, H. R. (1990). Chemosensory cell function in the behavior and development of Caenorhabditis elegans. Cold Spring Harb Symp Quant Biol *55*, 529-538.

Bassler, B. L., and Losick, R. (2006). Bacterially speaking. Cell *125*, 237-246.

Benzer, S. (1973). Genetic dissection of behavior. Sci Am *229*, 24-37.

Berg, H. C. (1988). A physicist looks at bacterial chemotaxis. Cold Spring Harb Symp Quant Biol *53 Pt 1*, 1-9.

Brenner, S. (1974). The genetics of Caenorhabditis elegans. Genetics *77*, 71-94.

Cavallaro, S., D'Agata, V., Manickam, P., Dufour, F., and Alkon, D. L. (2002). Memory-specific temporal profiles of gene expression in the hippocampus. Proc Natl Acad Sci U S A *99*, 16279-16284.

Chalfie, M., Sulston, J. E., White, J. G., Southgate, E., Thomson, J. N., and Brenner, S. (1985). The neural circuit for touch sensitivity in Caenorhabditis elegans. J Neurosci *5*, 956-964.

Chao, M. Y., Komatsu, H., Fukuto, H. S., Dionne, H. M., and Hart, A. C. (2004). Feeding status and serotonin rapidly and reversibly modulate a Caenorhabditis elegans chemosensory circuit. Proc Natl Acad Sci U S A *101*, 15512-15517.

Cheung, B. H., Arellano-Carbajal, F., Rybicki, I., and de Bono, M. (2004). Soluble guanylate cyclases act in neurons exposed to the body fluid to promote C. elegans aggregation behavior. Curr Biol *14*, 1105-1111.

Cheung, B. H., Cohen, M., Rogers, C., Albayram, O., and de Bono, M. (2005). Experience-dependent modulation of C. elegans behavior by ambient oxygen. Curr Biol *15*, 905-917.

Coates, J. C., and de Bono, M. (2002). Antagonistic pathways in neurons exposed to body fluid regulate social feeding in Caenorhabditis elegans. Nature *419*, 925-929.

Culotti, J. G., and Russell, R. L. (1978). Osmotic avoidance defective mutants of the nematode Caenorhabditis elegans. Genetics *90*, 243-256.

de Bono, M., and Bargmann, C. I. (1998). Natural variation in a neuropeptide Y receptor homolog modifies social behavior and food response in C. elegans. Cell *94*, 679-689.

de Bono, M., and Maricq, A. V. (2005). Neuronal substrates of complex behaviors in C. elegans. Annu Rev Neurosci *28*, 451-501.

de Bono, M., Tobin, D. M., Davis, M. W., Avery, L., and Bargmann, C. I. (2002). Social feeding in Caenorhabditis elegans is induced by neurons that detect aversive stimuli. Nature *419*, 899-903.

Delgado-Nixon, V. M., Gonzalez, G., and Gilles-Gonzalez, M. A. (2000). Dos, a heme-binding PAS protein from Escherichia coli, is a direct oxygen sensor. Biochemistry *39*, 2685-2691.

Flint, J. (2003). Analysis of quantitative trait loci that influence animal behavior. J Neurobiol *54*, 46-77.

Gilles-Gonzalez, M. A., Ditta, G. S., and Helinski, D. R. (1991). A haemoprotein with kinase activity encoded by the oxygen sensor of Rhizobium meliloti. Nature *350*, 170-172.

Gray, J. M., Hill, J. J., and Bargmann, C. I. (2005). A circuit for navigation in Caenorhabditis elegans. Proc Natl Acad Sci USA *102*, 3184-3191.

Gray, J. M., Karow, D. S., Lu, H., Chang, A. J., Chang, J. S., Ellis, R. E., Marletta, M. A., and Bargmann, C. I. (2004). Oxygen sensation and social feeding mediated by a C. elegans guanylate cyclase homologue. Nature *430*, 317-322.

Hilliard, M. A., Bargmann, C. I., and Bazzicalupo, P. (2002). C. elegans Responds to Chemical Repellents by Integrating Sensory Inputs from the Head and the Tail. Curr Biol *12*, 730-734.

Hilliard, M. A., Bergamasco, C., Arbucci, S., Plasterk, R. H., and Bazzicalupo, P. (2004). Worms taste bitter: ASH neurons, QUI-1, GPA-3 and ODR-3 mediate quinine avoidance in Caenorhabditis elegans. Embo J *23*, 1101-1111.

Hills, T., Brockie, P. J., and Maricq, A. V. (2004). Dopamine and glutamate control area-restricted search behavior in Caenorhabditis elegans. J Neurosci *24*, 1217-1225.

Horvitz, H. R., Chalfie, M., Trent, C., Sulston, J. E., and Evans, P. D. (1982). Serotonin and octopamine in the nematode Caenorhabditis elegans. Science *216*, 1012-1014.

Jordan, K. W., Morgan, T. J., and Mackay, T. F. (2006). Quantitative trait loci for locomotor behavior in Drosophila melanogaster. Genetics *174*, 271-284.

Kaelin, W. G., Jr. (2005). Proline hydroxylation and gene expression. Annu Rev Biochem *74*, 115-128.

Kaplan, J. M., and Horvitz, H. R. (1993). A dual mechanosensory and chemosensory neuron in Caenorhabditis elegans. Proc Natl Acad Sci U S A *90*, 2227-2231.

Kodama, E., Kuhara, A., Mohri-Shiomi, A., Kimura, K. D., Okumura, M., Tomioka, M., Iino, Y., and Mori, I. (2006). Insulin-like signaling and the neural circuit for integrative behavior in C. elegans. Genes Dev *20*, 2955-2960.

Langlais, K. K., Stewart, J. A., and Morton, D. B. (2004). Preliminary characterization of two atypical soluble guanylyl cyclases in the central and peripheral nervous system of Drosophila melanogaster. J Exp Biol *207*, 2323-2338.

Liu, D. W., and Thomas, J. H. (1994). Regulation of a periodic motor program in C. elegans. J Neurosci *14*, 1953-1962.

Marder, E., Bucher, D., Schulz, D. J., and Taylor, A. L. (2005). Invertebrate central pattern generation moves along. Curr Biol *15*, R685-699.

Menzel, R. (2001). Searching for the memory trace in a mini-brain, the honeybee. Learn Mem *8*, 53-62.

Morton, D. B. (2004). Atypical soluble guanylyl cyclases in Drosophila can function as molecular oxygen sensors. J Biol Chem *279*, 50651-50653.

Morton, D. B., Langlais, K. K., Stewart, J. A., and Vermehren, A. (2005). Comparison of the properties of the five soluble guanylyl cyclase subunits in Drosophila melanogaster. J Insect Sci *5*, 12.

Muto, A., Orger, M. B., Wehman, A. M., Smear, M. C., Kay, J. N., Page-McCaw, P. S., Gahtan, E., Xiao, T., Nevin, L. M., Gosse, N. J., *et al.* (2005). Forward genetic analysis of visual behavior in zebrafish. PLoS Genet *1*, e66.

Neuhauss, S. C. (2003). Behavioral genetic approaches to visual system development and function in zebrafish. J Neurobiol *54*, 148-160.

Pierce-Shimomura, J. T., Morse, T. M., and Lockery, S. R. (1999). The fundamental role of pirouettes in Caenorhabditis elegans chemotaxis. J Neurosci *19*, 9557-9569.

Rogers, C., Persson, A., Cheung, B., and de Bono, M. (2006). Behavioral motifs and neural pathways coordinating O2 responses and aggregation in C. elegans. Curr Biol *16*, 649-659.

Rogers, C., Reale, V., Kim, K., Chatwin, H., Li, C., Evans, P., and de Bono, M. (2003). Inhibition of *Caenorhabditis elegans* social feeding by FMRFamide-related peptide activation of NPR-1. Nat Neurosci *6*, 1178-1185.

Sambongi, Y., Nagae, T., Liu, Y., Yoshimizu, T., Takeda, K., Wada, Y., and Futai, M. (1999). Sensing of cadmium and copper ions by externally exposed ADL, ASE, and ASH neurons elicits avoidance response in Caenorhabditis elegans. Neuroreport *10*, 753-757.

Sambongi, Y., Takeda, K., Wakabayashi, T., Ueda, I., Wada, Y., and Futai, M. (2000). Caenorhabditis elegans senses protons through amphid chemosensory neurons: proton signals elicit avoidance behavior. Neuroreport *11*, 2229-2232.

Sawin, E. R., Ranganathan, R., and Horvitz, H. R. (2000). C. elegans locomotory rate is modulated by the environment through a dopaminergic pathway and by experience through a serotonergic pathway. Neuron *26*, 619-631.

Segalat, L., Elkes, D. A., and Kaplan, J. M. (1995). Modulation of serotonin-controlled behaviors by Go in Caenorhabditis elegans. Science *267*, 1648-1651.

Takahashi, J. S., Pinto, L. H., and Vitaterna, M. H. (1994). Forward and reverse genetic approaches to behavior in the mouse. Science *264*, 1724-1733.

Thomas, J. H. (1990). Genetic analysis of defecation in Caenorhabditis elegans. Genetics *124*, 855-872.

Trent, C., Tsuing, N., and Horvitz, H. R. (1983). Egg-laying defective mutants of the nematode Caenorhabditis elegans. Genetics *104*, 619-647.

Troemel, E. R., Kimmel, B. E., and Bargmann, C. I. (1997). Reprogramming chemotaxis responses: sensory neurons define olfactory preferences in C. elegans. Cell *91*, 161-169.

Weinshenker, D., Garriga, G., and Thomas, J. H. (1995). Genetic and pharmacological analysis of neurotransmitters controlling egg laying in C. elegans. J Neurosci *15*, 6975-6985.

White, J. G., Southgate, E., Thomson, J. N., and Brenner, S. (1986). The structure of the nervous system of the nematode *Caenorhabditis elegans*. Phil Transact R Soc Lond B *314*, 1-340.

Whitfield, C. W., Cziko, A. M., and Robinson, G. E. (2003). Gene expression profiles in the brain predict behavior in individual honey bees. Science *302*, 296-299.

Wright, D., Nakamichi, R., Krause, J., and Butlin, R. K. (2006). QTL analysis of behavioral and morphological differentiation between wild and laboratory zebrafish (Danio rerio). Behav Genet *36*, 271-284.

Yu, D., Akalal, D. B., and Davis, R. L. (2006). Drosophila alpha/beta Mushroom Body Neurons Form a Branch-Specific, Long-Term Cellular Memory Trace after Spaced Olfactory Conditioning. Neuron *52*, 845-855.

Zariwala, H. A., Miller, A. C., Faumont, S., and Lockery, S. R. (2003). Step response analysis of thermotaxis in Caenorhabditis elegans. J Neurosci *23*, 4369-4377.

Zhang, Y., Lu, H., and Bargmann, C. I. (2005). Pathogenic bacteria induce aversive olfactory learning in Caenorhabditis elegans. Nature *438*, 179-184.

Zuker, C. S. (1996). The biology of vision of Drosophila. Proc Natl Acad Sci U S A *93*, 571-576.

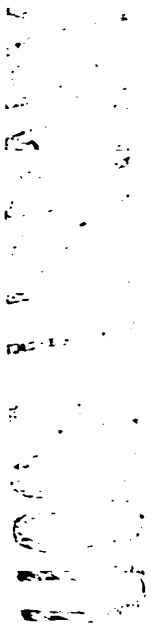

Chapter 2:

A Distributed Chemosensory Circuit for Oxygen Preference in *C. elegans*

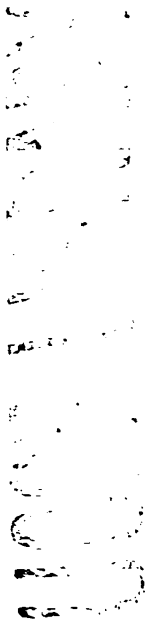

Statement of contributions:

A version of this chapter was published as Chang A.J., Chronis N., Karow D.S., Marletta M.A., and Bargmann C.I. (2006). PLoS Biology *4*: e274.

I performed all the experiments presented in this chapter. Nikolas Chronis performed G-CaMP calcium imaging experiments for oxygen-dependent response of ASH neurons (data not shown). David S. Karow and Michael A. Marletta contributed the *qaIs2241* strain used to kill URX, AQR, and PQR neurons. Cornelia I. Bargmann and I conducted the statistical analyses.

A Distributed Chemosensory Circuit for Oxygen Preference in *C. elegans*

by

Andy J. Chang[1], Nikolas Chronis[1], David S. Karow[2, 3, 4], Michael A. Marletta[2, 3, 4], Cornelia I. Bargmann[1,*]

[1]Howard Hughes Medical Institute and Laboratory of Neural Circuits and Behavior, The Rockefeller University, New York, New York, United States of America

[2]Graduate Program in Cellular and Molecular Biology, University of Michigan, Ann Arbor, Michigan, United States of America

[3]Departments of Chemistry and Molecular and Cell Biology, University of California, Berkeley, Berkeley, California, United States of America

[4]Division of Physical Biosciences, Lawrence Berkeley National Lab, Berkeley, California, United States of America

[*]To whom correspondence should be addressed. E-mail: cori@rockefeller.edu

Running title: A distributed oxygen-sensing circuit

Abbreviations: ANOVA, analysis of variance; cGMP, cyclic guanosine monophosphate; NGM, nematode growth medium; PCA, principal component analysis; sGCs, soluble guanylate cyclase homologs; TRPV, transient receptor potential channel, vanilloid

Summary

The nematode *Caenorhabditis elegans* has complex, naturally variable behavioral responses to environmental oxygen, food, and other animals. *C. elegans* detects oxygen through soluble guanylate cyclases (sGCs) and responds to it differently depending on the activity of the neuropeptide receptor NPR-1: *npr-1(lf)* and naturally-isolated *npr-1(215F)* animals avoid high oxygen and aggregate in the presence of food; *npr-1(215V)* animals do not. We show here that hyperoxia avoidance integrates food with *npr-1* activity through neuromodulation of a distributed oxygen-sensing network. Hyperoxia avoidance is stimulated by sGC-expressing oxygen-sensing neurons, nociceptive neurons, and ADF sensory neurons. In *npr-1(215V)* animals, the switch from weak aerotaxis on food to strong aerotaxis in its absence requires close regulation of the neurotransmitter serotonin in the ADF neurons; high levels of ADF serotonin promote hyperoxia avoidance. In *npr-1(lf)* animals, food regulation is masked by increased activity of the oxygen-sensing neurons. Hyperoxia avoidance is also regulated by the neuronal TGF-ß homolog DAF-7, a secreted mediator of crowding and stress responses. DAF-7 inhibits serotonin synthesis in ADF, suggesting that ADF serotonin is a convergence point for regulation of hyperoxia avoidance. Coalitions of neurons that promote and repress hyperoxia avoidance generate a subtle and flexible response to environmental oxygen.

Introduction

Sensory systems are shaped by evolution to detect the salient features of an animal's natural environment. At the simplest level, a sensory system is tuned to the most informative cues: specific ultrasonic wavelengths in the bat's echolocation system, or statistically likely features of natural scenes in the vertebrate visual system (Kossl and Vater, 1985; Sigman et al., 2001). At more complex levels of processing, the nervous system sets behavioral priorities based on context. Even the simplest animals generate distinct behaviors to the same sensory cue depending on the other cues that are present at the same time. Food, hunger, danger, and sleep elicit modulatory contexts that change the behavioral output to the same sensory input (Gu, 2002). Understanding behavior requires an understanding of the strategies that integrate context into sensory responses during ecologically relevant behaviors.

Oxygen is unevenly distributed in soil and water environments (Sylvia et al., 1998; Wannamaker and Rice, 2000; Wu, 2002), and is an important sensory cue for many organisms. Animals monitor both internal and environmental oxygen levels to maintain oxygen homeostasis (Hermes-Lima and Zenteno-Savin, 2002). Either hypoxia or hyperoxia is disruptive: molecular oxygen is essential for many biological processes, but excess oxygen promotes the production of toxic reactive oxygen species (Yu, 1994). The best-understood mechanism of oxygen homeostasis is the HIF-1 (hypoxia-inducible transcription factor) system, which is conserved in all metazoa (Kaelin, 2005). This relatively slow transcriptional pathway for oxygen homeostasis is supplemented by rapid neuronal mechanisms for oxygen sensation. In mammals, the carotid body senses reduced blood oxygenation to mediate a hyperventilatory response and strong arousal

(Lopez-Barneo, 2003). In the nematode *Caenorhabditis elegans,* certain chemosensory neurons detect environmental oxygen to generate aerotaxis behaviors in oxygen gradients (Gray et al., 2004). These neurons, called URX, AQR, and PQR, express five genes that encode soluble guanylate cyclase homologs (sGCs) with similarity to the NO-regulated sGCs from other animals. The sGC homolog GCY-35 is required for normal aerotaxis and binds directly to molecular oxygen through a heme cofactor (Gray et al., 2004), suggesting that oxygen regulates GCY-35 and cGMP production during aerotaxis. A second predicted sGC homolog encoded by the *gcy-36* gene is also needed for aerotaxis (Cheung et al., 2005). cGMP produced by these cyclases is thought to open a cGMP-gated sensory transduction channel encoded by the *tax-4* and *tax-2* genes (Gray et al., 2004). Through the activity of the cyclases and the cGMP-gated channel, animals accumulate at a preferred oxygen concentration of about 10% oxygen.

The behavioral response of *C. elegans* to oxygen is regulated by natural polymorphisms in a neuropeptide receptor gene, *npr-1* (Cheung et al., 2005; Gray et al., 2004). *npr-1* encodes a G protein-coupled receptor related to mammalian neuropeptide Y receptors, and exists in two allelic forms that differ at a single animal acid, NPR-1(215V) and NPR-1(215F) (de Bono and Bargmann, 1998). Both alleles are widely distributed in wild-caught *C. elegans* populations. Genetic analysis and biochemical characterization of ligand responses indicate that the 215V allele has high activity and the 215F allele has low activity (Coates and de Bono, 2002; Rogers et al., 2003). *npr-1(215F)* and *npr-1(lf)* animals have strong aerotaxis responses in oxygen gradients both in the presence of food and in its absence. *npr-1(215V)* animals, including the standard lab strain N2, have strong aerotaxis responses in the absence of food, but fail to avoid high oxygen when

food is present (Gray et al., 2004). *npr-1(lf)* and *npr-1(215V)* also differ in their locomotory responses to oxygen; reducing oxygen results in slowing of *npr-1(lf),* but not *npr-1(215V),* animals (Cheung et al., 2005). Slowing requires *gcy-35* and *gcy-36*, and is suppressed by expression of *npr-1(215V)* in URX, AQR, and PQR (Cheung et al., 2005). These results suggest that *npr-1(215V)* activity suppresses sGC-dependent oxygen responses in the presence of food.

The URX, AQR, and PQR oxygen-sensing neurons have an important role in a second behavior, the naturally polymorphic social feeding behavior of *C. elegans.* Animals with *npr-1(215F)* or *npr-1(lf)* alleles aggregate into feeding groups on bacterial lawns, a behavior that requires *gcy-35* and *gcy-36* in URX, AQR, and PQR neurons (Cheung et al., 2004; de Bono and Bargmann, 1998). Because aggregation is stimulated at high oxygen levels and accumulation into aggregates decreases local oxygen levels, it is likely that hyperoxia avoidance by URX, AQR, and PQR is a key component of aggregation (Gray et al., 2004; Rogers et al., 2006).

An unanswered question is the mechanism by which *npr-1* activity is integrated into the circuit that responds to food and oxygen. *npr-1(215V)* action in URX, AQR, and PQR neurons suppresses aggregation on food (Coates and de Bono, 2002). The simplest interpretation of this result would be that *npr-1(215V)* is an internal "food sensor" – a molecule that inhibits URX, AQR, and PQR activity when food is present. However, many other genes and cells can affect aggregation behavior. For example, aggregation in *npr-1(lf)* animals requires the function of TRPV channel genes *osm-9* and *ocr-2* and the receptor chaperone gene *odr-4* in ASH and ADL nociceptive neurons (de Bono et al., 2002). Aggregation is also inhibited by the TGF-β gene *daf-7,* which is expressed mainly

in a different class of sensory neurons called ASI (de Bono et al., 2002; Ren et al., 1996; Schackwitz et al., 1996; Thomas et al., 1993). Given the close relationship between genes and neurons involved in aggregation and hyperoxia avoidance, these other pathways are also candidate regulators of oxygen responses. Indeed, a recent study of oxygen responses in the *npr-1(lf)* background showed that *ocr-2* and the ASH nociceptive neurons regulate aerotaxis and oxygen-dependent locomotory responses (Rogers et al., 2006).

Other than *gcy-35* and *tax-4,* the genes and neurons required for aerotaxis in the food-regulated *npr-1(215V)* background are unknown. Here we undertake a systematic comparison of the cells and genes that mediate hyperoxia avoidance in *npr-1(215V)* and *npr-1(lf)* animals. Our results reveal a distributed network of aerotaxis-promoting neurons and antagonistic neurons that suppress aerotaxis on food. Neuromodulation by food is accomplished by the NPR-1 neuropeptide pathway, non-canonical peptide regulation by the TGF-ß-related protein DAF-7, and the neurotransmitter serotonin. Different coalitions of neurons dominate aerotaxis behavior in different conditions. Thus complex natural behaviors in *C. elegans,* like behaviors in other animals, are assembled by flexible, distributed neuronal networks.

Results

Two distinct groups of sGC-expressing neurons promote hyperoxia avoidance.

When N2 *npr-1(215V) C. elegans* is placed into a small chamber with a linear gradient from anoxia to atmospheric oxygen in the gas phase, animals rapidly move to an

intermediate preferred oxygen concentration between 7-14% O_2, avoiding both high and low oxygen levels (Gray et al., 2004) (Fig. 2-1A, B). We found that different genetic and sensory inputs affected the animals' distribution in complex ways (Figures 2-1 – 2-6). Some manipulations caused animals to shift toward higher or lower oxygen but preserved avoidance of oxygen extremes (e.g. Fig. 2-1F); other manipulations resulted in flattened distributions of animals between 7-21% oxygen but did not affect avoidance of low oxygen (e.g. Fig. 2-1G). Moreover, accumulation of animals at one oxygen concentration necessarily affected accumulation at all other concentrations – in other words, individual data points within an aerotaxis assay are not independent. Statistical approaches for analyzing aerotaxis data were developed to take the entire distribution into account in representing the mutant responses. Briefly, for each mutant and condition we first compared the complete distribution of animals in the gradient to appropriate control strains using a stringent nonparametric test, Chi-square analysis. Distributions that were significantly different at $p < 0.01$ were subjected to further analysis with additional tests, using appropriate corrections for multiple comparisons. The Methods include a full discussion of statistical considerations; primary aerotaxis data are included in Table 2-1.

In this study, we focused on genes and neurons that contribute to hyperoxia avoidance, the avoidance of oxygen levels above 14% O_2 (Fig. 2-1B, C). Many of the interesting differences between mutants were evident using a simple index for hyperoxia avoidance that compares the fraction of animals in the hyperoxia area (bins 1-3, >14% O_2) to the fraction in the preferred area (bins 4-6, 7-14% O_2). A hyperoxia avoidance index of 1.0 represents complete avoidance of hyperoxia, 0.0 represents no preference, and -1.0 represents a complete preference for hyperoxia. Because each mutant was

assayed at least three times, the hyperoxia avoidance index could be used for standard statistical methods such as ANOVA. In a few cases, the behavior of animals in the gradients showed a significant shift in the preferred oxygen concentration that was not well-described by the hyperoxia avoidance index, but could be described using the median preferred oxygen concentration. These cases are discussed individually as they arise. The analysis used here may underreport real differences, but should exclude false positive results. Throughout this paper, the term "aerotaxis" refers to the complete distribution of animals (Fig. 2-1B), and the phrase "hyperoxia avoidance" refers specifically to the hyperoxia avoidance index (Fig. 2-1 I).

Hyperoxia avoidance in N2 *npr-1(215V)* depends on the cGMP-gated channel *tax-4* and the sGC *gcy-35* (Gray et al., 2004). Four additional candidate sGCs, *gcy-32, gcy-34, gcy-36,* and *gcy-37,* are co-expressed with *gcy-35* and *tax-4* in the URX, AQR, and PQR sensory neurons. Existing loss-of-function mutations in all of these sGCs except *gcy-37* were tested to ask whether other sGCs are involved in oxygen sensing in N2 *npr-1(215V)* animals. *gcy-35* and *gcy-36* mutants were significantly different from wild-type N2 animals based on the hyperoxia avoidance index, whereas *gcy-32* and *gcy-34* mutants were not affected by this measure (Fig. 2-1D, E, I). Analysis of the entire aerotaxis distribution showed a significant shift toward higher median preferred oxygen concentrations in *gcy-34* mutants ($p < 0.05$), and a shift in *gcy-32* animals that is unlikely to be significant. In an independent study, *gcy-35* and *gcy-36* were found to affect aerotaxis in the *npr-1(lf)* background, but *gcy-32* and *gcy-34* had no effect under standard assay conditions (Cheung et al., 2005).

The hyperoxia avoidance defects of *gcy-35* and *tax-4* mutants can be rescued by transgenes expressed in the URX, AQR, and PQR neurons (Gray et al., 2004). To ask whether these neurons are also necessary for aerotaxis, we expressed the cell-death activator gene *egl-1* (Conradt and Horvitz, 1998) under the control of the *gcy-36* promoter to generate a strain in which the URX, AQR, and PQR neurons were absent (*qaIs2241*). No URX, AQR, and PQR neurons could be detected in animals bearing the integrated *qaIs2241* transgene, as assessed either by expression of *gcy-35::GFP* or by Nomarski microscopy ($n > 100$ and $n = 10$, respectively). Surprisingly, the *qaIs2241* strain exhibited robust hyperoxia avoidance that was unlike the sGC mutants *gcy-34, gcy-35,* and *gcy-36* (Fig. 2-1F, I). Their hyperoxia avoidance index was normal, but *qaIs2241* animals were shifted to significantly lower oxygen concentrations in a 0-21% gradient than wild-type animals ($p < 0.01$). These results imply the existence of oxygen-sensing neurons other than URX, AQR, and PQR. They also show that altering sGC gene function leads to qualitatively different results from killing URX, AQR, and PQR neurons (see Discussion).

gcy-35::GFP reporter genes are expressed reliably in URX, AQR, PQR, SDQ, ALN, and BDU neurons, and variably in AVM, PLM, and PLN neurons (Cheung et al., 2004; Gray et al., 2004). AVM and PLM are mechanosensory neurons; little is known about the functional properties of SDQ, ALN, BDU, and PLN. *gcy-35; qaIs2241* animals were defective in hyperoxia avoidance, unlike *qaIs2241* (Fig. 2-1G, I). This result indicates that *gcy-35* has an additional site of action outside the URX, AQR, and PQR neurons. Expressing *gcy-35* in SDQ, ALN, and PLN was sufficient to restore hyperoxia avoidance to *gcy-35* mutants (Fig. 2-1H, I), suggesting that SDQ, ALN, and PLN might

also serve as oxygen-sensing neurons. Thus at least two sets of sGC-expressing neurons promote hyperoxia avoidance: (1) some or all of URX, AQR, and PQR and (2) some or all of SDQ, ALN, and PLN (Fig. 2-1J). The two SDQ neurons are similar in lineage, morphology, and neural connectivity to the AQR and PQR neurons, so they are attractive candidate oxygen sensors.

The nociceptive ASH TRPV neurons and serotonergic ADF TRPV neurons promote hyperoxia avoidance.

In further screens for effects of sensory mutants on aerotaxis, we found that two *C. elegans* TRPV sensory channels, *osm-9* and *ocr-2*, affected hyperoxia avoidance in *npr-1(215V)* strains. *osm-9* mutants were highly defective in hyperoxia avoidance; *ocr-2* mutants had significant defects in hyperoxia avoidance, and a shifted median preference towards higher oxygen ($p < 0.05$) (Fig. 2-2A, I).

osm-9 and *ocr-2* function in chemotaxis toward some odors and in avoidance of high osmolarity, nose touch, and chemical repellents (Colbert et al., 1997; Tobin et al., 2002). The expression of *osm-9* and *ocr-2* overlaps in the chemosensory neurons AWA, ADF, ADL, ASH, PHA, and PHB; *osm-9* is expressed in numerous additional neurons. Several cell-specific transgenes were tested for the ability to rescue *osm-9* hyperoxia avoidance in the N2 *npr-1(215V)* strain. The ASH nociceptive neurons are required for avoidance of chemical, mechanical, and osmotic repellents (Bargmann and Mori, 1997). Expressing *osm-9* in the ASH nociceptive neurons, together with the posterior PHA and PHB neurons, restored hyperoxia avoidance to *osm-9* mutants (Zhang et al., 2004) (Fig. 2-2B, I). A close correlation was observed between rescue of osmotic avoidance, an

ASH-mediated behavior, and rescue of hyperoxia avoidance (see Methods). These results match with those previously observed in the *npr-1(lf)* background, where expression of OCR-2 in ASH rescued both aggregation and aerotaxis (de Bono et al., 2002; Rogers et al., 2006).

Unexpectedly, a second transgene that rescued an *osm-9* mutant only in ADF neurons also rescued *osm-9* hyperoxia avoidance (Zhang et al., 2004) (Fig. 2-2C, I). ADF is a chemosensory neuron that affects formation of the alternative dauer larva stage, chemotaxis towards water-soluble attractants, and olfactory learning (Bargmann and Horvitz, 1991; Bargmann and Mori, 1997; Zhang et al., 2005); it has not previously been implicated in oxygen-related behaviors. Unlike the rescuing ASH transgene, the ADF transgene did not rescue osmotic avoidance (see Methods), and the ASH transgene did not rescue other roles of *osm-9* in ADF (Zhang et al., 2004). These results suggest that *osm-9* acts in both ASH and ADF neurons to promote hyperoxia avoidance.

The ADF neurons produce serotonin, a neurotransmitter that modulates egg-laying, feeding, locomotion, learning, and other food- and stress-related responses (Estevez et al., 2004; Horvitz et al., 1982; Sze et al., 2000; Zhang et al., 2005). The rate-limiting enzyme for serotonin biosynthesis is tryptophan hydroxylase, which is encoded by the *tph-1* gene in *C. elegans* (Sze et al., 2000). *osm-9* and *ocr-2* mutants have reduced levels of *tph-1* expression in ADF (Zhang et al., 2004). To ask whether serotonin might contribute to the activity of ADF neurons, we examined *tph-1* null mutants. These animals avoided hyperoxia about half as well as wild-type animals (Fig. 2-2D, I). Their intermediate defect is consistent with the idea that ADF functions as one of several neurons that promote hyperoxia avoidance. A transgene that expressed *tph-1* only in the

ADF sensory neurons rescued the hyperoxia avoidance defect of *tph-1* mutants (Fig. 2-2E, I). A different transgene that expressed *tph-1* in the NSM neurons in the pharynx did not rescue hyperoxia avoidance (Fig. 2-2F, I), although it does rescue some effects of *tph-1* on locomotion (Zhang et al., 2005). This result suggests that serotonin produced by ADF promotes hyperoxia avoidance.

tph-1 was also required for hyperoxia avoidance in the *qaIs2241* strain that lacked URX, AQR, and PQR neurons, as were *ocr-2* and *osm-9* TRPV genes (Fig. 2-2G-I). These results provide further evidence that TRPV channel-expressing neurons cooperate with sGC-expressing neurons in the oxygen response. The analysis of the sGC and TRPV mutants suggests that no single class of neuron is required for hyperoxia avoidance in N2 *npr-1(215V)* animals. Either of two sets of sGC-expressing neurons can cooperate with either of two sets of TRPV-expressing neurons to generate hyperoxia avoidance in oxygen gradients (Fig. 2-1J, 2-2J).

npr-1(lf) strains can respond to food if sGC or _ocr-2_ TRPV activity is reduced.

The basic aerotaxis responses of *npr-1(lf)* animals were similar to those of N2 *npr-1(215V)* animals (Gray et al., 2004) (Fig. 2-3A), and most of the cells and genes required for hyperoxia avoidance appeared to be similar. *npr-1(lf)* animals with the *qaIs2241* transgene that killed URX, AQR, and PQR neurons showed robust hyperoxia avoidance, but the aerotaxis distribution was significantly shifted compared to *npr-1(lf)* alone (Fig. 2-3B, G). *npr-1(lf)* hyperoxia avoidance was reduced by mutations in *gcy-35*, *osm-9*, and *ocr-2* (Fig. 2-3C-E, G); similar results were obtained independently by de Bono and colleagues (Cheung et al., 2005; Rogers et al., 2006). One significant

difference between N2 and *npr-1(lf)* was that a *tph-1* mutation did not significantly diminish hyperoxia avoidance in the *npr-1(lf)* strain (Fig. 2-3F, G).

The presence of a small amount of bacterial food in the aerotaxis chamber strongly suppressed hyperoxia avoidance of N2 strains (Gray et al., 2004) (Fig. 2-4A, K). In *npr-1(lf)* strains, the hyperoxia avoidance index was nearly unchanged by food (Gray et al., 2004) (Fig. 2-4B, 2-4K), and aerotaxis was shifted slightly but significantly toward lower oxygen levels ($p < 0.05$). N2; *qaIs2241* animals in which URX, AQR, and PQR were killed were regulated by food, like N2 animals (Fig. 2-4C, K). Hyperoxia avoidance in *npr-1 qaIs2241* animals was also strongly regulated by food, unlike the response of *npr-1(lf)* animals (Fig. 2-4D, K). The reappearance of food regulation was surprising, but consistent with observations that oxygen-dependent slowing on food is restored in *npr-1(lf)* animals with *gcy* mutations or hyperpolarized URX, AQR, and PQR neurons (Cheung et al., 2005) (Fig. 2-4E, F, K). The recovery of food regulation also supports the model from aggregation studies that the main site of *npr-1* action is the sGC-expressing URX, AQR, and PQR neurons (de Bono et al., 2002), which are not required for food regulation (Fig. 2-4C, K).

osm-9 and *ocr-2* TRPV mutations affected both food regulation and hyperoxia avoidance in the *npr-1(lf)* background. *osm-9* mutants were defective in hyperoxia avoidance in all *npr-1* backgrounds, with or without food (Fig. 2-4G, H, K). The hyperoxia avoidance index of *ocr-2; npr-1(lf)* double mutants was significantly regulated by food, unlike that of *npr-1(lf)* mutants (Fig. 2-4I - 2-4K).

The simplest initial model explaining *npr-1* aerotaxis behavior would have been that *npr-1(215V)* is the essential link between food sensation and hyperoxia avoidance,

but this model must be incorrect. *npr-1* contributes to food regulation of aerotaxis, but the analysis of double mutants shows that alternative pathways retain covert food sensitivity in *npr-1(lf)* strains.

Increases and decreases in ADF serotonin affect hyperoxia avoidance on food.

Serotonin regulates numerous food-associated behaviors in *C. elegans,* and therefore was considered as a possible regulator of aerotaxis. Indeed, in the N2 *npr-1(215V)* strain, the serotonin biosynthesis gene *tph-1* was required both for robust hyperoxia avoidance (Fig. 2-2) and for food regulation: the residual hyperoxia avoidance of *tph-1* mutants was not regulated by food (Fig. 2-5A, B, F). Hyperoxia avoidance in *tph-1; npr-1* double mutants was unregulated by food, as observed for each single mutant (Fig. 2-5C, F). These results implicate *tph-1* in food regulation in *npr-1(215V)* strains.

The hyperoxia avoidance defect of *tph-1* mutants off food was rescued in *tph-1; ADF::tph-1* transgenic animals (Fig. 2-2), but these rescued animals were not regulated by food (Fig. 2-5D, F). These results are consistent with models in which food regulation requires the endogenous *tph-1* promoter, accurate regulation of ADF serotonin levels, or additional serotonergic neurons. The *ADF::tph-1* transgene was introduced into wild-type animals to distinguish among possible mechanisms of food regulation. This strain should have increased *tph-1* expression in ADF, and the *srh-142* ADF promoter should be resistant to normal transcriptional pathways for *tph-1* regulation. Hyperoxia avoidance in wild-type animals bearing the *ADF::tph-1* transgene was poorly regulated by food compared to N2 controls (Fig. 2-5E, F). Thus regulation of hyperoxia avoidance by food requires appropriate regulation of ADF serotonin: either loss of ADF *tph-1* or

unregulated ADF *tph-1* expression disrupted food regulation of *npr-1(215V)* strains. These results point toward *tph-1* in ADF as a possible site of food regulation in the *npr-1(215V)* strain. In particular, they suggest that high levels of ADF *tph-1* generate strong hyperoxia avoidance on or off food.

daf-7/TGF-ß reduces ADF serotonin to block hyperoxia avoidance on food.

The *C. elegans* TGF-ß homolog DAF-7 responds to food and crowding to regulate formation of the alternative dauer larva stage; low levels of *daf-7* activity are associated with stressful conditions that favor dauer formation (Ren et al., 1996; Schackwitz et al., 1996). *daf-7* mutants aggregate on food, suggesting a possible interaction with oxygen-regulated behaviors (Thomas et al., 1993), but this process is genetically different from *npr-1* aggregation (Cheung et al., 2004; de Bono et al., 2002). We found that *daf-7* mutants exhibit robust hyperoxia avoidance in the presence or absence of food (Fig. 2-6A, B, J). These results suggest that like *npr-1(215V)*, *daf-7* activity suppresses hyperoxia avoidance on food.

During reproductive growth, secreted DAF-7 antagonizes the activity of the SMAD transcription factor DAF-3 in target cells (Patterson et al., 1997; Thomas et al., 1993). *daf-3* mutants are dauer-defective, *daf-7* mutants are dauer-constitutive, and *daf-7; daf-3* mutants resemble *daf-3* mutants. Similar epistasis relationships were observed in hyperoxia avoidance. *daf-3* hyperoxia avoidance was regulated by food (Fig. 2-6C, J), and hyperoxia avoidance of *daf-7; daf-3* animals was also regulated by food, resembling *daf-3* mutants rather than *daf-7* mutants (Fig. 2-6D, J). These results suggest that *daf-7* regulates hyperoxia avoidance through the transcriptional *daf-3/SMAD* pathway.

Hyperoxia avoidance in *daf-3 npr-1* mutants resembled that of *npr-1* single mutants and was not regulated by food (Fig. 2-6E, J). These results indicate that *npr-1* does not act through the *daf-3* transcriptional pathway.

daf-7 is expressed most strongly in the ASI sensory neurons, where its transcription is induced by food and suppressed by crowding (Ren et al., 1996). This activity-dependent pathway for *daf-7* expression in ASI requires the cGMP-gated sensory channel *tax-4* (Coburn et al., 1998) (Fig. 2-6F, G). To ask whether *daf-7* expression in ASI might affect aerotaxis, we examined a strain in which *tax-4* was mutant in ASI and other sensory neurons, but rescued in URX, AQR, and PQR neurons. Hyperoxia avoidance in these strains was not regulated by food (Fig. 2-6H, J), suggesting that food could act in part by regulating *daf-7* expression in ASI.

Both *daf-7* and the serotonin biosynthetic enzyme *tph-1* function in food and stress responses, and *tph-1* has complex positive and negative interactions with genes in the dauer formation pathway, including *daf-7* (Estevez et al., 2004; Sze et al., 2000). We found that *daf-7* mutants had significantly increased *tph-1::GFP* expression in ADF neurons (Fig. 2-7A-C). *tph-1* is the rate-limiting enzyme for serotonin synthesis, so this induction should increase total ADF serotonin levels and therefore promote aerotaxis. *tph-1::GFP* expression in ADF was also increased in *tax-4* mutants (Fig. 2-7C), which have a low level of *daf-7* expression in ASI. These observations suggest that *tph-1* in ADF might act at a hub between aerotaxis-promoting and aerotaxis-suppressing networks.

Increased ADF serotonin stimulates hyperoxia avoidance on food in N2 *npr-1(215V)* animals (Fig. 2-5E, F), so the induction of *tph-1* in *daf-7* mutants could explain

why *daf-7* mutants retained strong hyperoxia avoidance on food. This hypothesis was supported by molecular and genetic epistasis results. At a molecular level, *daf-3* suppressed the *tph-1::GFP* induction caused by the *daf-7* mutation (Fig. 2-7C), as well as suppressing *daf-7* hyperoxia avoidance on food (Fig. 2-6D, J). These results indicate that *daf-7* activity inhibits *daf-3* to inhibit *tph-1* expression in ADF (Fig. 2-7D). At a genetic level, *tph-1* was epistatic to *daf-3*, so that hyperoxia avoidance in *tph-1; daf-3* double mutants was unregulated by food, as in *tph-1* single mutants (Fig. 2-6I, J). These results are consistent with the model that *daf-3* functions by regulating *tph-1* expression. *daf-3* is not required for basal *tph-1* expression in ADF, only for its regulation by *daf-7* (Fig. 2-7C); since *tph-1* is also regulated by TRPV and calcium signaling pathways (Zhang et al., 2004), *daf-3* may not be the only link between food and *tph-1* expression (Fig. 2-7D).

By both molecular and genetic criteria, *daf-7* and *npr-1* appeared to act in separate pathways to regulate hyperoxia avoidance on food. The expression of *tph-1::GFP* in ADF was not increased in *npr-1* animals compared to wild-type animals (Fig. 2-7C), and *daf-3 npr-1* mutants resembled *npr-1* single mutants in hyperoxia avoidance (Fig. 2-6E, J), indicating that *daf-3* is not the target for *npr-1*.

These results implicate two different pathways in food regulation of aerotaxis: one mediated by neuropeptide *npr-1* suppression of sGC neurons, and one mediated by *daf-7* suppression of *tph-1* expression in ADF. Neurons that promote and regulate hyperoxia avoidance belong to partly redundant coalitions that antagonize each other: no unique system directs either hyperoxia avoidance or food regulation. A model for this network is presented in Figure 2-8.

Discussion

Oxygen-sensing neurons interact in a distributed aerotaxis circuit.

The *C. elegans* nervous system consists of 302 neurons with reproducible morphologies and synapses (White et al., 1986). Many of these neurons have characteristic sensory or motor functions (Bargmann and Mori, 1997; Chalfie et al., 1985; Gray et al., 2005). However, food is able to alter the neurons required for several *C. elegans* behaviors (Chao et al., 2004; Sawin et al., 2000), often through serotonin-dependent pathways (Estevez et al., 2004; Horvitz et al., 1982; Sze et al., 2000; Zhang et al., 2005). Our results suggest that the network for oxygen-regulated behavior is flexible and distributed. Like the crustacean feeding circuit, the leech escape circuit, and the mammalian hippocampus, oxygen responses are encoded in the behavior of neuronal populations, not just individual neurons (Briggman et al., 2005; Nusbaum and Beenhakker, 2002; Wills et al., 2005).

At least four sets of sensory neurons promote avoidance of high oxygen: (1) some or all of URX, AQR, and PQR, which express multiple soluble guanylate cyclases (sGCs), (2) some or all of SDQ, ALN, and PLN, which express the sGC GCY-35 and (3 and 4) the *osm-9* (TRPV)-expressing neurons ADF and ASH (Fig. 2-8A). In the absence of food, either URX, AQR, and PQR neurons or the other sGC neurons can be sufficient for hyperoxia avoidance, although they result in different peak oxygen preferences: about 10% O_2 for URX, AQR, and PQR, and about 8% O_2 for the alternative neurons. Avoidance of hypoxia (below 7% O_2) appears to represent a separate system that is largely independent of these pathways.

At least three predicted soluble guanylate cyclases, *gcy-34, gcy-35,* and *gcy-36,* contribute to hyperoxia avoidance in a N2 background. Mammalian sGCs function as obligate dimers (Koesling, 1999), so the possible complement of different cyclases in URX, AQR, and PQR is substantial, perhaps explaining why sGC mutations are different from killing URX, AQR, and PQR. In an independent study, *gcy-35* and *gcy-36,* but not *gcy-32* or *gcy-34,* were found to be required for hyperoxia avoidance in *npr-1* strains (Cheung et al., 2005). Enhanced aerotaxis activity of URX, AQR, and PQR in *npr-1* mutants may relieve the requirement for *gcy-34* activity. However, even in *npr-1* mutants, either *gcy-32* or *gcy-34* contributes to avoidance of high oxygen levels under sensitized conditions (Cheung et al., 2005).

URX, AQR, PQR, SDQ, ALN, and PLN express soluble guanylate cyclases that bind to molecular oxygen, consistent with a primary oxygen-sensing function (Gray et al., 2004). We suggest that these neurons are activated by high oxygen to trigger avoidance behavior. An avoidance function is consistent with the neuronal connectivity of URX, AQR, PQR, and SDQ neurons; like ASH and other sensory neurons that mediate avoidance, these neurons synapse onto the command interneurons that regulate the choice between forward and backward movement (White et al., 1986) (Fig. 2-8A).

The TRPV-expressing neurons ADF and ASH also promote hyperoxia avoidance, and an *osm-9* mutant can be rescued by expression in either of those cells. Additionally, ASH neurons contribute to aggregation in *npr-1* strains (de Bono et al., 2002). No direct molecular mediators of oxygen sensation have been defined in ADF and ASH. These neurons might sense oxygen directly through an unknown mechanism, or they might act indirectly to stimulate the activity of the sGC-expressing neurons. ASH neurons are

polymodal nociceptors that generate robust calcium transients to noxious stimuli such as high osmotic strength, quinine, and touch (Hilliard et al., 2004), but ASH does not respond with strong calcium transients when exposed to decreases or increases in oxygen in the range where hyperoxia avoidance is observed (data not shown). It is possible that a subtle modulation of ASH activity by oxygen contributes to a distributed oxygen response, or that other noxious signals sensed by ASH converge with oxygen at downstream neurons (de Bono et al., 2002).

The ADF neurons have not been implicated in aggregation, but our results indicate that ADF has a significant role in aerotaxis of *npr-1(215V)* animals. ADF stimulates aerotaxis in the absence of food by producing serotonin. A variety of results suggest that ADF serotonin may be a stress signal in *C. elegans;* this possibility is considered below.

The wiring diagram of synaptic connections in *C. elegans* suggests that the network of aerotaxis neurons converges on AVA, the command interneuron responsible for generating backward motion; ASH, AQR, PQR, and SDQ all make connections to AVA (White et al., 1986) (Fig. 2-8A). Another likely site of signal integration is the interneuron AUA, which receives most of its synaptic inputs from ADF and URX and synapses onto AVA and other neurons.

TGF-ß signaling, serotonin, and aerotaxis on food.

C. elegans egg-laying, feeding, locomotion and olfactory behavior are all regulated by food, in part through serotonin-dependent pathways (Estevez et al., 2004;

Horvitz et al., 1982; Sze et al., 2000; Zhang et al., 2005). Our results identify serotonin and the TGF-ß homolog DAF-7 as interacting modulators of hyperoxia avoidance in *npr-1(215V)* strains. Either decreased or increased serotonin disrupts food regulation: *tph-1* mutants have poor hyperoxia avoidance that is not regulated by food, whereas *daf-7* strains that overexpress *tph-1* have robust aerotaxis that is not regulated by food. Unregulated expression of *tph-1* from the *srh-142* promoter results in food-resistant aerotaxis. These results suggest that *tph-1* expression in ADF functions as a dose-dependent stimulator of hyperoxia avoidance.

Genetic and molecular results indicate that *daf-7* suppresses hyperoxia avoidance on food by repressing *tph-1* expression in ADF neurons. The expression of *daf-7* in ASI is stimulated by food and *tax-4*, providing a link between food availability and *daf-7* activity (Coburn et al., 1998; Ren et al., 1996). Thus the *daf-7/tph-1* regulatory loop may be a component of normal food regulation of hyperoxia avoidance. It is possible that other serotonergic neurons affect food regulation as well.

tph-1 expression in ADF can be induced by infection with bacterial pathogens, high temperature, calcium signaling, and genes in the dauer formation pathway (Estevez et al., 2004; Zhang et al., 2004; Zhang et al., 2005). High temperature and pathogenic infection are natural stressors for *C. elegans*, and the dauer pathway is a general physiological response to stress states, suggesting that induction of serotonin in ADF is a common stress-related response. Hyperoxia is a metabolic stressor and a mutagen; the nociceptive ASH neurons and the ADF serotonergic neurons may function to stimulate hyperoxia avoidance (and thus decrease oxidative stress) in the presence of other environmental or metabolic stressors.

Paradoxically, serotonin can substitute for the effects of food in many behavioral assays (Horvitz et al., 1982), and therefore may communicate either food or stress signals depending on the amount of serotonin or the neuronal source of serotonin. An interesting contrast to hyperoxia avoidance is provided by ASH nociception, which is stimulated by serotonin and heightened in the presence of food, the condition in which hyperoxia avoidance is suppressed (Chao et al., 2004). The behaviors associated with serotonin signaling – enhancement of feeding or egg-laying, enhanced slowing on food, alteration of nociceptive pathways, and olfactory learning – are all highly sensitive to the transition between well-fed and starved states (Chao et al., 2004; Horvitz et al., 1982; Nuttley et al., 2002; Sawin et al., 2000; Zhang et al., 2005). ADF serotonin release might be used to signal and enhance the transition between these states, rather than representing either the positive or the negative sensory context.

Aerotaxis, social feeding, and foraging: Flexibility and plasticity of natural behavior.

By repressing the activity of oxygen-sensing neurons (Cheung et al., 2005; Rogers et al., 2006), *npr-1(215V)* activity in N2 strains enhances the food sensitivity of an existing oxygen-sensing network regulated by *daf-7* and *tph-1*. The phenotypes of *npr-1(lf)* strains are consistent with increased URX, AQR, and PQR activity, and subsequent stimulation of both hyperoxia avoidance and aggregation on food. *C. elegans* consumes oxygen, so oxygen levels within an aggregate of *C. elegans* are lower than those in the surrounding bacterial lawn ((Rogers et al., 2006); M. Peliti, personal communication). Aggregation only occurs in strains that maintain strong hyperoxia

avoidance in the presence of food (Table 2-3). These results suggest that aggregation behavior is partly driven by hyperoxia avoidance, and that animals within an aggregate cooperate to lower ambient oxygen to a preferred level. Aggregation in microaerophilic flagellates has been shown to have a similar oxygen-lowering effect (Fox, 1921).

More generally, hyperoxia avoidance may represent a foraging behavior in which *C. elegans* searches for the lower oxygen concentrations that correspond to food. In the soil, pockets of bacteria growing on decaying organic matter create local sinks of oxygen; even *E. coli* colonies on an agar surface consume oxygen faster than it can diffuse through the lawn (Gray et al., 2004). N2 *npr-1(215V)* animals suppress the drive to find low oxygen in the presence of adequate *E. coli* food, a strategy that may allow them to exploit a greater range of environments. Thus the recent evolutionary appearance of *C. elegans* strains with *npr-1(215V)* activity may have added flexibility to *C. elegans* feeding behavior (Rogers et al., 2003).

The analysis of wild-type and *npr-1* animals on and off food shows that despite its stereotyped neuroanatomy, *C. elegans* can generate hyperoxia avoidance using flexible configurations of neurons. The preferred oxygen concentration can be altered by changing the class of sensory neurons that dominate the response, or by changing the properties of the sensory neurons. The strength of the avoidance response can be regulated by different food signals that modulate oxygen-sensing circuits. Our results suggest that the simple nervous system of *C. elegans* has the potential to assemble alternative functional circuits analogous to the dynamic modulated networks in crustacean feeding circuits, leech escape response circuit, or hippocampal place cells (Briggman et al., 2005; Nusbaum and Beenhakker, 2002; Wills et al., 2005). The

complexity and subtlety of these pathways suggest that oxygen – a highly variable stimulus in the soil environment – is an important regulator of natural *C. elegans* behavior.

Materials and Methods

Strains

Strains were cultured under standard conditions (Brenner, 1974) and fed *E. coli* HB101. Wild-type animals were *C. elegans* Bristol strain N2. Other strains used in this study include: AX1297 *gcy-36 (db66)* X, CX6448 *gcy-35 (ok769)* I, RB1062 *gcy-34 (ok1012)* V, CX6804 *gcy-32 (ok995)* V, CX7102 *lin-15 (n765) qaIs2241* [*gcy-36::egl-1, gcy-35::gfp, lin-15(+)*] X, CX7104 *gcy-35 (ok769)* I; *qaIs2241* X, CX8142 *gcy-35 (ok769)* I; *kyEx1248* [*lad-2::gcy-35, unc-122::dsRed*], CX4544 *ocr-2 (ak47)* IV, CX4537 *osm-9 (ky10)* IV, CX7265 *osm-9 (ky10)* IV; *yzEx53* [*osm-10::osm-9, elt-2::gfp*], CX7264 *osm-9 (ky10)* IV; *yzEx51* [*cat-1::osm-9, elt-2::gfp*], CX7456 *ocr-2 (ak47)* IV; *qaIs2241* X, CX7250 *osm-9 (ky10)* IV; *qaIs2241* X, DA609 *npr-1 (ad609)* X, CX7158 *npr-1 (ad609) qaIs2241* X, CX7157 *gcy-35 (ok769)* I; *npr-1 (ad609)* X, CX4821 *osm-9 (ky10)* IV; *npr-1 (ad609)* X, CX4649 *ocr-2 (ak47)* IV; *npr-1 (ad609)* X, CB1372 *daf-7 (e1372)* III, CB1376 *daf-3 (e1376)* X, JT5464 *daf-7 (e1372)* III; *daf-3 (e1376)* X, CX7926 *daf-3 (e1376) npr-1 (ad609)* X, DR1808 *mIs6* [*daf-7::gfp, rol-6 (su1006)*] X, CX7394 *tax-4 (ks28)* III; *mIs6* X, CX6858 *tax-4 (ks28)* III; *kyIs342* [*gcy-32::tax-4::gfp, unc-122::gfp*], GR1321 *tph-1 (mg280)* II, CX7749 *tph-1 (mg280)* II; *kyEx1087* [*ceh-2::tph-1::gfp, unc-122::gfp*], CX76741 *tph-1 (mg280)* II; *kyEx953* [*srh-142::tph-1::gfp, unc-122::gfp*], CX8060 *kyEx953*, CX7888 *tph-1 (mg280)* II; *qaIs2241* X, CX8151 *tph-1 (mg280)* II; *npr-1 (ad609)* X, GR1334 *tph-1 (mg280)* II; *daf-3 (mgDf90)* X, GR1333 *yzIs71* [*tph-1::gfp, rol-6 (su1006)*] V, CX7248 *tax-4 (ks28)* III; *yzIs71* V, CX8013 *daf-7 (e1372)* III; *yzIs71* V, CX8012 *yzIs71* V; *daf-3 (e1376)* X, CX8059 *daf-7 (e1372)* III; *yzIs71* V; *daf-3*

(e1376) X, CX8105 *yzIs71* V; *npr-1 (ad609)* X. Additional strains used in Figures 2-10S and 2-11S include: CZ3805 *gcy-33 (ok232)* V; *gcy-31 (ok296)* X, CX6803 *gcy-35 (ok769)* I; *gcy-33 (ok232)* V; *gcy-31 (ok296)* X, CX6422 *gcy-35 (ok769)* I; *gcy-33 (ok232)* V; *gcy-31 (ok296) qaIs2241* X, CX4651 *osm-9 (ky10) ocr-2 (ak47)* IV, CX5104 *osm-9 (ky10) ocr-2 (ak47)* IV; *npr-1 (ad609)* X, RB982 *flp-21 (ok889)* V, NY192 *flp-21 (pk1601)* V, CX7887 *daf-7 (e1372)* III; *qaIs2241* X. In all cases, null alleles or strong loss-of-function alleles were used.

Molecular Biology

A *lad-2::gcy-35* rescuing plasmid was constructed by PCR amplification of the *lad-2* promoter from genomic DNA and insertion into FseI to AscI in an expression vector containing *gcy-35* cDNA in pSM1, a modified pPD49.26 with extra cloning sites (Gray et al., 2004). The *lad-2* promoter contains 4.0 kb sequence upstream of the start codon. Expression of the *lad-2::gfp* transcriptional reporter fusion was reported in the SMD, SAA, SDQ, ALN, and PLN neurons (Oliver Hobert, personal communication); we made independent strains that confirmed this expression pattern (data not shown). The *lad-2::gcy-35* plasmid was injected at 50 ng/µl with 30 ng/µl *unc-122::dsRed* as a co-injection marker.

Behavioral Assays

Aerotaxis assays were performed by placing animals on NGM agar in custom-made microfluidic devices fabricated from polydimethylsiloxane (PDMS) with a gas-phase linear gradient from 0-21% oxygen, and monitoring animals' accumulation in nine

bins across the gradient (Gray et al., 2004). Gradients were generated by delivering gases under laminar flow to source and drain chambers immediately outside the behavioral arena, using a syringe pump; diffusion of the gases established the gradient in the small assay chamber. Gases were obtained from Airgas, Matheson, and TW Smith. Animals were prepared for assays as described except that animals were picked instead of washed from their culture plate onto NGM assay plates before the devices were placed onto the assay plate. For assays on food, thin bacterial lawns of *E. coli* HB101 were made by seeding NGM plates for overnight growth at 37°C and returning plates to room temperature for at least 1 hour before assay.

Results from two devices were binned for one assay (~80-100 animals per assay). At least three independent assays on three different days for each genotype were used to generate results in the Figures. Data presented represent distributions 25 minutes from start of the assay.

Glycerol osmotic avoidance assays for rescued *osm-9* strains were performed using a ring of 20 µl 4M glycerol and xylene cyanol pipetted onto a NGM plate. The fraction of animals that escaped the ring was scored at 8 minutes after exposure. *osm-9; ADF::osm-9* animals were not rescued for osmotic avoidance (fraction escaping osmotic ring ± standard error of the mean for N2, 0.04±0.02; for *osm-9,* 0.82±0.06; for *osm-9; ADF::osm-9,* 0.73±0.06). *osm-9; osm-10(ASH, PHA, PHB)::osm-9* animals were partially rescued for osmotic avoidance (fraction escaping osmotic ring, 0.43±0.06), suggesting variable expression of the transgene. To select for *osm-9; osm-10::osm-9* transgenic animals that strongly avoided high osmolarity, animals were washed and tested in the 4M glycerol ring. Transgenic animals that stayed inside the ring after 8-10

minutes were picked off and recovered on a well-fed culture plate for at least 4 hours before testing for aerotaxis.

Statistical Analysis

Statistical analysis of aerotaxis was conducted in multiple steps. The nine individual points in the aerotaxis assay are not independent – accumulation of animals in one bin necessarily affects all other bins – so they cannot be analyzed individually. A first test to assess the overall distribution of animals in the aerotaxis assay was a comparison of experimental strains or conditions to controls by Chi-square analysis (nine bins per aerotaxis assay x 2 strains = 8 degrees of freedom). Chi-square analysis takes into account the non-Gaussian nature of the aerotaxis distributions as well as the total number of animals tested. It is overly conservative, because it combines all animals tested into a single contingency table, and does not take into account the fact that each assay was repeated multiple times. Therefore, assays that are not statistically different by this criterion may actually be different. With this issue in mind, we have emphasized positive findings in this study. For controls such as N2 that were compared to multiple mutants, $p < 0.01$ was used as the level of significance for the Chi-square test. Most results described in the paper were significant at $p < 0.001$ (Table 2-2). In the text, any stated differences in a secondary measure, such as hyperoxia avoidance index or median preferred oxygen concentration (see below), had also passed this first test using Chi-square analysis of the entire distribution ($p < 0.01$).

The hyperoxia avoidance index has been previously described (Gray et al., 2004) and is defined as [(fraction of animals in 7-14% O_2) - (fraction of animals in 14-21% O_2)]

/ (fraction of animals in 7-21% O_2). This standard performance index varies from –1.0 (all animals in hyperoxic regions) to +1.0 (all animals in normoxic regions) with 0 representing no preference between normoxia and hyperoxia. The response to hypoxia, the region between 0-7% oxygen, was not reliably affected in any of the assays described here; hypoxia avoidance appears to be a distinct behavior with a distinct genetic basis, and this part of the curve was not informative for any analysis. Each strain or condition was tested in at least 3 assays with ~80-100 animals each, and the mean hyperoxia avoidance index across all assays was used to test significance. *t* tests were used to compare the hyperoxia avoidance indices between two distributions (Statview). ANOVA plus Bonferroni *t* tests or Dunnett tests were used for multiple comparisons of hyperoxia avoidance indices between strains (Statview). For controls such as N2 that were compared to multiple mutants, $p < 0.01$ was used as the level of significance.

The median oxygen preference was calculated for each assay as the position of the 50th percentile of animals. Results from multiple assays were combined for each strain or condition using at least 3 assays with ~80-100 animals per assay, generating a mean median oxygen preference. For ANOVA, all strains were compared to one control (N2 in the absence of food), and Dunnett tests for multiple comparisons were used. Significant differences were observed with *gcy-34, gcy-36,* and *ocr-2* (all off food, higher oxygen preference than N2), and *qaIs2241* off food, *npr-1* on food, and *daf-7* on food (lower oxygen preference than N2).

In almost every case, the hyperoxia avoidance index or the median oxygen preference uncovered and simplified the differences between strains and conditions that were apparent in the overall assays.

Two concerns remained after this analysis: (1) Is it valid to consider the hyperoxia avoidance index and the median preferred oxygen concentration as independent values? (2) Are there important features of the behavior that were overlooked using these parameters? As an independent, unbiased way to identify important sources of variance in the data, we analyzed the distribution of animals in 279 aerotaxis assays by principal component analysis (PCA), an unsupervised data reduction method.

PCA was conducted on 48 data points that described each aerotaxis curve: the fraction of animals in each of the nine bins, the sums of fractions in adjacent bins or adjacent groups of three or four bins, and the differences between adjacent bins or adjacent groups of two or three bins. These 48 data points reflected features of the aerotaxis assay that were not necessarily represented in the standard parameters, such as the steepness of the curve at each point in the assay. Aerotaxis assays representing 36 genotypes with or without food were analyzed for PCA using Cluster 3.0 for Mac OSX (Michiel de Hoon, Seiya Imoto, and Satoru Miyano, University of Tokyo). The first principle component (PC1) described the basic bell-shape of the aerotaxis assay, the second component (PC2) resembled the peak preferred oxygen concentration, and the third component (PC3) resembled the hyperoxia avoidance index. Each principal component represents a complex vector that is most easily understood by showing the assays with the highest and lowest value of that vector (Fig. 2-9). For PC2, the highest values were the assays where the peak response was at high oxygen concentrations (e.g. *gcy-34, gcy-36, ocr-2*), and the lowest values were the assays in which the peak response was at low oxygen concentrations (e.g. *qaIs2241*); wild-type N2 animals had an

intermediate value (Fig. 2-9A). For PC3, the highest values were the assays with a strong aerotaxis peak (e.g. *npr-1, daf-7, ADF::tph-1*) and the lowest values were the assays that were nearly flat (e.g. N2-like genotypes on food); wild-type N2 animals off food had a high value (Fig. 2-9B).

The conclusion of this analysis is that an unbiased assessment of the variance in the aerotaxis assays yields features that are substantially related to the parameters identified by direct inspection of the aerotaxis data: the hyperoxia avoidance index and the median preferred oxygen concentration. Since PC2 and PC3 are by definition independent of each other, it is valid to consider these two components of the aerotaxis assay (its peak and its strength) separately.

We reasoned that if the principle components defined in this manner were biologically significant, they would correlate with the genotype and condition of the assay. Therefore, after PCA of individual assays, assays were grouped by genotype and condition, and the mean and standard error for each principal component were defined for each strain and condition and subjected to ANOVA. This analysis demonstrated significant effects of genotype and condition on PC2 and PC3. Detailed statistical analysis of PC2 and PC3 by genotype and condition led to conclusions similar to those reported in the results (data not shown).

Acknowledgments

We thank Jesse Gray, Massimo Hilliard, Greg Lee, Hang Lu, Navin Pokala, Makoto Tsunozaki, Yun Zhang, and Manuel Zimmer for helpful discussions and advice during this work, Joel Cohen and Alon Kaufman for statistical advice, Ji Ying Sze, Mario de Bono, Chris Li, and Jim Thomas for sharing strains, Martin Hudson for integrating the *qaIs2241* transgene, the *C. elegans* Knockout Consortium for deletion alleles of *gcy-32*, *gcy-34*, and *gcy-35*, and the *Caenorhabditis* Genetics Center for providing strains.

Author contributions

AJC and CIB conceived and designed the experiments. AJC and NC performed the experiments. AJC and CIB analyzed the data. DSK and MAM contributed reagents/materials/analysis tools. AJC and CIB wrote the paper.

Funding

This work was supported by the Howard Hughes Medical Institute. AJC was supported by a National Science Foundation Predoctoral Fellowship. CIB is an Investigator of the Howard Hughes Medical Institute.

Supplementary Data

Additional experiments not explicitly addressed in the text of Chapter 2 are included as Figures 2-10S and 2-11S.

References

Bargmann, C. I., and Horvitz, H. R. (1991). Control of larval development by chemosensory neurons in Caenorhabditis elegans. Science *251*, 1243-1246.

Bargmann, C. I., and Mori, I. (1997). Chemotaxis and thermotaxis. In C. elegans II, T. B. D.L. Riddle, B.J. Meyer, J.R. Priess, ed. (Cold Spring Harbor, New York, Cold Spring Harbor Laboratory Press), pp. 717-737.

Brenner, S. (1974). The genetics of Caenorhabditis elegans. Genetics *77*, 71-94.

Briggman, K. L., Abarbanel, H. D., and Kristan Jr., W. B. (2005). Optical imaging of neuronal populations during decision-making. Science *307*, 896-901.

Chalfie, M., Sulston, J. E., White, J. G., Southgate, E., Thomson, J. N., and Brenner, S. (1985). The neural circuit for touch sensitivity in Caenorhabditis elegans. J Neurosci *5*, 956-964.

Chao, M. Y., Komatsu, H., Fukuto, H. S., Dionne, H. M., and Hart, A. C. (2004). Feeding status and serotonin rapidly and reversibly modulate a Caenorhabditis elegans chemosensory circuit. Proc Natl Acad Sci U S A *101*, 15512-15517.

Cheung, B. H., Arellano-Carbajal, F., Rybicki, I., and de Bono, M. (2004). Soluble guanylate cyclases act in neurons exposed to the body fluid to promote C. elegans aggregation behavior. Curr Biol *14*, 1105-1111.

Cheung, B. H., Cohen, M., Rogers, C., Albayram, O., and de Bono, M. (2005). Experience-dependent modulation of C. elegans behavior by ambient oxygen. Curr Biol *15*, 905-917.

Coates, J. C., and de Bono, M. (2002). Antagonistic pathways in neurons exposed to body fluid regulate social feeding in Caenorhabditis elegans. Nature *419*, 925-929.

Coburn, C. M., Mori, I., Ohshima, Y., and Bargmann, C. I. (1998). A cyclic nucleotide-gated channel inhibits sensory axon outgrowth in larval and adult Caenorhabditis elegans: a distinct pathway for maintenance of sensory axon structure. Development *125*, 249-258.

Colbert, H. A., Smith, T. L., and Bargmann, C. I. (1997). OSM-9, a novel protein with structural similarity to channels, is required for olfaction, mechanosensation, and olfactory adaptation in Caenorhabditis elegans. J Neurosci *17*, 8259-8269.

Conradt, B., and Horvitz, H. R. (1998). The C. elegans protein EGL-1 is required for programmed cell death and interacts with the Bcl-2-like protein CED-9. Cell *93*, 519-529.

de Bono, M., and Bargmann, C. I. (1998). Natural variation in a neuropeptide Y receptor homolog modifies social behavior and food response in C. elegans. Cell *94*, 679-689.

de Bono, M., Tobin, D. M., Davis, M. W., Avery, L., and Bargmann, C. I. (2002). Social feeding in Caenorhabditis elegans is induced by neurons that detect aversive stimuli. Nature *419*, 899-903.

Estevez, M., Estevez, A. O., Cowie, R. H., and Gardner, K. L. (2004). The voltage-gated calcium channel UNC-2 is involved in stress-mediated regulation of tryptophan hydroxylase. J Neurochem *88*, 102-113.

Fox, H. M. (1921). An investigation into the case of the spontaneous aggregation of flagellates and into the reactions of flagellates to dissolved oxygen. J Gen Phys *3*, 483-512.

Gray, J. M., Hill, J. J., and Bargmann, C. I. (2005). A circuit for navigation in Caenorhabditis elegans. Proc Natl Acad Sci USA *102*, 3184-3191.

Gray, J. M., Karow, D. S., Lu, H., Chang, A. J., Chang, J. S., Ellis, R. E., Marletta, M. A., and Bargmann, C. I. (2004). Oxygen sensation and social feeding mediated by a C. elegans guanylate cyclase homologue. Nature *430*, 317-322.

Gu, Q. (2002). Neuromodulatory transmitter systems in the cortex and their role in cortical plasticity. Neuroscience *111*, 815-835.

Hermes-Lima, M., and Zenteno-Savin, T. (2002). Animal response to drastic changes in oxygen availability and physiological oxidative stress. Comp Biochem Physiol C *133*, 537-556.

Hilliard, M. A., Bergamasco, C., Arbucci, S., Plasterk, R. H., and Bazzicalupo, P. (2004). Worms taste bitter: ASH neurons, QUI-1, GPA-3 and ODR-3 mediate quinine avoidance in Caenorhabditis elegans. Embo J *23*, 1101-1111.

Horvitz, H. R., Chalfie, M., Trent, C., Sulston, J. E., and Evans, P. D. (1982). Serotonin and octopamine in the nematode Caenorhabditis elegans. Science *216*, 1012-1014.

Kaelin, W. G., Jr. (2005). Proline hydroxylation and gene expression. Annu Rev Biochem *74*, 115-128.

Koesling, D. (1999). Studying the structure and regulation of soluble guanylyl cyclase. Methods *19*, 485-493.

Kossl, M., and Vater, M. (1985). The cochlear frequency map of the mustache bat, Pteronotus parnellii. J Comp Physiol [A] *157*, 687-697.

Lopez-Barneo, J. (2003). Oxygen and glucose sensing by carotid body glomus cells. Curr Opin Neurobiol *13*, 493-499.

Nolan, K. M., Sarafi-Reinach, T. R., Horne, J. G., Saffer, A. M., and Sengupta, P. (2002). The DAF-7 TGF-beta signaling pathway regulates chemosensory receptor gene expression in C. elegans. Genes Dev *16*, 3061-3073.

Nusbaum, M. P., and Beenhakker, M. P. (2002). A small-systems approach to motor pattern generation. Nature *417*, 343-350.

Nuttley, W. M., Atkinson-Leadbeater, K. P., and Van Der Kooy, D. (2002). Serotonin mediates food-odor associative learning in the nematode Caenorhabditiselegans. Proc Natl Acad Sci U S A *99*, 12449-12454.

Patterson, G. I., Koweek, A., Wong, A., Liu, Y., and Ruvkun, G. (1997). The DAF-3 Smad protein antagonizes TGF-beta-related receptor signaling in the Caenorhabditis elegans dauer pathway. Genes Dev *11*, 2679-2690.

Ren, P., Lim, C. S., Johnsen, R., Albert, P. S., Pilgrim, D., and Riddle, D. L. (1996). Control of C. elegans larval development by neuronal expression of a TGF-beta homolog. Science *274*, 1389-1391.

Rogers, C., Persson, A., Cheung, B., and de Bono, M. (2006). Behavioral motifs and neural pathways coordinating O2 responses and aggregation in C. elegans. Curr Biol *16*, 649-659.

Rogers, C., Reale, V., Kim, K., Chatwin, H., Li, C., Evans, P., and de Bono, M. (2003). Inhibition of *Caenorhabditis elegans* social feeding by FMRFamide-related peptide activation of NPR-1. Nat Neurosci *6*, 1178-1185.

Sawin, E. R., Ranganathan, R., and Horvitz, H. R. (2000). C. elegans locomotory rate is modulated by the environment through a dopaminergic pathway and by experience through a serotonergic pathway. Neuron *26*, 619-631.

Schackwitz, W. S., Inoue, T., and Thomas, J. H. (1996). Chemosensory neurons function in parallel to mediate a pheromone response in C. elegans. Neuron *17*, 719-728.

Sigman, M., Cecchi, G. A., Gilbert, C. D., and Magnasco, M. O. (2001). On a common circle: natural scenes and Gestalt rules. Proc Natl Acad Sci U S A *98*, 1935-1940.

Sylvia, D. M., Fuhrmann, J. J., Hartel, P. G., and Zuberer, D. A. (1998). Principles and Applications of Soil Microbiology (Upper Saddle River, New Jersey, Prentice Hall).

Sze, J. Y., Victor, M., Loer, C., Shi, Y., and Ruvkun, G. (2000). Food and metabolic signalling defects in a Caenorhabditis elegans serotonin-synthesis mutant. Nature *403*, 560-564.

Thomas, J., Birnby, D., and Vowels, J. (1993). Evidence for parallel processing of sensory information controlling dauer formation in Caenorhabditis elegans. Genetics *134*, 1105-1117.

Tobin, D., Madsen, D., Kahn-Kirby, A., Peckol, E., Moulder, G., Barstead, R., Maricq, A., and Bargmann, C. (2002). Combinatorial expression of TRPV channel proteins defines their sensory functions and subcellular localization in C. elegans neurons. Neuron *35*, 307-318.

Wannamaker, C. M., and Rice, J. A. (2000). Effects of hypoxia on movements and behavior of selected estuarine organisms from the southeastern United States. J Exp Mar Biol Ecol *249*, 145-163.

White, J. G., Southgate, E., Thomson, J. N., and Brenner, S. (1986). The structure of the nervous system of the nematode *Caenorhabditis elegans*. Phil Transact R Soc Lond B *314*, 1-340.

Wills, T. J., Lever, C., Cacucci, F., Burgess, N., and O'Keefe, J. (2005). Attractor dynamics in the hippocampal representation of the local environment. Science *308*, 873-876.

Wu, R. S. (2002). Hypoxia: from molecular responses to ecosystem responses. Mar Pollut Bull *45*, 35-45.

Yu, B. (1994). Cellular defenses against damage from reactive oxygen species. Physiol Rev *74*, 139-162.

Zhang, S., Sokolchik, I., Blanco, G., and Sze, J. Y. (2004). Caenorhabditis elegans TRPV ion channel regulates 5HT biosynthesis in chemosensory neurons. Development *131*, 1629-1638.

Zhang, Y., Lu, H., and Bargmann, C. I. (2005). Pathogenic bacteria induce aversive olfactory learning in Caenorhabditis elegans. Nature *438*, 179-184.

Table 2-1. Distributions of different genotypes and conditions in aerotaxis assays in a 0-21% oxygen gradient.

Bins are equally spaced along the gradient as depicted in Figure 1A. Values are the fractions of animals in each bin. n, number of assays. Each assay represents 80-100 animals.

Genotype	Food	n	1	2	3	4	5	6	7	8	9
N2	off	28	0.039	0.057	0.094	0.163	0.280	0.214	0.104	0.039	0.011
gcy-32	off	3	0.043	0.060	0.139	0.164	0.203	0.231	0.119	0.032	0.010
gcy-34	off	4	0.034	0.078	0.201	0.230	0.232	0.134	0.068	0.021	0.002
gcy-35	off	9	0.062	0.117	0.156	0.140	0.176	0.147	0.112	0.070	0.019
gcy-36	off	6	0.103	0.150	0.199	0.172	0.189	0.124	0.045	0.014	0.004
osm-9	off	7	0.122	0.113	0.161	0.142	0.160	0.130	0.102	0.056	0.015
ocr-2	off	3	0.046	0.149	0.217	0.268	0.175	0.096	0.045	0.004	0.000
qaIs2241	off	8	0.028	0.056	0.091	0.132	0.133	0.267	0.224	0.056	0.013
gcy-35; qaIs2241	off	4	0.088	0.104	0.139	0.104	0.151	0.180	0.161	0.057	0.016
osm-9; qaIs2241	off	4	0.086	0.113	0.126	0.165	0.141	0.177	0.119	0.047	0.026
ocr-2; qaIs2241	off	4	0.119	0.094	0.109	0.110	0.134	0.150	0.176	0.072	0.037
tph-1; qaIs2241	off	3	0.085	0.129	0.120	0.151	0.152	0.158	0.159	0.024	0.021
npr-1	off	4	0.013	0.037	0.086	0.236	0.287	0.210	0.082	0.031	0.018
npr-1 qaIs2241	off	3	0.027	0.053	0.102	0.113	0.182	0.202	0.208	0.089	0.023
gcy-35; npr-1	off	3	0.068	0.097	0.122	0.208	0.173	0.168	0.089	0.055	0.020
osm-9; npr-1	off	3	0.087	0.114	0.184	0.156	0.195	0.148	0.083	0.022	0.012
ocr-2; npr-1	off	3	0.020	0.084	0.181	0.244	0.259	0.128	0.059	0.022	0.002
tph-1; npr-1	off	4	0.029	0.054	0.118	0.196	0.259	0.169	0.132	0.033	0.010
daf-3 npr-1	off	3	0.039	0.053	0.082	0.168	0.242	0.188	0.139	0.058	0.030
daf-7	off	4	0.015	0.041	0.105	0.186	0.296	0.197	0.121	0.035	0.005
daf-3	off	3	0.068	0.069	0.117	0.148	0.221	0.174	0.119	0.059	0.025
daf-7; daf-3	off	4	0.036	0.047	0.123	0.180	0.221	0.172	0.140	0.059	0.021
tax-4; kyIs342	off	4	0.054	0.111	0.105	0.153	0.188	0.188	0.120	0.049	0.031
ADF::tph-1	off	4	0.044	0.066	0.065	0.151	0.263	0.254	0.117	0.030	0.010
tph-1	off	11	0.075	0.109	0.123	0.129	0.204	0.197	0.117	0.037	0.009
tph-1; daf-3	off	3	0.065	0.088	0.125	0.167	0.213	0.175	0.099	0.048	0.020
gcy-35; SDQ::gcy-35	off	3	0.051	0.087	0.109	0.202	0.244	0.195	0.069	0.038	0.006
osm-9; ASH::osm-9	off	3	0.036	0.094	0.152	0.172	0.265	0.197	0.081	0.004	0.000
osm-9; ADF::osm-9	off	6	0.078	0.093	0.108	0.137	0.200	0.257	0.103	0.023	0.002
tph-1; ADF::tph-1	off	5	0.031	0.066	0.114	0.145	0.183	0.244	0.141	0.064	0.010
tph-1; NSM::tph-1	off	3	0.046	0.145	0.123	0.119	0.101	0.217	0.194	0.049	0.006
N2	on	10	0.152	0.109	0.119	0.152	0.154	0.120	0.088	0.071	0.035
gcy-35	on	3	0.254	0.109	0.089	0.120	0.172	0.116	0.070	0.044	0.026
gcy-36	on	3	0.204	0.096	0.128	0.128	0.183	0.087	0.087	0.063	0.025
osm-9	on	3	0.203	0.097	0.122	0.183	0.159	0.112	0.071	0.049	0.005
ocr-2	on	3	0.162	0.093	0.112	0.135	0.177	0.150	0.100	0.050	0.021
qaIs2241	on	4	0.159	0.108	0.089	0.108	0.099	0.137	0.161	0.095	0.043
npr-1	on	7	0.047	0.031	0.070	0.109	0.253	0.227	0.127	0.091	0.046
npr-1 qaIs2241	on	3	0.179	0.074	0.092	0.096	0.120	0.158	0.125	0.091	0.065
gcy-35; npr-1	on	4	0.181	0.099	0.116	0.131	0.151	0.127	0.101	0.077	0.017
osm-9; npr-1	on	3	0.142	0.089	0.140	0.134	0.189	0.122	0.092	0.064	0.028
ocr-2; npr-1	on	3	0.107	0.088	0.133	0.157	0.224	0.144	0.090	0.038	0.020
tph-1; npr-1	on	3	0.045	0.061	0.114	0.167	0.155	0.218	0.161	0.059	0.020
daf-3 npr-1	on	3	0.035	0.047	0.066	0.130	0.170	0.239	0.173	0.076	0.064
daf-7	on	6	0.038	0.058	0.086	0.139	0.188	0.212	0.147	0.084	0.048
daf-3	on	3	0.150	0.064	0.080	0.099	0.165	0.141	0.136	0.091	0.073
daf-7; daf-3	on	3	0.183	0.093	0.090	0.100	0.132	0.139	0.125	0.091	0.048
tax-4; kyIs342	on	3	0.052	0.085	0.109	0.117	0.155	0.212	0.195	0.048	0.025
tph-1	on	5	0.075	0.120	0.103	0.173	0.147	0.179	0.125	0.057	0.023
tph-1; daf-3	on	3	0.048	0.069	0.103	0.131	0.205	0.192	0.152	0.078	0.021
tph-1; ADF::tph-1	on	5	0.060	0.089	0.083	0.158	0.192	0.178	0.144	0.068	0.029
ADF::tph-1	on	5	0.078	0.073	0.095	0.123	0.175	0.198	0.127	0.092	0.040

Table 2-2 (p. 1). Chi-square comparisons from this study.

n, total number of animals tested for a given genotype and condition.

Group 1			Group 2			Chi-Square
Genotype	Food	n	Genotype	Food	n	
N2	off	2774	*qcy-36*	off	553	191 **
N2	off	2774	*qcy-35*	off	823	117 **
N2	off	2774	*qcy-34*	off	384	53 **
N2	off	2774	*qcy-32*	off	306	13
N2	off	2774	*qaIs2241*	off	801	121 **
N2	off	2774	*osm-9*	off	601	158 **
N2	off	2774	*ocr-2*	off	203	82 **
N2	off	2774	*tph-1*	off	1076	79 **
N2	off	2774	*npr-1*	off	414	20
N2	off	2774	*daf-7*	off	403	13
N2	off	2774	*daf-3*	off	289	18
N2	off	2774	*tax-4; kyIs342*	off	396	42 **
N2	off	2774	*ADF::tph-1*	off	422	8
qcy-35; qaIs2241	off	427	*qaIs2241*	off	801	44 **
qcy-35; qaIs2241	off	427	*qcy-35*	off	823	18
osm-9; qaIs2241	off	429	*qaIs2241*	off	801	76 **
osm-9; qaIs2241	off	429	*osm-9*	off	601	7
ocr-2; qaIs2241	off	378	*qaIs2241*	off	801	64 **
ocr-2; qaIs2241	off	378	*ocr-2*	off	203	76 **
tph-1; qaIs2241	off	282	*qaIs2241*	off	801	50 **
tph-1; qaIs2241	off	282	*tph-1*	off	1076	13
npr-1 qaIs2241	off	318	*npr-1*	off	414	51 **
npr-1 qaIs2241	off	318	*qaIs2241*	off	801	10
qcy-35; npr-1	off	311	*npr-1*	off	414	42 **
qcy-35; npr-1	off	311	*qcy-35*	off	823	12
osm-9; npr-1	off	364	*npr-1*	off	414	69 **
osm-9; npr-1	off	364	*osm-9*	off	601	16
ocr-2; npr-1	off	404	*npr-1*	off	414	39 **
ocr-2; npr-1	off	404	*ocr-2*	off	203	13
tph-1; npr-1	off	406	*npr-1*	off	414	13
tph-1; npr-1	off	406	*tph-1*	off	1076	34 **
daf-3 npr-1	off	274	*npr-1*	off	414	5
daf-3 npr-1	off	274	*daf-3*	off	289	19
daf-7; daf-3	off	388	*daf-7*	off	403	16
daf-7; daf-3	off	388	*daf-3*	off	289	6
tph-1; daf-3	off	303	*tph-1*	off	1076	8
tph-1; daf-3	off	303	*daf-3*	off	289	2
qcy-35; SDQ::gcy-35	off	325	*qcy-35*	off	823	31 **
qcy-35; SDQ::gcy-35	off	325	N2	off	2774	16
osm-9; ASH::osm-9	off	269	*osm-9*	off	601	52 **
osm-9; ASH::osm-9	off	269	N2	off	2774	28 **
osm-9; ADF::osm-9	off	532	*osm-9*	off	601	50 **
osm-9; ADF::osm-9	off	532	N2	off	2774	50 **
tph-1; ADF::tph-1	off	500	*tph-1*	off	1076	30 **
tph-1; ADF::tph-1	off	500	N2	off	2774	32 **
tph-1; NSM::tph-1	off	308	*tph-1*	off	1076	32 **
tph-1; NSM::tph-1	off	308	N2	off	2774	92 **

* $P < 0.01$
** $P < 0.001$

Table 2-2 (p. 2). Chi-square comparisons from this study.

n, total number of animals tested for a given genotype and condition.

Group 1			Group 2			Chi-Square
Genotype	Food	n	Genotype	Food	n	
N2	off	2774	N2	on	848	248 **
qcy-35	off	823	*qcy-35*	on	240	81 **
qaIs2241	off	801	*qaIs2241*	on	346	103 **
osm-9	off	601	*osm-9*	on	249	19
ocr-2	off	203	*ocr-2*	on	254	49 **
npr-1	off	414	*npr-1*	on	627	44 **
npr-1 qaIs2241	off	318	*npr-1 qaIs2241*	on	243	49 **
qcy-35; npr-1	off	311	*qcy-35; npr-1*	on	294	26 **
osm-9; npr-1	off	364	*osm-9; npr-1*	on	337	19
ocr-2; npr-1	off	404	*ocr-2; npr-1*	on	308	41 **
tph-1; npr-1	off	406	*tph-1; npr-1*	on	312	19
daf-3 npr-1	off	274	*daf-3 npr-1*	on	281	13
daf-7	off	403	*daf-7*	on	589	47 **
daf-3	off	289	*daf-3*	on	197	22 *
daf-7; daf-3	off	388	*daf-7; daf-3*	on	233	58 **
tax-4; kyIs342	off	396	*tax-4; kyIs342*	on	311	12
tph-1	off	1076	*tph-1*	on	436	23 *
tph-1; daf-3	off	303	*tph-1; daf-3*	on	287	9
tph-1; ADF::tph-1	off	500	*tph-1; ADF::tph-1*	on	488	18
ADF::tph-1	off	422	*ADF::tph-1*	on	458	37 **
N2	on	848	*qaIs2241*	on	346	19
N2	on	848	*qcy-35*	on	240	19
N2	on	848	*osm-9*	on	249	15
N2	on	848	*ocr-2*	on	254	6
N2	on	848	*npr-1*	on	627	114 **
N2	on	848	*daf-7*	on	589	82 **
N2	on	848	*daf-3*	on	197	18
N2	on	848	*tax-4; kyIs342*	on	311	56 **
N2	on	848	*tph-1*	on	436	27 **
N2	on	848	*tph-1; daf-3*	on	287	40 **
N2	on	848	*tph-1; ADF::tph-1*	on	488	43 **
N2	on	848	*ADF::tph-1*	on	458	35 **
npr-1 qaIs2241	on	243	*npr-1*	on	627	61 **
npr-1 qaIs2241	on	243	*qaIs2241*	on	346	6
qcy-35; npr-1	on	294	*npr-1*	on	627	86 **
qcy-35; npr-1	on	294	*qcy-35*	on	240	8
osm-9; npr-1	on	337	*npr-1*	on	627	63 **
osm-9; npr-1	on	337	*osm-9*	on	249	15
ocr-2; npr-1	on	308	*npr-1*	on	627	53 **
ocr-2; npr-1	on	308	*ocr-2*	on	254	8
tph-1; npr-1	on	312	*npr-1*	on	627	34 **
tph-1; npr-1	on	312	*tph-1*	on	436	13
daf-3 npr-1	on	281	*npr-1*	on	627	18
daf-3 npr-1	on	281	*daf-3*	on	197	28 **
daf-7; daf-3	on	233	*daf-7*	on	589	54 **
daf-7; daf-3	on	233	*daf-3*	on	197	3
tph-1; daf-3	on	287	*tph-1*	on	436	14
tph-1; daf-3	on	287	*daf-3*	on	197	25 *

* $P < 0.01$
** $P < 0.001$

Table 2-3. Hyperoxia avoidance and aggregation behavior

Genotype	Hyperoxia Avoidance (off food)[1]	Hyperoxia Avoidance (on food)[1]	Aggregation (on food)
N2[2]	++	-	-
npr-1[2]	++	++	++
gcy-35; npr-1[3]	+	-	-
npr-1 qaIs2241	+	-	-
osm-9; npr-1[4]	-	-	-
ocr-2; npr-1[4]	+	-	-
daf-3 npr-1[4]	++	++	++
tph-1; npr-1	++	+	+
daf-7[5]	++	++	++
daf-7; daf-3[5]	++	-	-
tph-1	+	+	-
tph-1; daf-3	+	+	-
tph-1; ADF::tph-1	++	+	-
ADF::tph-1	++	+	-

[1] Hyperoxia avoidance index. ++, >0.45; +, 0.25-0.45; -, <0.25
[2] Aggregation reported in de Bono and Bargmann, 1998.
[3] Aggregation reported in Cheung et al., 2004.
[4] Aggregation reported in de Bono et al., 2002.
[5] Aggregation reported in Thomas et al., 1993.
All other results are from this study.

Figure 2-1. Two distinct groups of sGC-expressing neurons promote hyperoxia avoidance.

(A) A cartoon of the typical distribution of 100 wild-type N2 animals (red dots) in a 0-21% oxygen gradient. Adult animals are placed on an agar surface under a 3-cm x 1.5-cm PDMS chamber; laminar flow of gases at either end of the chamber generates an oxygen gradient within the chamber. The positions of animals are scored after 25 minutes. For counting, animals are binned in nine equally spaced regions along the device.

(B) In a 0-21% oxygen gradient, wild-type N2 animals avoid both hyperoxia (14-21% O_2) and hypoxia (0-7% O_2), preferring the center of the gradient (7-14% O_2) (n = 28 assays, 80-100 animals/assay).

(C) Neurons (top row) and genes that appear in this study. *npr-1* is expressed in SDQ and ASH, but not known to affect their function (de Bono and Bargmann, 1998).

(D, E) Aerotaxis of *gcy-35* and *gcy-36* mutants (D) and *gcy-32* and *gcy-34* mutants (E).

(F) Aerotaxis of *qaIs2241* animals, which bear a transgene that kills the URX, AQR, and PQR neurons.

(G) Aerotaxis of *gcy-35; qaIs2241* mutants.

(H) Aerotaxis of *gcy-35* mutants in which SDQ, ALN, and PLN were rescued with a *lad-2::gcy-35* transgene.

In D-H, asterisks denote distributions different by Chi-square analysis at $p < 0.01$ from the first distribution in the panel, unless otherwise noted. $n \geq 3$ assays per genotype, 80-100 animals/assay. Error bars are standard error of the mean (SEM). Aerotaxis assays in all figures follow a standard color code: red and blue colors are used for mutants, green

is used for transgenic rescue strains, and gray is used for results repeated from an earlier figure.

(I) The hyperoxia avoidance index is defined as [(fraction of animals in 7-14% O_2) - (fraction of animals in 14-21% O_2)] / (fraction of animals in 7-21% O_2).

In I, asterisks denote values different from N2 controls at $p < 0.01$ by Dunnett test.

Cross, value different from the *gcy-35* control at $p < 0.05$ by Bonferroni t test with N2 and *gcy-35* controls. Error bars denote SEM.

(J) Hyperoxia avoidance is promoted by two sets of sGC-expressing neurons: (1) some or all of URX, PQR, and PQR and (2) some or all of SDQ, ALN, and PLN.

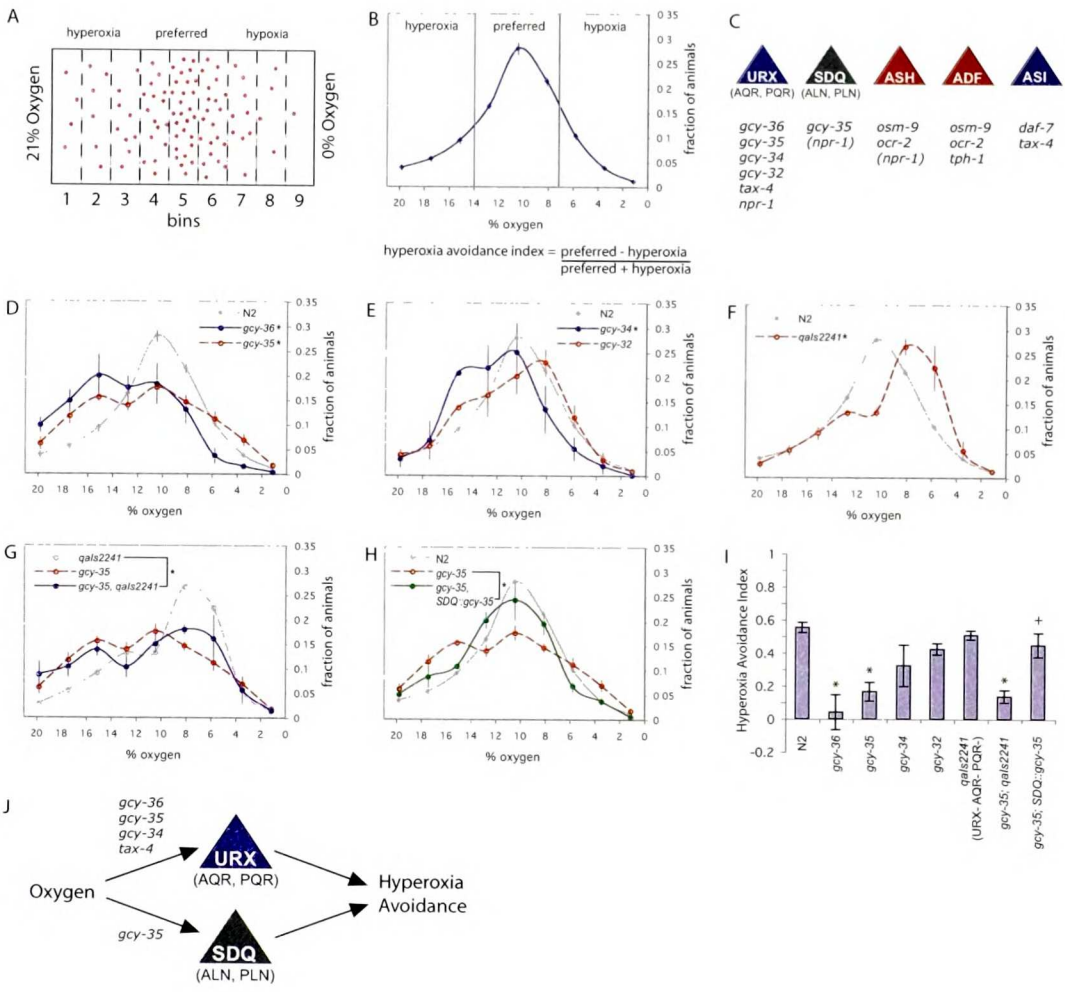

Figure 2-2. Multiple TRPV-expressing neurons contribute to hyperoxia avoidance.

(A) Aerotaxis of *TRPV* single mutants. The median preferred oxygen concentration of *ocr-2* mutants was significantly higher than N2 ($p < 0.05$ by Dunnett test).

(B) Aerotaxis of *osm-9* mutants in which ASH, PHA, and PHB were rescued with an *osm-10::osm-9* transgene (Zhang et al., 2004). Animals rescued for ASH function were preselected for avoidance of high osmolarity, an ASH behavior (see Methods).

(C) Aerotaxis of *osm-9* mutants in which ADF was rescued by expression from a *cat-1::osm-9* transgene (Zhang et al., 2004).

(D) Aerotaxis of *tph-1* mutants.

(E) Aerotaxis of *tph-1* mutants rescued in ADF neurons using a *srh-142::tph-1::gfp* transgene (Zhang et al., 2005).

(F) Aerotaxis of *tph-1* mutants rescued in NSM neurons using a *ceh-2::tph-1::gfp* transgene (Zhang et al., 2005).

(G) Aerotaxis of *TRPV; qaIs2241* double mutants.

(H) Aerotaxis of *tph-1; qaIs2241* double mutants.

For A-H, asterisks denote distributions different by Chi-square analysis at $p < 0.01$ from the first distribution in the panel, unless otherwise noted. $n \geq 3$ assays per genotype, 80-100 animals/assay. Error bars denote SEM.

(I) Hyperoxia avoidance index as defined in Figure 2-1. Asterisks, values different from N2 controls at $p < 0.01$ by Dunnett test. Single crosses, values different from the *osm-9* or *tph-1* control at $p < 0.05$ by Bonferroni *t* test with N2 and mutant controls. Double crosses, values different from *qaIs2241* controls at $p < 0.01$ by Dunnett test. NS, not significant. Error bars denote SEM.

(J) ASH and ADF sensory neurons promote hyperoxia avoidance through the activity of TRPV channels *osm-9* and *ocr-2*. Serotonin production in ADF by *tph-1*, which is regulated by TRPV channels, also drives this behavior.

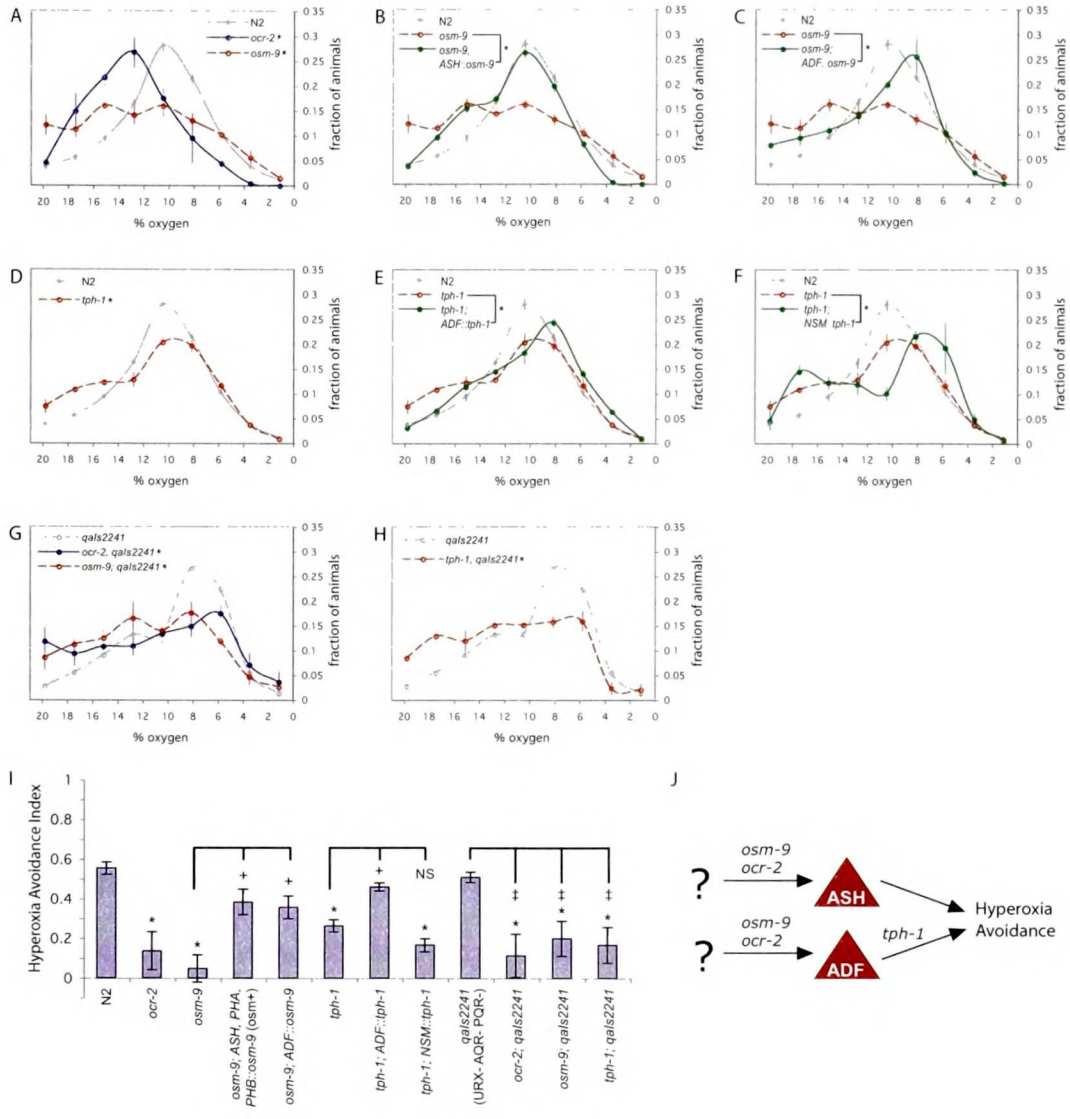
A
N2
ocr-2*
osm-9*
B
N2
osm-9
osm-9; ASH::osm-9
C
N2
osm-9
osm-9; ADF::osm-9
D
N2
tph-1*
E
N2
tph-1
tph-1; ADF::tph-1
F
N2
tph-1
tph-1; NSM::tph-1
G
qals2241
ocr-2; qals2241*
osm-9; qals2241*
H
qals2241
tph-1; qals2241*
fraction of animals
% oxygen
I
Hyperoxia Avoidance Index
N2
ocr-2
osm-9
osm-9; ASH, PHA, PHB::osm-9 (osm+)
osm-9; ADF::osm-9
tph-1
tph-1; ADF::tph-1
tph-1; NSM::tph-1
qals2241 (URX-, AQR-, PQR-)
ocr-2; qals2241
osm-9; qals2241
tph-1; qals2241
NS
J
osm-9
ocr-2
ASH
osm-9
ocr-2
ADF
tph-1
Hyperoxia Avoidance

Figure 2-3. Hyperoxia avoidance of *npr-1* mutants requires sGC and TRPV activity, but not serotonin.

(A) Aerotaxis of *npr-1* mutants.

(B) Aerotaxis of *npr-1; qaIs2241* strain.

(C) Aerotaxis of *gcy-35; npr-1* double mutants.

(D) Aerotaxis of *osm-9; npr-1* double mutants.

(E) Aerotaxis of *ocr-2; npr-1* double mutants.

(F) Aerotaxis of *tph-1; npr-1* double mutants.

For A-F, asterisks denote distributions different by Chi-square analysis at $p < 0.01$ from the first distribution in the panel. $n \geq 3$ assays per genotype, 80-100 animals/assay. Error bars denote SEM. For B-E, all double mutants are significantly different from *npr-1* controls, but not significantly different from animals carrying the other mutation ($p < 0.01$ by Chi-square analysis of the complete distribution).

(G) Hyperoxia avoidance index as defined in Figure 2-1. Asterisks and double asterisks, values different from *npr-1* controls at $p < 0.05$ and $p < 0.01$, respectively, by Dunnett test. Error bars denote SEM.

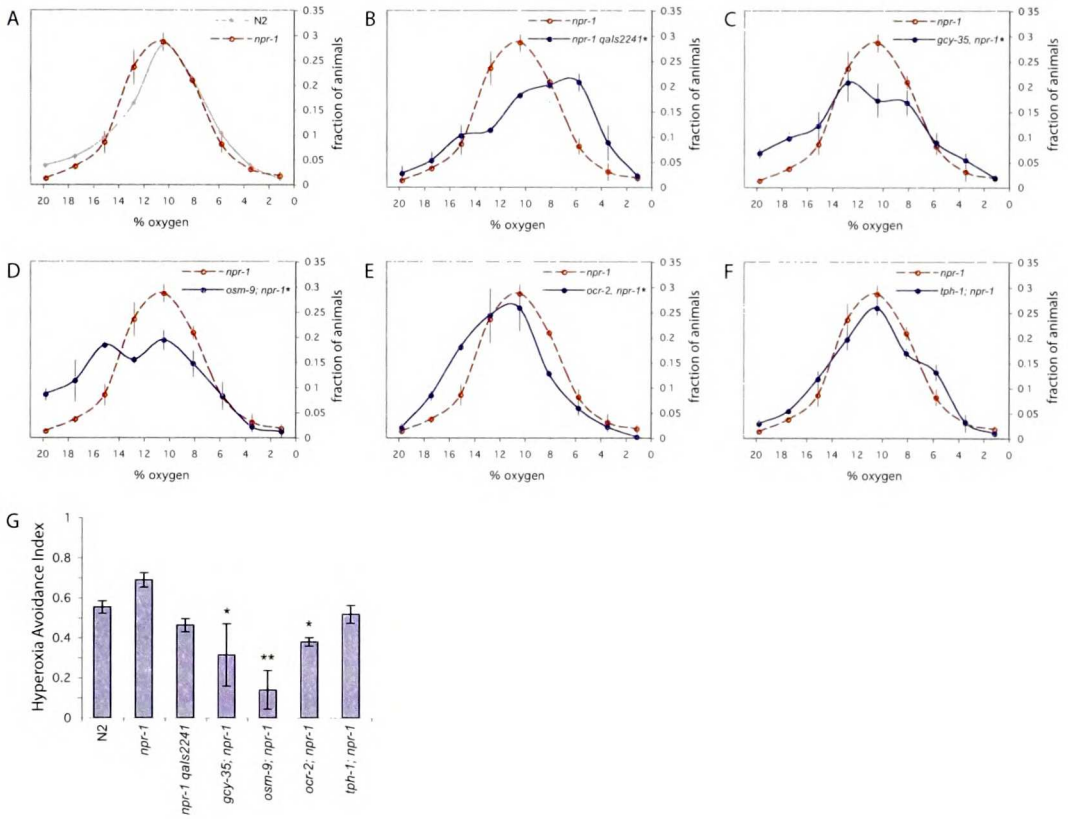
A
N2
npr-1
B
npr-1
npr-1 qals2241*
C
npr-1
gcy-35; npr-1*
D
npr-1
osm-9; npr-1*
E
npr-1
ocr-2; npr-1*
F
npr-1
tph-1; npr-1
fraction of animals
% oxygen
G
Hyperoxia Avoidance Index
N2
npr-1
npr-1 qals2241
gcy-35; npr-1
osm-9; npr-1
ocr-2; npr-1
tph-1; npr-1

Figure 2-4. sGC and *ocr-2* TRPV mutations restore food regulation of hyperoxia avoidance to *npr-1*.

(A-J) In all panels, dotted lines indicate aerotaxis in the presence of a small amount of bacterial food.

(A) Aerotaxis of wild-type N2 animals.

(B) Aerotaxis of *npr-1* mutants.

(C) Aerotaxis of *qaIs2241* strain (URX, AQR, PQR killed).

(D) Aerotaxis of *npr-1 qaIs2241* strain.

(E) Aerotaxis of *gcy-35* mutants.

(F) Aerotaxis of *gcy-35; npr-1* double mutants.

(G) Aerotaxis of *osm-9* mutants.

(H) Aerotaxis of *osm-9; npr-1* double mutants.

(I) Aerotaxis of *ocr-2* mutants.

(J) Aerotaxis of *ocr-2; npr-1* double mutants.

For A-J, asterisks denote distributions different by Chi-square analysis at $p < 0.01$ from the same genotype without food. $n \geq 3$ assays per genotype and condition, 80-100 animals/assay. Error bars denote SEM.

(K) Hyperoxia avoidance index as defined in Figure 2-1. Asterisks denote values significantly different from the same genotype without food at $p < 0.05$ by t test. Error bars denote SEM. Double crosses indicate that *ocr-2* mutants are significantly regulated by food using Chi-square analysis of the entire distribution ($p < 0.01$), and that *ocr-2; npr-1* on food is significantly different from *ocr-2; npr-1* off food and *npr-1* on food ($p < 0.01$ by Chi-square analysis) and not significantly different from *ocr-2* mutants on food.

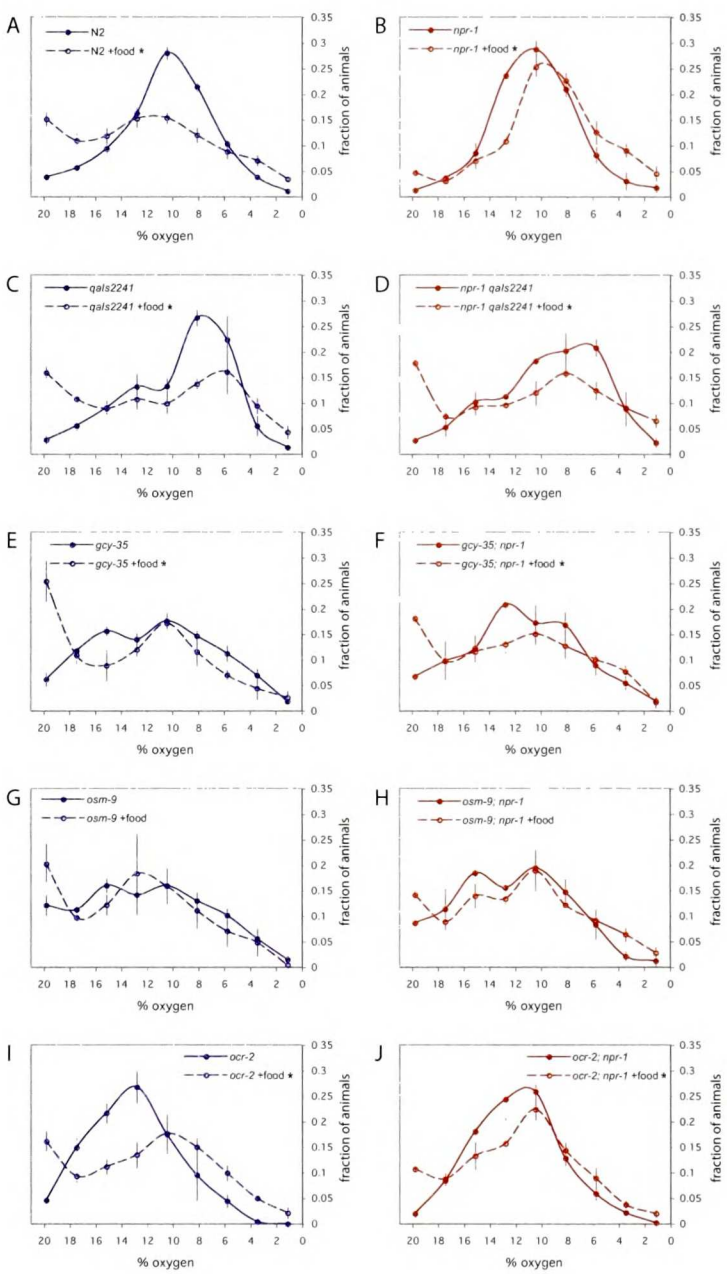
A
N2
N2 +food *
B
npr-1
npr-1 +food *
C
qals2241
qals2241 +food *
D
npr-1 qals2241
npr-1 qals2241 +food *
E
gcy-35
gcy-35 +food *
F
gcy-35; npr-1
gcy-35; npr-1 +food *
G
osm-9
osm-9 +food
H
osm-9; npr-1
osm-9; npr-1 +food
I
ocr-2
ocr-2 +food *
J
ocr-2; npr-1
ocr-2; npr-1 +food *
fraction of animals
% oxygen
K
Hyperoxia Avoidance Index
off food
on food
N2
npr-1
qals2241
npr-1 qals2241
gcy-35
gcy-35; npr-1
osm-9
osm-9; npr-1
ocr-2
ocr-2; npr-1

Figure 2-5. Levels of serotonin in ADF neurons affect food regulation of hyperoxia avoidance.

(A-E) In all panels, dotted lines indicate aerotaxis in the presence of a small amount of bacterial food.

(A) Aerotaxis of wild-type N2 animals.

(B) Aerotaxis of *tph-1* mutants.

(C) Aerotaxis of *tph-1; npr-1* double mutants.

(D) Aerotaxis of *tph-1* animals rescued in ADF with a *srh-142::tph-1::gfp* transgene (Zhang et al., 2005).

(E) Aerotaxis of wild-type animals expressing *tph-1* in ADF from a *srh-142::tph-1::gfp* transgene.

For A-E, asterisks denote distributions different by Chi-square analysis at $p < 0.01$ from the same genotype without food. $n \geq 3$ assays per genotype and condition, 80-100 animals/assay. Error bars denote SEM.

(F) Hyperoxia avoidance index as defined in Figure 2-1. Asterisks, values significantly different from the same genotype without food at $p < 0.05$ by t test. Crosses, values significantly different from N2 on food at $p < 0.01$ by Dunnett test. NS, not significant. Error bars denote SEM.

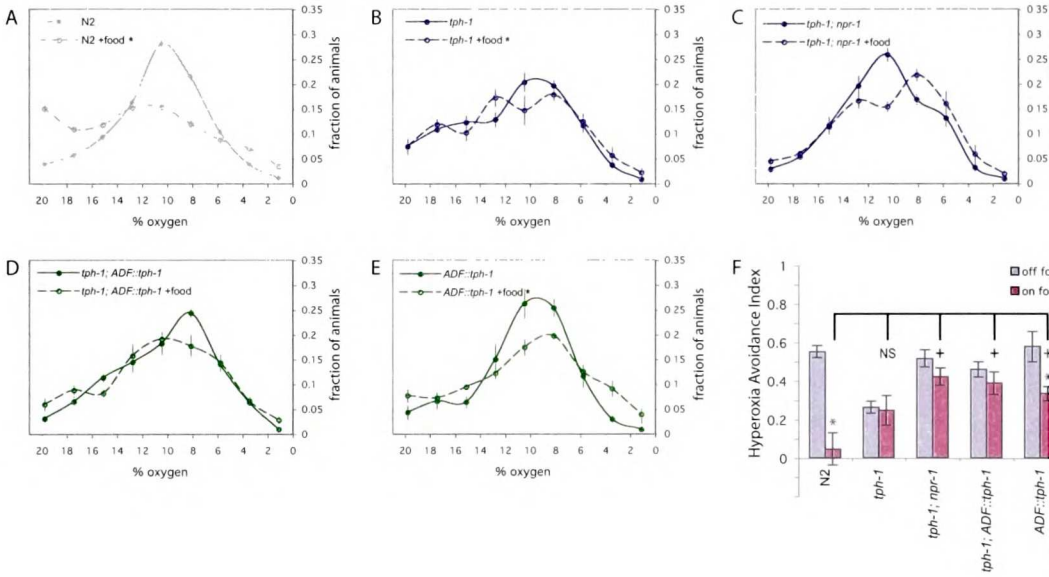
A
N2
N2 +food *
fraction of animals
% oxygen
B
tph-1
tph-1 +food *
C
tph-1; npr-1
tph-1; npr-1 +food
D
tph-1; ADF::tph-1
tph-1; ADF::tph-1 +food
E
ADF::tph-1
ADF::tph-1 +food *
F
Hyperoxia Avoidance Index
off fo
on fo
NS
+
N2
tph-1
tph-1; npr-1
tph-1; ADF::tph-1
ADF::tph-1

Figure 2-6. TGF-ß signaling mediates food suppression of hyperoxia avoidance.

(A-E, H, I) In all panels, dotted lines indicate aerotaxis in the presence of a small amount of bacterial food.

(A) Aerotaxis of wild-type N2 animals.

(B) Aerotaxis of *daf-7* mutants.

(C) Aerotaxis of *daf-3* mutants.

(D) Aerotaxis of *daf-7; daf-3* double mutants.

(E) Aerotaxis of *daf-3 npr-1* double mutants.

(F, G) *daf-7::GFP* expression in ASI was reduced in a *tax-4* mutant. Anterior is to the left.

(H) Aerotaxis of *tax-4; kyIs342* animals, which bear a transgene that rescues *tax-4* in URX, AQR, and PQR, but not in ASI or other neurons.

(I) Aerotaxis of *tph-1; daf-3* double mutants.

For A-E, H, and I, asterisks denote distributions different by Chi-square analysis at $p < 0.01$ from the same genotype without food. $n \geq 3$ assays per genotype and condition, 80-100 animals/assay. Error bars denote SEM.

(J) Hyperoxia avoidance index as defined in Figure 2-1. Asterisks, values significantly different from the same genotype without food at $p < 0.05$ by t test. In the absence of food, no strain is different from N2 controls by Dunnett test. In the presence of food, *daf-7*, *daf-3 npr-1*, and *tph-1; daf-3* are different from N2 at $p < 0.01$ and *tax-4; kyIs342* different from N2 at $p < 0.05$ by Dunnett test. Error bars denote SEM.

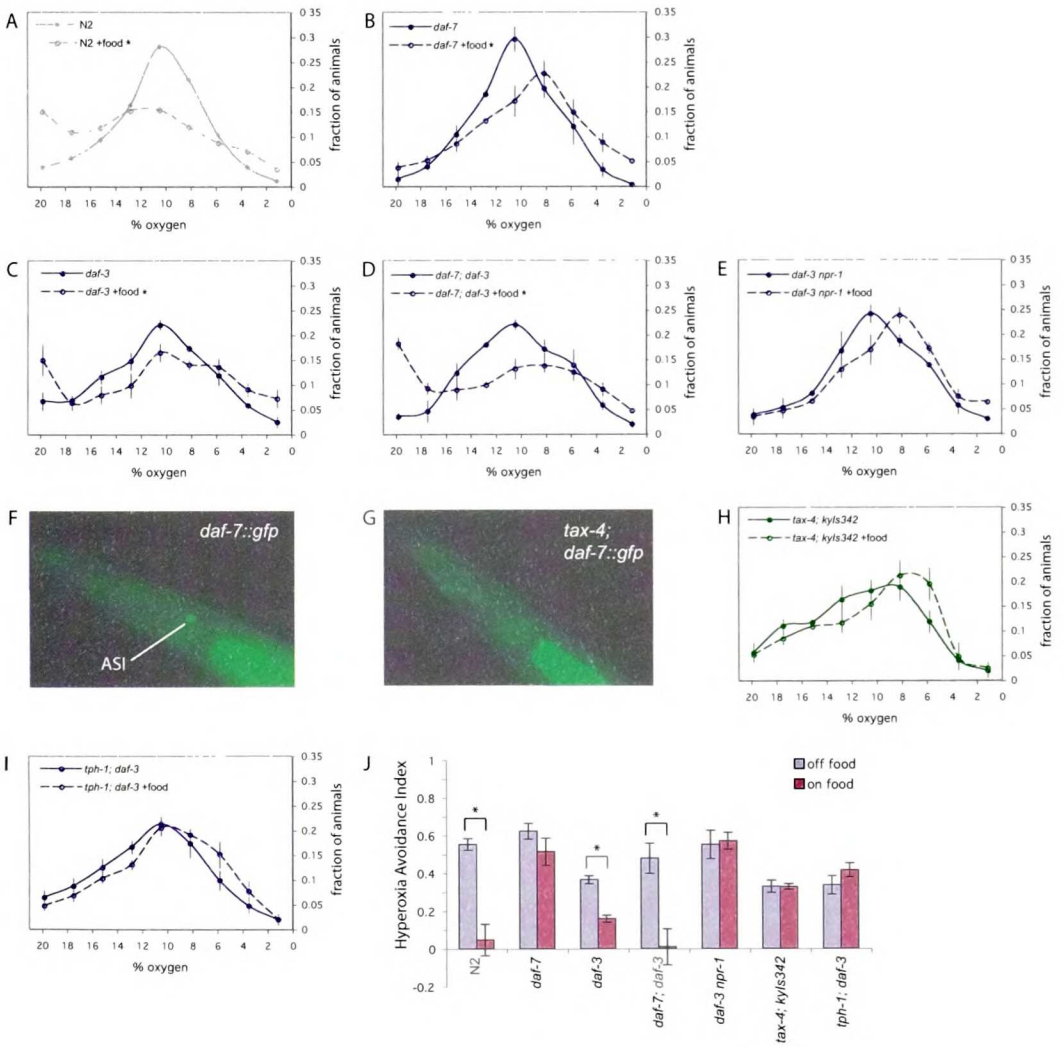
A
N2
N2 +food *
B
daf-7
daf-7 +food *
C
daf-3
daf-3 +food *
D
daf-7; daf-3
daf-7; daf-3 +food *
E
daf-3 npr-1
daf-3 npr-1 +food
F
daf-7::gfp
ASI
G
tax-4;
daf-7::gfp
H
tax-4; kyIs342
tax-4; kyIs342 +food
I
tph-1; daf-3
tph-1; daf-3 +food
J
off food
on food
Hyperoxia Avoidance Index
N2
daf-7
daf-3
daf-7; daf-3
daf-3 npr-1
tax-4; kyIs342
tph-1; daf-3
fraction of animals
% oxygen

Figure 2-7. Serotonin production in ADF neurons is regulated by TGF-ß signaling.

(A, B) *tph-1::GFP* expression in wild-type (A) and *daf-7* (B) adults. Anterior is to the left. Two NSM neurons and two ADF neurons are visible in each animal.

(C) Quantitation of *tph-1::GFP* fluorescence in ADF neurons. Asterisks, values different from N2 controls at $p < 0.01$ by Dunnett test. *daf-7* mutants were different from N2, *daf-3*, and *daf-7; daf-3* at $p < 0.05$ by Bonferroni t test. $n \geq 18$ animals per genotype. Error bars denote SEM.

(D) Model for food regulation of aerotaxis, combining genetic results from Figure 2-6 with molecular results from this Figure.

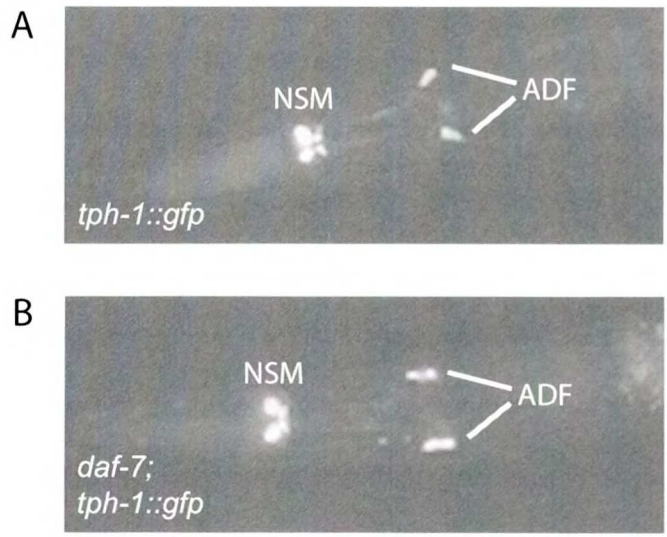
A
NSM
ADF
tph-1::gfp
B
NSM
ADF
daf-7;
tph-1::gfp
C
ADF tph-1::GFP Fluorescence (AU)
3000
2500
2000
1500
1000
500
0
*
*
N2
tax-4
daf-7
daf-3
daf-7;
daf-3
npr-1
D
Food
tax-4
daf-7
daf-3
tph-1
osm-9
ocr-2

Figure 2-8. A distributed network of oxygen-sensing neurons.

(A) Aerotaxis-promoting neurons. In the absence of food, parallel networks of sensory neurons generate hyperoxia avoidance. Triangles denote sensory neurons; hexagons denote interneurons. URX, AQR, and PQR, and SDQ, ALN, and BDU neurons (abbreviated as "SDQ" for simplicity) express sGCs; these neurons are likely oxygen sensors. ASH and ADF neurons express the TRPV channels *osm-9* and *ocr-2;* they might be modulatory neurons, or might respond to oxygen directly. ADF promotes aerotaxis by producing serotonin. Our genetic results suggest that robust aerotaxis requires at least one class of sGC neuron and at least one class of TRPV neuron. Synaptic connections to the AUA interneurons and AVA backward command neurons are shown; additional synapses are omitted (White et al., 1986).

(B) Aerotaxis-suppressing pathways. In the presence of food, the aerotaxis neurons are inhibited by the TGF-ß homolog DAF-7 and the neuropeptide receptor NPR-1. Food and *tax-4* activity in ASI neurons stimulate the synthesis of DAF-7, which acts through DAF-3 to inhibit serotonin production in ADF and suppress aerotaxis. Increased or unregulated serotonin expression in ADF allows aerotaxis in the presence of food. Food inhibition may involve additional food-sensing pathways in ADF (perhaps via *osm-9* and *ocr-2*) or serotonin signaling from other food-sensing neurons (such as NSM). NPR-1 is expressed in URX, AQR, PQR, ASH, SDQ, and AUA neurons (Coates and de Bono, 2002) and could inhibit their function in a food-dependent or food-independent fashion. Many of the signaling pathways and neurons described here have the potential to regulate each others' activity. *tph-1* mutants have decreased *daf-7* expression (Sze et al., 2000), and *daf-7* affects gene expression in the ASH neurons (Nolan et al., 2002). A food-

related change in serotonin levels affects nociceptive signaling in ASH (Chao et al., 2004). The NPR-1 ligand FLP-21 is expressed by ASH and ADL (Rogers et al., 2003). The regulatory relationships in Figure 2-8B are supported by the genetics, molecular biology, and behavioral assays in this paper, but these relationships could be reconfigured under different conditions.

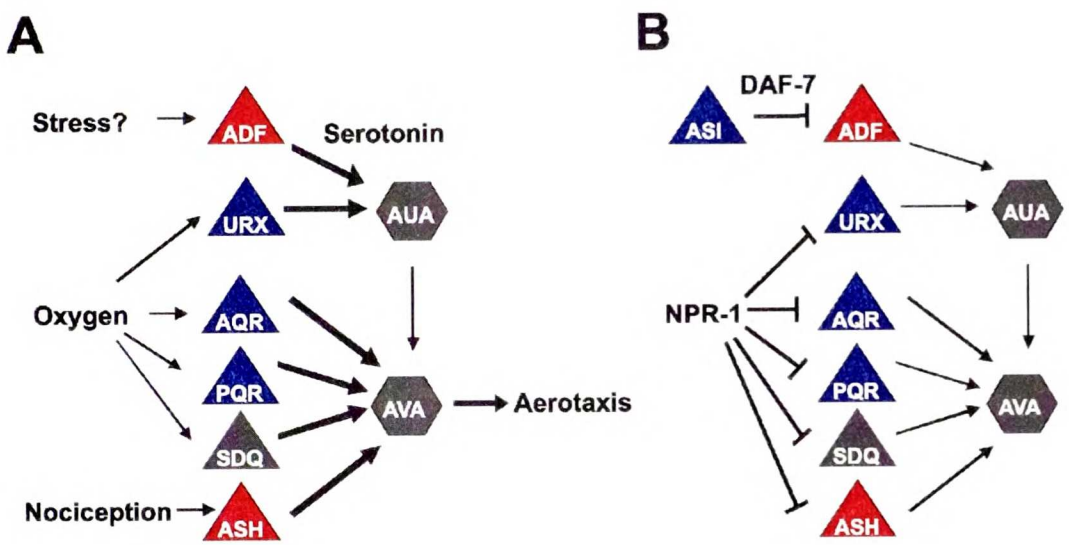
A
Stress?
ADF
Serotonin
URX
AUA
Oxygen
AQR
PQR
SDQ
AVA
Aerotaxis
Nociception
ASH
B
DAF-7
ASI
ADF
URX
AUA
NPR-1
AQR
PQR
SDQ
AVA
ASH

Figure 2-9. Second and third principal components of aerotaxis data (PC2, PC3).

(A) Assays with the highest (blue) and lowest (red) values for the second principal component (PC2), out of 36 sets of assays examined. Wild-type N2 animals off food are included for comparison (black, thick lines).

(B) Assays with the highest (blue) and lowest (red) values for the third principal component (PC3), out of 36 sets of assays examined. Wild-type N2 animals off food are included for comparison (black, thick lines).

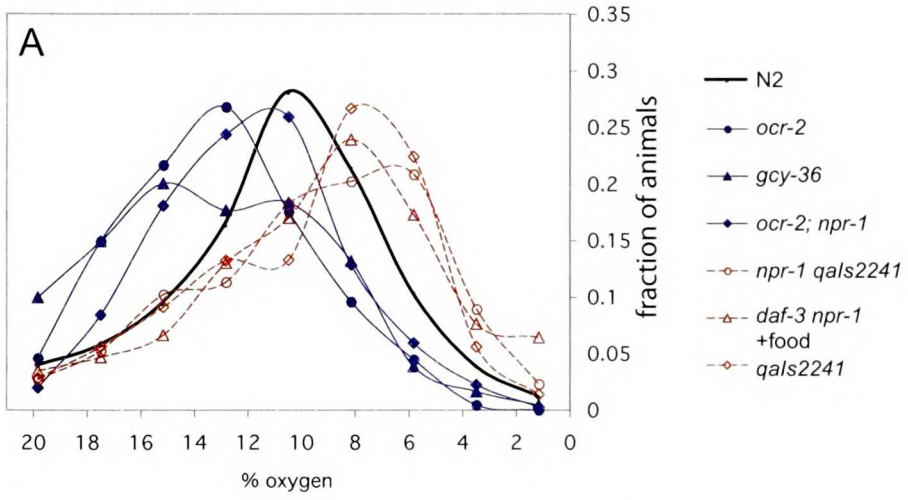
A
0.35
0.3
0.25
0.2
0.15
0.1
0.05
0
fraction of animals
20 18 16 14 12 10 8 6 4 2 0
% oxygen
N2
ocr-2
gcy-36
ocr-2; npr-1
npr-1 qals2241
daf-3 npr-1
+food
qals2241

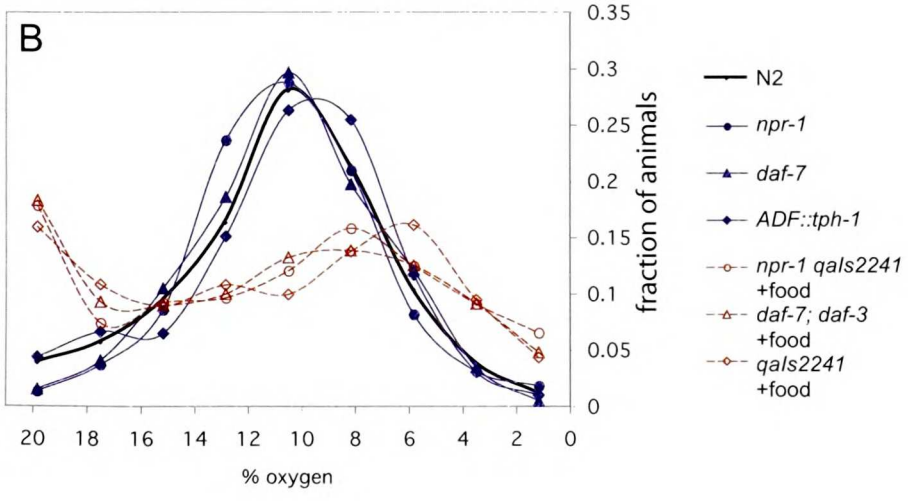
B
0.35
0.3
0.25
0.2
0.15
0.1
0.05
0
fraction of animals
20 18 16 14 12 10 8 6 4 2 0
% oxygen
N2
npr-1
daf-7
ADF::tph-1
npr-1 qals2241
+food
daf-7; daf-3
+food
qals2241
+food

Figure 2-10S. Additional aerotaxis experiments off food.

(A) Aerotaxis of *gcy-33; gcy-31* and *gcy-35; gcy-33; gcy-31* mutants.

(B) Aerotaxis of *gcy-35; gcy-33; gcy-31 qaIs2241* mutants.

(C) Aerotaxis of *osm-9 ocr-2* mutants.

(D) Aerotaxis of *osm-9 ocr-2; npr-1* mutants.

(E) Aerotaxis of *flp-21 (ok889)* and *flp-21 (pk1601)* mutants.

(F) Aerotaxis of *daf-7; qaIs2241* mutants.

For A-F, asterisks denote distributions different by Chi-square analysis at $p < 0.01$ from the first distribution in the panel. $n \geq 3$ assays per genotype, 80-100 animals/assay. Error bars denote SEM.

(G) Hyperoxia avoidance index as defined in Figure 2-1. None of these strains are significantly different from N2 controls by ANOVA ($p = 0.193$). Error bars denote SEM.

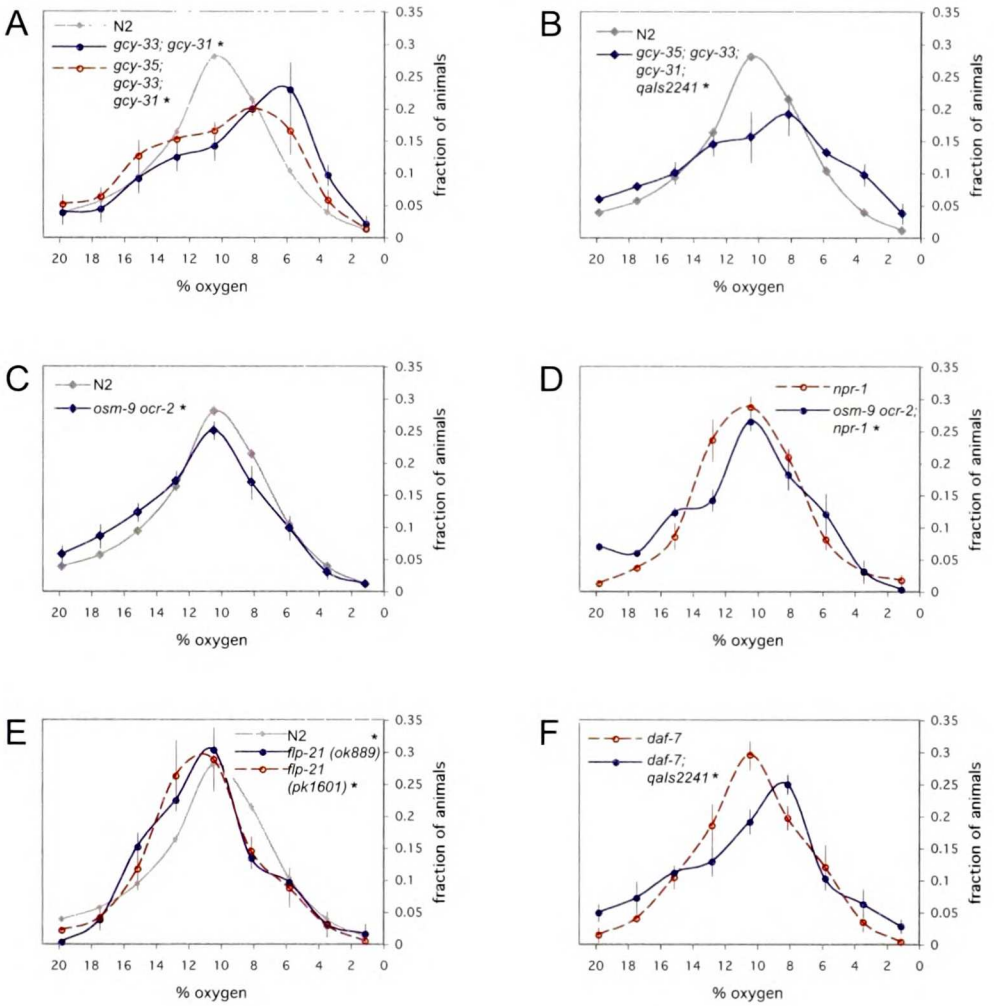
A
N2
gcy-33; gcy-31 *
gcy-35; gcy-33; gcy-31 *
B
N2
gcy-35; gcy-33; gcy-31; qals2241 *
C
N2
osm-9 ocr-2 *
D
npr-1
osm-9 ocr-2; npr-1 *
E
N2 *
flp-21 (ok889)
flp-21 (pk1601) *
F
daf-7
daf-7; qals2241 *
fraction of animals
% oxygen

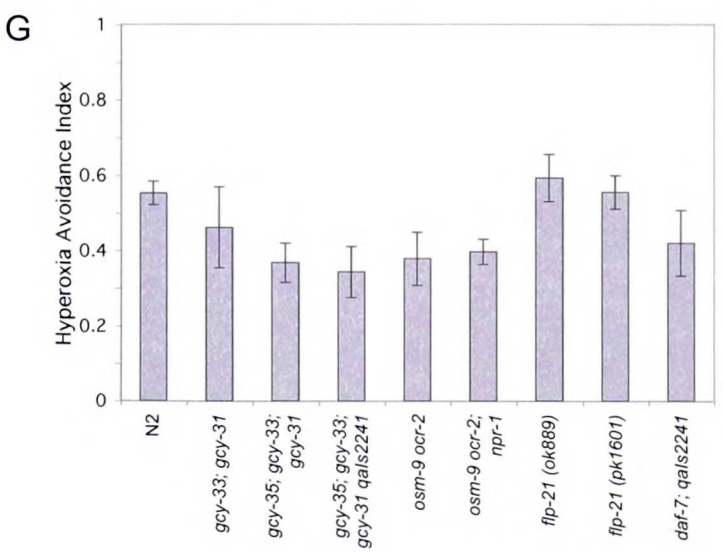
G
Hyperoxia Avoidance Index
N2
gcy-33; gcy-31
gcy-35; gcy-33; gcy-31
gcy-35; gcy-33; gcy-31 qals2241
osm-9 ocr-2
osm-9 ocr-2; npr-1
flp-21 (ok889)
flp-21 (pk1601)
daf-7; qals2241

Figure 2-11S. Additional aerotaxis experiments off and on food.

(A-E) In all panels, dotted lines indicate aerotaxis in the presence of a small amount of bacterial food.

(A) Aerotaxis of *osm-9 ocr-2* mutants.

(B) Aerotaxis of *osm-9 ocr-2; npr-1* mutants.

(C) Aerotaxis of *flp-21 (ok889)* mutants.

(D) Aerotaxis of *flp-21 (pk1601)* mutants.

(E) Aerotaxis of *daf-7; qaIs2241* mutants.

For A-E, asterisks denote distributions different by Chi-square analysis at $p < 0.01$ from the same genotype without food. $n \geq 3$ assays per genotype, 80-100 animals/assay. Error bars denote SEM.

(F) Hyperoxia avoidance index as defined in Figure 2-1. Asterisks, values significantly different from the same genotype without food at $p < 0.05$ by t test. Error bars denote SEM.

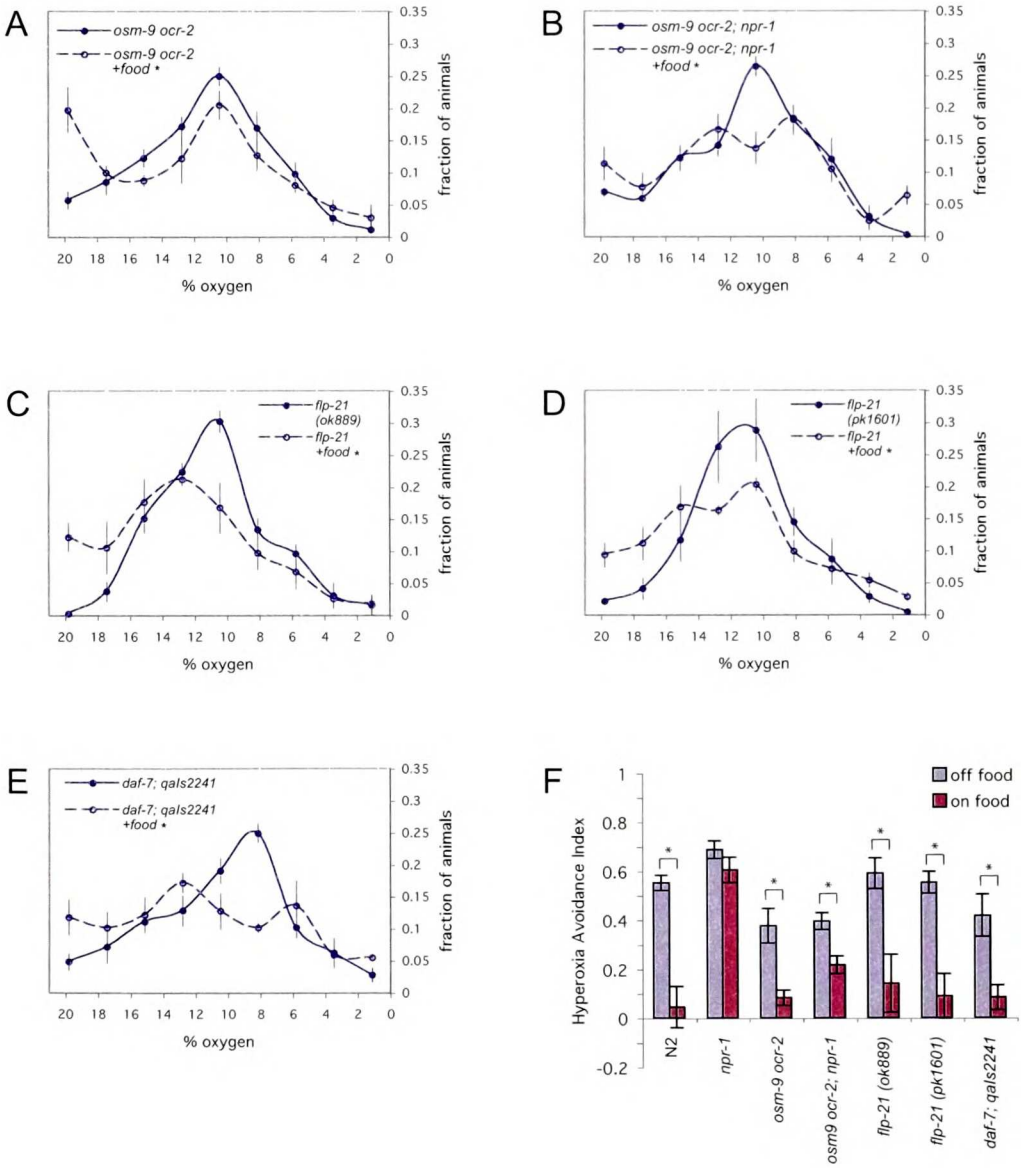
A
osm-9 ocr-2
osm-9 ocr-2 +food *
fraction of animals
% oxygen
B
osm-9 ocr-2; npr-1
osm-9 ocr-2; npr-1 +food *
fraction of animals
% oxygen
C
flp-21 (ok889)
flp-21 +food *
fraction of animals
% oxygen
D
flp-21 (pk1601)
flp-21 +food *
fraction of animals
% oxygen
E
daf-7; qals2241
daf-7; qals2241 +food *
fraction of animals
% oxygen
F
off food
on food
Hyperoxia Avoidance Index
N2
npr-1
osm-9 ocr-2
osm9 ocr-2; npr-1
flp-21 (ok889)
flp-21 (pk1601)
daf-7; qals2241

Chapter 3:

Regulation of the Circuit for Oxygen Preference by the HIF-1 Pathway

Introduction

Oxygen is an important molecule for the life of most organisms. Aerobic organisms require oxygen for metabolism while obligate anaerobic organisms need to avoid oxygen to survive. Animals living in soil and water environments, where oxygen levels are highly variable, are likely to have mechanisms to detect oxygen in their external environment to find optimal oxygen concentrations for their survival and growth (Sylvia et al., 1998; Wannamaker and Rice, 2000; Wu, 2002). For terrestial animals living on the surface, external oxygen levels are rarely limiting, but internal oxygen homeostasis is critical to deliver oxygen to tissues as needed (Hermes-Lima and Zenteno-Savin, 2002).

Many proteins can potentially act as oxygen sensors, as any enzymatic activity that is sensitive to oxidation state can be affected by changes in oxygen levels. Oxygen sensors that couple oxygen binding to enzymatic activity have been identified in bacteria and invertebrates. In bacteria, FixL in *Bradyrhizobium japonicum* and DOS in *Escherichia coli* bind oxygen through heme domains to regulate kinase and phosphodiestrase activities, respectively (Delgado-Nixon et al., 2000; Gilles-Gonzalez et al., 1991). In invertebrate animals, soluble guanylate cyclase homologs (sGCs) are implicated in oxygen sensing. Although canonical sGCs are regulated by nitric oxide binding to heme domains (Cary et al., 2006), *Drosophila melanogaster* has three atypical neuronally-expressed sGCs, Gyc-88E, Gyc-89Da, and Gyc-89Db, that can be activated by hypoxia when expressed in heterologous COS7 cells (Langlais et al., 2004; Morton, 2004; Morton et al., 2005). In *C. elegans*, the sGC GCY-35 binds oxygen through its

heme domain and promotes avoidance of hyperoxia (>14%) (Gray et al., 2004). Two additional sGCs, GCY-36 and GCY-34, are also implicated in hyperoxia avoidance (Chang et al., 2006; Cheung et al., 2005).

In mammals, the proposed oxygen sensors include NADPH oxidase, mitochondrial complexes, AMP kinase, and hemoxygenase-2 (Kemp, 2006). These enzymes use oxygen directly as a substrate or catalyze oxygen-dependent chemical reactions. Acute sensing of oxygen in the bloodstream is mediated by the carotid body (CB), which generates a hyperventilatory response and strong arousal in response to hypoxia (Lopez-Barneo, 2003). Recently, hemoxygenase-2 (HO-2) activity was proposed to signal hypoxia through inhibition of calcium-sensitive potassium (BK) channels in the CB (Williams et al., 2004). However, while HO-2 null mice have oxygen-related developmental and gene expression phenotypes in the CB, they show the same CB hypoxia sensitivity as control littermates. Furthermore, pharmacological blockage of BK channels does not abolish hypoxia sensitivity in the CB from mouse and rat, challenging the role of HO-2 activity and BK channels in acute hypoxia sensing (Ortega-Saenz et al., 2006). Thus, the acute oxygen sensor in the carotid body remains elusive.

The best described oxygen-sensing mechanism in metazoa is the hypoxia-inducible factor-1 (HIF-1) pathway, a transcriptional pathway for oxygen homeostasis (Kaelin, 2005). In mammals, HIF-1 signaling regulates diverse cellular and systemic processes from vascular biology and erythropoiesis to metabolism and cell survival/proliferation. The HIF-1 transcription factor is a heteromeric dimer of HIF-1α and HIF-1β subunits; HIF-1β is constitutively expressed while HIF-1α expression and

activity are dependent on oxygen concentration (Semenza, 2001). In normoxia, HIF-1α is constitutively modified by prolyl hydroxylase-2 (PHD-2), which uses oxygen as a co-substrate in the hydroxylation reaction (Berra et al., 2003). Prolyl hydroxylation allows HIF-1α to be recognized by the von Hippel-Lindau tumor suppressor protein (VHL), which forms an E3 ubiquitin ligase complex that targets HIF-1α for degradation via the ubiquitin-proteosome system. In hypoxic conditions, PHD-2 activity is reduced, and HIF-1α is not modified and degraded, allowing the HIF-1 transcription factor to act on its targets (Semenza, 2001).

The major components of the HIF-1 pathway have been identified in *C. elegans*: the genes encoding homologs of PHD-2, VHL, and HIF-1α are named *egl-9*, *vhl-1*, and *hif-1*, respectively (Epstein et al., 2001; Jiang et al., 2001). While HIF-1 knockout mice die embryonically, *C. elegans hif-1* mutants are completely viable in normal culture conditions, where environmental oxygen levels vary from 12-21% (Gray et al., 2004; Jiang et al., 2001). *C. elegans*'s metabolic rates do not begin to slow until environmental oxygen drops below 4%; at 1% oxygen, metabolic rates are at half of normal levels (Van Voorhies and Ward, 2000). At 1% oxygen, almost all wild-type N2 animals develop from embryo to fertile adults, but two-thirds of *hif-1* mutants do not survive embryogenesis (Jiang et al., 2001). As with other animals, *C. elegans* HIF-1 protein levels are low in normoxia and induced in hypoxia. At 1% and 0.1% oxygen, HIF-1 levels are strongly induced within 4-8 hours, but disappear rapidly within minutes upon reoxygenation (Epstein et al., 2001; Jiang et al., 2001). Mutants in *egl-9* and *vhl-1* show constitutive upregulation of HIF-1 protein in normoxic and hyperoxic conditions (Epstein et al., 2001). Genome-wide microarray studies of *egl-9*, *vhl-1*, and *hif-1* mutants grown

at normoxia and hypoxia show highly overlapping sets of oxygen-dependent transcriptional targets, supporting the idea that these genes function in the same pathway (Bishop et al., 2004; Shen et al., 2005). The existence of other targets regulated by oxygen, but not by *egl-9*, *vhl-1*, and *hif-1*, suggests that the HIF-1 pathway is not the only mechanism for oxygen homeostasis in *C. elegans*.

Strong evidence supports the role of HIF-1 signaling in oxygen-dependent development and physiology. Can the HIF-1 pathway also regulate oxygen-dependent behaviors? A circuit for oxygen preference in *C. elegans* was proposed in Chapter 2 and Chang et al., 2006. In this chapter, I will describe the role of the HIF-1 pathway in regulating hyperoxia avoidance behavior. Upregulation of HIF-1 signaling by loss of *egl-9* activity alters oxygen preference and food regulation of hyperoxia avoidance. In *egl-9* mutants, the circuit for oxygen preference changes from a flexible, distributed network to a more fixed configuration utilizing fewer sensory components. I will also present evidence for interactions between HIF-1 signaling and sensory experience in hyperoxia avoidance.

Results

Upregulation of the HIF-1 pathway alters oxygen preference and sensory requirements for hyperoxia avoidance.

To investigate the role of the HIF-1 oxygen-sensing pathway in aerotaxis, I tested mutants defective for HIF-1 signaling in linear gradient assays. Wild-type N2 animals have undetectable levels of HIF-1 protein in normoxic conditions and maximal levels of

HIF-1 protein at low oxygen (≤1%) (Epstein et al., 2001; Jiang et al., 2001). Mut
egl-9, an oxygen sensor that negatively regulates HIF-1 stability, have higher leve
HIF-1 protein in both normoxic and hypoxic conditions (Epstein et al., 2001). Fo
purposes of this study, normal culture conditions are considered to be in normoxia
(Brenner, 1974). In a linear gradient from anoxia to atmospheric oxygen (0-21%)
mutants preferred slightly, but significantly, lower oxygen concentrations than wi
animals (Chang et al., 2006; Gray et al., 2004) (Fig. 3-1A and Table 3-3). This ch
was dependent on *hif-1* activity, as both *hif-1* and *egl-9 hif-1* mutants preferred the
oxygen range as N2 animals (Fig. 3-1B). To examine the lower oxygen range mo
carefully, I tested these animals in 0-10% oxygen gradients. *egl-9* mutants accum
in lower oxygen than N2, *hif-1*, and *egl-9 hif-1* animals in 0-10% oxygen gradient
well as 0-21% gradients (Fig. 3-1C, D) (see also Chapter 4). These results sugges
egl-9 acts through *hif-1* to shift animals' preference to lower oxygen.

To account for the shift in preferred oxygen levels of *egl-9* mutants, a mod
hyperoxia avoidance index is used in this chapter that differs from the hyperoxia
avoidance index used in Chapter 2. In Chapter 3, the hyperoxia avoidance index
compares the average of the fractions of animals in the hyperoxia area (bins 1-3, >
O_2) to the average of the fractions in the preferred area (bins 4-7, 5-14% O_2). A
hyperoxia avoidance index of 1.0 represents complete avoidance of hyperoxia, 0.0
represents no preference, and -1.0 represents a complete preference for hyperoxia.
Throughout this chapter, the term "aerotaxis" refers to the complete distribution o
animals (Fig. 3-1A, Table 3-1), and the phrase "hyperoxia avoidance" refers speci
to the hyperoxia avoidance index (Fig. 3-1K)

A circuit for hyperoxia avoidance in wild-type N2 and mutant *npr-1(lf)* animals was proposed in Chapter 2 and Chang et al., 2006. To investigate how upregulation of the *hif-1* pathway may affect this circuit, I constructed and tested various combination mutants in the *egl-9* mutant background. The combination mutants were selected by a candidate approach based on the known effects of various mutations on N2 and *npr-1(lf)* aerotaxis.

Hyperoxia avoidance of wild-type N2 animals depends on the cyclic nucleotide gated-channel *tax-4* and the soluble guanylate cyclase homologs *gcy-36, gcy-35,* and *gcy-34* in URX, AQR, and PQR neurons (Chang et al., 2006; Gray et al., 2004). In *egl-9* mutants, *gcy-36* significantly suppressed hyperoxia avoidance while *gcy-35* had only a weak effect (Fig. 3-1E, F, K). *gcy-34; egl-9* double mutants were not tested. Interestingly, killing URX, AQR, and PQR using the *qaIs2241* transgene strongly suppressed hyperoxia avoidance in *egl-9* mutants (Fig. 1G, 1K); this transgene did not diminish hyperoxia avoidance of N2 and *npr-1(lf)* animals (Chang et al., 2006).

Two sets of sGC-expressing neurons (URX, AQR, and PQR and SDQ, ALN, and PLN) cooperate with TRPV channel-expressing neurons ASH and ADF to promote hyperoxia avoidance in wild-type N2 animals. Single mutants in the TRPV channels *osm-9* and *ocr-2* exhibited strong defects in hyperoxia avoidance (Chang et al., 2006). Combining *egl-9* with single mutations in *osm-9* or *ocr-2* or both *osm-9* and *ocr-2* had no effect on *egl-9* hyperoxia avoidance (Fig. 3-1H-K). Taken together, these results show that *egl-9* mutants require the activity of URX, AQR, and PQR and not that of TRPV channel-expressing neurons for hyperoxia avoidance, in contrast with the distributed circuit of wild-type N2 animals.

Hyperoxia avoidance of *egl-9* mutants requires serotonin in multiple neurons.

In *C. elegans*, the tryptophan hydroxylase enzyme encoded by the *tph-1* gene is required for serotonin biosynthesis (Sze et al., 2000). Five classes of *C. elegans* neurons express *tph-1* and synthesize serotonin. Serotonin signaling from ADF neurons is important in modulating hyperoxia avoidance of wild-type N2 animals (Chang et al., 2006). Like N2 animals, *egl-9* mutants required *tph-1* for hyperoxia avoidance (Chang et al., 2006) (Fig. 3-2A, E). However, unlike *tph-1* single mutants, *tph-1; egl-9* double mutants were not rescued by transgenic expression of *tph-1* in ADF neurons alone (Fig. 3-2B, E). Transgenic expression of *tph-1* in only the NSM neurons resulted in weak, statistically insignificant improvements in aerotaxis (Fig. 3-2C, E), whereas expression in both NSM and ADF neurons together resulted in strong rescue of the *tph-1; egl-9* defect (Fig. 3-2D, E). These results differ from rescue results in the N2 background; using the same transgenes, expression of *tph-1* in ADF, but not NSM, neurons was sufficient to restore hyperoxia avoidance to *tph-1* mutants (Chang et al., 2006).

tph-1 is the rate-limiting enzyme for serotonin biosynthesis (Sze et al., 2000), and its expression levels can provide insight into cells that are producing high or low amounts of serotonin. Expression of a *tph-1::GFP* transcriptional reporter in *egl-9*, *hif-1*, and *egl-9 hif-1* mutants was comparable to expression in wild-type animals (Fig. 3-2F). However, ADF *tph-1::GFP* expression was strongly reduced in *osm-9; egl-9*, *ocr-2; egl-9*, and *osm-9 ocr-2; egl-9* mutants (Fig. 3-2F), matching the role of TRPV channels in upregulating ADF *tph-1::GFP* expression in the N2 background (Zhang et al., 2004). Because *TRPV::egl-9* mutants showed strong hyperoxia avoidance (Fig. 3-1H-K), these expression results suggest that high levels of serotonin in ADF neurons are not required

for hyperoxia avoidance of *egl-9* mutants. NSM *tph-1::GFP* expression were normal i these mutant backgrounds (data not shown).

The *tph-1* rescue and expression experiments suggest that serotonin from NSM neurons is required for hyperoxia avoidance of *egl-9* mutants, although NSM serotonin not important in wild-type. The NSM neurons are the major neuronal source of seroto in *C. elegans* and exhibit very strong *tph-1::GFP* expression and serotonin immunoreactivity (Sze et al., 2000; Zhang et al., 2004; Zhang et al., 2005). The limite rescue of hyperoxia avoidance of *tph-1; egl-9* mutants by *tph-1* expression in NSM neurons may reflect a specific benefit to at least some expression in ADF as well as NSM. Alternatively, the NSM and ADF enhancement could result from an increase in total serotonin levels in the animal. NSM neurons are able to take up serotonin from other neuronal sources (Sze et al., 2002; Zhang et al., 2005); expression of *tph-1* in bot NSM and ADF neurons may allow NSM neurons in *tph-1; egl-9* mutants to take up serotonin produced by ADF and reach high serotonin levels that promote strong hyperoxia avoidance.

egl-9 mutants avoid hyperoxia in the presence of food.

In the presence of bacterial food, wild-type N2 animals have diminished hyperoxia avoidance (Fig. 3-3A, K), whereas mutants in the neuropeptide receptor *npr* and the TGF-ß homolog *daf-7* continue to avoid hyperoxia strongly (Chang et al., 2006 Gray et al., 2004). Like *npr-1* and *daf-7* mutants, *egl-9* mutants exhibited strong hyperoxia avoidance in the absence and presence of a bacterial lawn (Fig. 3-3B, K). Food regulation was restored by a mutation in *hif-1* (Fig. 3-3C, D, K), suggesting that t

egl-9/hif-1 transcriptional pathway regulates targets that affect food regulation of hyperoxia avoidance.

The unregulated hyperoxia avoidance in *npr-1* and *daf-7* mutants correlated to two other behaviors: aggregation into feeding groups that lower local oxygen and accumulation at the edge of a bacterial lawn, where oxygen concentrations are reduced (Chang et al., 2006; de Bono and Bargmann, 1998; Gray et al., 2004; Thomas et al., 1993). *egl-9* mutants accumulated at the lawn border, but did not aggregate as strongly as *npr-1* or *daf-7* (Darby et al., 1999) (data not shown). The bordering behavior of *egl-9* mutants was dependent on *hif-1* (data not shown).

In *npr-1* mutants, reduction of either soluble guanylate cyclase or *ocr-2* TRPV activity restores food regulation to hyperoxia avoidance (Chang et al., 2006). In *egl-9* mutants, reduction of soluble guanylate cyclase activity in URX, AQR, and PQR neurons by mutations in *gcy-36* or *gcy-35* did not restore food regulation of hyperoxia avoidance (Fig. 3-3E-G, K). Similarly, mutations in the TRPV channels *osm-9* and *ocr-2* were unable to restore food regulation to hyperoxia avoidance in an *egl-9* background (Fig. 3-3H-K). These results suggest that *egl-9* mutants have a fundamentally different mechanism for decreased food regulation than *npr-1* mutants.

The HIF-1 pathway acts in parallel to the NPR-1 and DAF-7 pathways for food regulation of hyperoxia avoidance.

To determine the relationship between NPR-1, DAF-7, and HIF-1 pathways in modulation of hyperoxia avoidance, I tested various double mutants between components from different pathways. A mutation in *hif-1*, which strongly suppressed hyperoxia

avoidance of *egl-9* mutants on food (Fig. 3-3D, K), did not suppress hyperoxia avoidance of *npr-1* mutants on food (Fig. 3-4D, I). These results suggest that *egl-9* and *npr-1* use different mechanism to confer food regulation on hyperoxia avoidance. *daf-7; hif-1* double mutants were not tested for aerotaxis because very few animals developed to adult. Most of these double mutants arrested in an alternate larval stage called the dauer (data not shown).

Like EGL-9, DAF-7 is an inhibitor of a transcription factor, the SMAD DAF-3. In *daf-7* mutants, food regulation of hyperoxia avoidance can be restored by a mutation in *daf-3* (Chang et al., 2006), but *daf-3* failed to suppress *egl-9* hyperoxia avoidance on food (Fig. 3-4F, I). These results suggest that the *egl-9/hif-1* and *daf-7/daf-3* transcriptional pathways work in parallel to regulate hyperoxia avoidance, and not in a sequential cascade.

Transcriptional reporters can be used to ask how pathways interact at a molecular level. *daf-7* activity inhibits *tph-1* expression in ADF, an interaction that defines at least one transcriptional target for food regulation of hyperoxia avoidance (Chang et al., 2006). ADF *tph-1::gfp* expression was not significantly affected in *egl-9* mutants (Fig. 3-2F), confirming that the transcriptional targets of *egl-9/hif-1* and *daf-7/daf-3* differ. In addition, wild-type N2 animals grown at 1% oxygen for 3 days before adult or 6 hours as adults, conditions which should stimulate *hif-1* activity, did not exhibit any change in ADF *tph-1::gfp* expression (data not shown).

I also asked whether the *egl-9/hif-1* and *daf-7/daf-3* pathways regulate each other. *egl-9* mutants had half as much *daf-7::gfp* as wild-type N2 animals in ASI neurons (*t* test, $p < 0.001$), suggesting a regulatory relationship between these two systems. However,

egl-9 did not act through the *daf-7* pathway for food regulation of hyperoxia avoidance, since it was not suppressed by *daf-3* (see above). This result indicates that the two pathways do interact, but that this is not their main output.

I also examined aerotaxis *daf-7; egl-9* and *egl-9; npr-1* double mutants. These double mutant exhibited strong hyperoxia avoidance that was not regulated by food, like the single mutants (Chang et al., 2006) (Fig. 3-4B, C, E, I).

Other than *hif-1*, only one genetic background restored food regulation to *egl-9* mutants. *tph-1; egl-9; NSM+ADF::tph-1* strain rescued for hyperoxia avoidance off food (Fig. 3-2C, D) showed strong regulation by food (Fig. 3-4H, I), which was not seen either in *tph-1* alone (Chang et al., 2006) or in *egl-9* alone (Fig. 3-4B, I). This result suggests that a particular configuration of serotonin expression can uncover a food regulation pathway that persists in *egl-9* mutants. One explanation for this result is that this transgenic strain had different serotonin levels in NSM and ADF than *egl-9* and that absolute levels of serotonin have a specific effect. An alternate possibility is that other cellular sources of serotonin are recruited for *egl-9* hyperoxia avoidance on food.

Site of *egl-9* action for food regulation of hyperoxia avoidance.

As an important regulator of cellular physiology, *hif-1* is expressed in virtually all cells in *C. elegans* (Jiang et al., 2001). Similarly, *egl-9* is broadly expressed in pharyngeal muscle, body wall muscle, vulval hypodermis, gonadal distal tip cells, and sensory neurons and interneurons of the head and tail (Darby et al., 1999). I attempted to restore food regulation to *egl-9* mutants by transgenic expression of an *egl-9* cDNA in subsets of cells. Expression of *egl-9* from an endogenous promoter was able to restore

some degree of food regulation of hyperoxia avoidance to *egl-9* mutants (Fig. 3-5A-D, However, expression of *egl-9* in most neurons from the H20 promoter or in serotonerg cells (NSM ADF, HSN, gut) from the *tph-1* promoter did not rescue food regulation (F 3-5E, F, I). Neither did expression of *egl-9* in body wall muscle from the *myo-3* promoter nor in pharyngeal muscle from the *myo-2* promoter (Fig. 3-5G-I).

Because I have not performed an exhaustive set of rescue experiments in all cel expressing *egl-9*, I may not have rescued *egl-9* in the relevant cell(s) yet. Some future rescue experiments should include rescue in URX, AQR, and PQR neurons, pharyngea neurons, and gut. Alternatively, rescue in multiple cell types may be required to restor food regulation. Finally, perhaps the *egl-9* cDNA I am using for these experiments is l effective for rescue than other shorter isoforms of *egl-9*.

Behavioral role of the HIF-1 pathway in response to hypoxia treatment.

Because *hif-1* activity is normally only induced in hypoxia, *egl-9* mutants with constitutively high *hif-1* activity can be considered to be animals that are adapted to hypoxia even when they are in normoxia. Conversely, *hif-1* mutants are adapted to normoxia even when they are in hypoxia. Animals living in hypoxia may be behaviora as well as physiologically adapted for a low oxygen environment. This can be one explanation for the lower oxygen preference of *egl-9* mutants.

To test this possibility, I asked whether growth in hypoxia caused any behavior changes similar to those caused by *egl-9*. *npr-1* mutants have been reported to shift the oxygen preference to lower oxygen if they are grown at 1% oxygen for ≥4 hours; N2 animals do not show this altered preference (Cheung et al., 2005) (data not shown).

Because HIF-1 protein levels are induced when animals are grown in hypoxia for ≥4 hours (Epstein et al., 2001; Jiang et al., 2001), I tested whether the HIF-1 pathway was involved in the behavioral shift in *npr-1* mutants. When *npr-1* mutants were grown at 1% for 6 hours, their peak preference shifted from 10% to 6% oxygen (Fig. 3-6A and Table 3-3). A similar shift was observed for *hif-1; npr-1* double mutants (Fig. 3-6B-D and Table 3-3), suggesting that an increase in *hif-1* activity during hypoxia was not necessary for the change in preference of *npr-1* mutants.

Although N2 animals grown in low oxygen did not shift preference to hypoxia like *npr-1*, they did show altered oxygen response. In N2, this change caused a loss of food regulation rather than the hypoxic shift seen in *npr-1*. When adult N2 animals were grown in 1% oxygen for 6 hours, they exhibited hyperoxia avoidance on food (Fig. 3-6E, G). Like the hypoxic shift in *npr-1* mutants, this response to low oxygen did not require *hif-1* (Fig. 3-6E, G). However, a role for *hif-1* in behavioral adaptation to hypoxia was uncovered when animals were grown at 1% oxygen during larval stages. Wild-type N2 animals grown in 1% oxygen for 2 days before adult showed strong hyperoxia avoidance on food (Fig. 3-6F, G). *hif-1* mutants did not show strong oxygen preference on food with the same treatment (Fig. 3-6F, G). These results suggest that *hif-1* signaling impacts on oxygen-sensing behavioral pathways when animals develop in hypoxia, but only when animals are exposed to hypoxia before adult. Animals transferred to hypoxia as adults may have alternative, *hif-1*-independent pathways to sense hypoxic stress and promote hyperoxia avoidance on food. To test if these effects are due to a requirement for *hif-1* activity during a critical period before adult or duration of hypoxia treatment, animals

should be transferred to hypoxia as adults for 2 days and tested for hyperoxia avoidance on food.

Physiological responses to hypoxia.

One question about the relevance of studying aerotaxis in 0-21% oxygen is whether any known physiological changes occur in this range of oxygen concentrations. In *C. elegans*, FOXO signaling through the DAF-16 transcription factor is important for regulating lifespan (Lin et al., 2001) and increased survival during oxidative stress in some long-lived mutants (Honda and Honda, 1999). One target of DAF-16 that is induced in oxidative stress is superoxide dismutase-3 (*sod-3*), an enzyme that rapidly converts cell-damaging reactive oxygen species to hydrogen peroxide (Honda and Honda, 1999). Because reactive oxygen species are produced during respiration, *sod-3* expression may be regulated by oxygen levels. *sod-3::gfp* expression in the pharynx was reduced by 40% when animals were grown at 1% oxygen for 2 days before adult instead of at normoxia (*t* test, $p < 0.001$). These results show that a physiological change linked to oxygen metabolism does occur in the 0-21% oxygen range. Regulation of *sod-3* expression by hypoxia is likely to be dependent on *daf-16* FOXO signaling, and not on the *hif-1* pathway, because *sod-3* is already a known transcriptional target of *daf-16* (Honda and Honda, 1999), and a change in *sod-3::gfp* expression was not observed between *egl-9* mutants with high *hif-1* activity and wild-type animals (*t* test, $p > 0.05$). Nevertheless, *sod-3::gfp* expression should be also be examined for *daf-16* and *hif-1* mutants grown in hypoxia to confirm this hypothesis.

Discussion

In wild-type N2 animals, a flexible, distributed circuit is used to generate oxygen preference (Chang et al., 2006). Upregulation of the *hif-1* pathway in *egl-9* mutants changes the oxygen preference of animals and alters the circuit for hyperoxia avoidance. URX, AQR, and PQR become crucial for hyperoxia avoidance in *egl-9*, but they are dispensable in wild-type. Conversely, TRPV channel-expressing neurons are required for hyperoxia avoidance in a wild-type background, but not in an *egl-9* mutant. Serotonin is important for hyperoxia avoidance in both contexts, but in *egl-9* the NSM neurons rather than ADF neurons appear to be the primary source of serotonin. These sensory requirements reveal an altered circuit for hyperoxia avoidance in *egl-9* mutants, involving fewer neurons and less redundancy (Fig. 3-7).

From the wiring diagram of synaptic connections in *C. elegans,* the oxygen-sensing, sGC-expressing neurons converge on AVA, a command interneuron for generating backward locomotion. The NSM neurons in the pharynx receives inputs from other pharyngeal neurons and form *en passant* connections to the ventral nerve cord (White et al., 1986). NSM does not form anatomical synapses with other neurons in the circuit in Figure 3-7, but serotonin can probably act at a distance as a neuromodulator from extra-synaptic sites. In this way, it may affect the activity of the neurons described in Figure 3-7 or other cells that have not yet been implicated in hyperoxia avoidance. Because serotonin signaling is often associated with behaviors modulated by well-fed and starved states (Chao et al., 2004; Horvitz et al., 1982; Nuttley et al., 2002; Sawin et al.,

2000; Zhang et al., 2005), NSM may sense food intake in the pharynx to modulate hyperoxia avoidance.

Where and how the *hif-1* pathway acts to inhibit hyperoxia avoidance on food remains to be determined. Further rescue experiments for the *egl-9* food regulation defect are necessary to address these questions. My experiments indicate that *egl-9* can regulate at least one other gene in the pathway, *daf-7*, although that is not its primary target based on genetic epistasis interactions. One interesting additional result is that *egl-9* mutants have enhanced expression of *flp-21::gfp* in PQR neurons (data not shown) compared to wild-type animals. *flp-21* encodes a neuropeptide ligand for the NPR-1 receptor (Rogers et al., 2003). To understand if this change in *flp-21* expression could affect food regulation will require further investigations into the specific role of PQR in aerotaxis.

daf-7/TGF-ß signaling is regulated by environmental factors such as food availability and population density as assessed through a pheromone; unfavorable conditions such as starvation and high pheromone levels inhibit *daf-7* expression (Ren et al., 1996; Schackwitz et al., 1996). Because *daf-7* mutants avoid hyperoxia on food, loss of food regulation of hyperoxia avoidance may reflect behavior of animals in unfavorable conditions (Chang et al., 2006). *egl-9* mutants, which perceive themselves to be under hypoxia even when they are not, may also uncouple food from hyperoxia avoidance as part of a stress pathway.

Materials and Methods

Strains

Strains were cultured under standard conditions (Brenner, 1974) and fed *E. coli* HB101. Wild-type animals were *C. elegans* Bristol strain N2. Other strains used in this work include: JT307 *egl-9 (sa307)* V, ZG31 *hif-1 (ia4)* V, CX6571 *egl-9 (sa307) hif-1 (ia4)* V, CX7103 *egl-9 (sa307)* V; *qaIs2241* X, CX7466 *egl-9 (sa307)* V; *gcy-36 (db66)* X, CX6745 *gcy-35 (ok769)* I; *egl-9 (sa307)* V, CX7033 *osm-9 (ky10)* IV; *egl-9 (sa307)* V, CX7034 *ocr-2 (ak47)* IV; *egl-9 (sa307)* V, CX7035 *osm-9 (ky10) ocr-2 (ak47)* IV; *egl-9 (sa307)* V, CX8220 *tph-1 (mg280)* II; *egl-9 (sa307)* V, CX8221 *tph-1 (mg280)* II; *egl-9 (sa307)* V; *kyEx953 [srh-142::tph-1::gfp, unc-122::gfp]*, CX8429 *tph-1 (mg280)* II; *egl-9 (sa307)* V; *kyEx1087 [ceh-2::tph-1::gfp, unc-122::gfp]*, CX8428 *tph-1 (mg280)* II; *egl-9 (sa307)* V; *kyEx848 [srh-142::tph-1::gfp, ceh-2::tph-1::gfp, unc-122::gfp], yzIs71-4 [tph-1::gfp, rol-6 (su1006)]* I, CX8556 *yzIs71-4* I; *egl-9 (sa307)* V, CX8557 *yzIs71-4* I; *hif-1 (ia4)* V, CX8550 *yzIs71-4* I; *egl-9 (sa307) hif-1 (ia4)* V, CX8725 *yzIs71-4* I; *osm-9 (ky10))* IV; *egl-9 (sa307)* V, CX8755 *yzIs71-4* I; *ocr-2 (ak47)* IV; *egl-9 (sa307)* V, CX8590 *yzIs71-4* I; *osm-9 (ky10) ocr-2 (ak47)* IV; *egl-9 (sa307)* V, CX8131 *egl-9 (sa307)* V; *npr-1 (ad609)* X, CX8306 *hif-1 (ia4)* V; *npr-1 (ad609)* X, CX8029 *daf-7 (e1372)* III; *egl-9 (sa307)* V, CX8014 *egl-9 (sa307)* V; *daf-3 (e1376)* X, DR1808 *mIs6 [daf-7::gfp, rol-6 (su1006)]* X, CX7395 *egl-9 (sa307)* V; *mIs6* X, CX7285 *egl-9 (sa307)* V; *ynIs80 [flp-21::gfp]*, CF1553 *muIs84 [sod-3::gfp]*, CX8754 *egl-9 (sa307)* V; *muIs84*, CX8757 *egl-9 (sa307)* V; *kyEx1518 [egl-9::egl-9::gfp]* Line #1, CX8756 *egl-9 (sa307)* V; *kyEx1593 [egl-9::egl-9::gfp]* Line #2, CX8628 *egl-9 (sa307)* V; *kyEx1525 [H20::egl-*

9::gfp], CX8632 *egl-9 (sa307)* V; *kyEx1529 [tph-1::egl-9::gfp]*, CX8630 *egl-9 (sa307)* V; *kyEx1527 [myo-3::egl-9::gfp]*, CX8792 *egl-9 (sa307)* V; *kyEx1616 [myo-2::egl-9::gfp]*. In all cases, null alleles or strong loss-of-function alleles were used.

Molecular Biology

egl-9 rescuing plasmids were constructed by PCR amplification of promoters and insertion into FseI to AscI in an expression vector containing *egl-9* cDNA (F22E12.4a) in pSM, a modified pPD49.26 with extra cloning sites, and *gfp* following a SL2 trans-splicing sequence for co-expression from the same promoter. The promoter fragments for *egl-9, tph-1, myo-3,* and *myo-2* respectively contain 4.6, 3.1, 2.4, and 1.2 kb of sequence upstream of the start codons of these genes. The H20 promoter is a 2.7 kb genomic DNA fragment that drives expression in most neurons.

Behavioral Assays

Aerotaxis assays were performed by placing animals on nematode growth medium (NGM) agar in custom-made microfluidic devices fabricated from polydimethylsiloxane with a gas-phase linear gradient from 0-21% and 0-10% oxygen, and monitoring animals' accumulation in nine bins across the gradient (Gray et al., 2004). Gradients were generated by delivering gases under laminar flow to source and drain chambers immediately outside the behavioral arena, using a syringe pump; diffusion of the gases established the gradient in the small assay chamber. For 0-21% gradients, 100% nitrogen gas and air were used; for 0-10% gradients, 100% nitrogen and 10% oxygen/90% nitrogen gases were used. Gases were obtained from Airgas (Radnor,

Pennsylvania), Matheson (Montgomeryville, Pennsylvania), and TW Smith (Brooklyn, New York). Animals were prepared for assays as described (Chang et al., 2006). For assays on food, thin bacterial lawns of *E. coli* HB101 were made by seeding NGM plates for overnight growth at 37°C and returning plates to room temperature for at least 1 hour before assay.

Results from two devices were binned for one assay (~80-100 animals per assay). At least three independent assays on three different days for each genotype were used to generate results in the Figures. Data presented represent distributions 25 minutes from start of the assay.

For experiments growing animals at 1% oxygen, ambient oxygen concentrations were controlled by a gas-tight hypoxic chamber (Coy Laboratory Products, Grass Lake, Michigan) in which culture plates were placed. At various stages of development, animals were transferred from culture plates at normal growth conditions to new culture plates that had been equilibrated in 1% oxygen for at least 24 hours. Animals were assayed immediately upon removal from the hypoxic chamber.

Statistical Analysis

Statistical analysis of aerotaxis was conducted in multiple steps. The nine individual points in the aerotaxis assay are not independent – accumulation of animals in one bin necessarily affects all other bins – so they cannot be analyzed individually. A first test to assess the overall distribution of animals in the aerotaxis assay was a comparison of experimental strains or conditions to controls by Chi-square analysis (nine bins per aerotaxis assay x 2 strains = 8 degrees of freedom). Chi-square analysis takes

into account the non-Gaussian nature of the aerotaxis distributions as well as the total number of animals tested. It is overly conservative, because it combines all animals tested into a single contingency table and does not take into account the fact that each assay was repeated multiple times. Therefore, assays that are not statistically different by this criterion may actually be different. With this issue in mind, we have emphasized positive findings in this chapter. For controls such as N2 or *egl-9* that were compared to multiple mutants, $p < 0.01$ was used as the level of significance for the Chi-square test. Most results described in this chapter were significant at $p < 0.001$ (Table 3-2). In the text, any stated differences in a secondary measure, such as hyperoxia avoidance index or median preferred oxygen concentration, had also passed this first test using Chi-square analysis of the entire distribution ($p < 0.01$).

The hyperoxia avoidance index used in this chapter differs from that used in Chapter 2 to account for the shift in oxygen preference of *egl*-9 mutants to lower oxygen (5-14%). In Chapter 3, the hyperoxia avoidance index is defined as [average(fraction of animals in 5-14% O_2) - average(fraction of animals in 14-21% O_2)] / [average(fraction of animals in 5-14% O_2) + average(fraction of animals in 14-21% O_2)]. This standard performance index varies from –1.0 (all animals in hyperoxic regions) to +1.0 (all animals in normoxic regions) with 0 representing no preference between normoxia and hyperoxia. Each strain or condition was tested in at least 3 assays with ~80-100 animals each, and the mean hyperoxia avoidance index across all assays was used to test significance. *t* tests were used to compare the hyperoxia avoidance indices between two distributions. Analysis of variance (ANOVA) plus Bonferroni *t* tests or Dunnett tests were used for multiple comparisons of hyperoxia avoidance indices or median preferred

oxygen concentrations between strains and conditions (Statview, Cary, North Carolina). For controls such as N2 or *egl-9* that were compared to multiple mutants, $p < 0.01$ was usually used as the level of significance.

References

Berra, E., Benizri, E., Ginouves, A., Volmat, V., Roux, D., and Pouyssegur, J. (2003). HIF prolyl-hydroxylase 2 is the key oxygen sensor setting low steady-state levels of HIF-1alpha in normoxia. Embo J *22*, 4082-4090.

Bishop, T., Lau, K. W., Epstein, A. C., Kim, S. K., Jiang, M., O'Rourke, D., Pugh, C. W., Gleadle, J. M., Taylor, M. S., Hodgkin, J., and Ratcliffe, P. J. (2004). Genetic analysis of pathways regulated by the von Hippel-Lindau tumor suppressor in Caenorhabditis elegans. PLoS Biol *2*, e289.

Brenner, S. (1974). The genetics of Caenorhabditis elegans. Genetics *77*, 71-94.

Cary, S. P., Winger, J. A., Derbyshire, E. R., and Marletta, M. A. (2006). Nitric oxide signaling: no longer simply on or off. Trends Biochem Sci *31*, 231-239.

Chang, A. J., Chronis, N., Karow, D. S., Marletta, M. A., and Bargmann, C. I. (2006). A distributed chemosensory circuit for oxygen preference in C. elegans. PLoS Biol *4*, e274.

Chao, M. Y., Komatsu, H., Fukuto, H. S., Dionne, H. M., and Hart, A. C. (2004). Feeding status and serotonin rapidly and reversibly modulate a Caenorhabditis elegans chemosensory circuit. Proc Natl Acad Sci U S A *101*, 15512-15517.

Cheung, B. H., Cohen, M., Rogers, C., Albayram, O., and de Bono, M. (2005). Experience-dependent modulation of C. elegans behavior by ambient oxygen. Curr Biol *15*, 905-917.

Darby, C., Cosma, C. L., Thomas, J. H., and Manoil, C. (1999). Lethal paralysis of Caenorhabditis elegans by Pseudomonas aeruginosa. Proc Natl Acad Sci U S A *96*, 15202-15207.

de Bono, M., and Bargmann, C. I. (1998). Natural variation in a neuropeptide Y receptor homolog modifies social behavior and food response in C. elegans. Cell *94*, 679-689.

Delgado-Nixon, V. M., Gonzalez, G., and Gilles-Gonzalez, M. A. (2000). Dos, a heme-binding PAS protein from Escherichia coli, is a direct oxygen sensor. Biochemistry *39*, 2685-2691.

Epstein, A. C., Gleadle, J. M., McNeill, L. A., Hewitson, K. S., O'Rourke, J., Mole, D. R., Mukherji, M., Metzen, E., Wilson, M. I., Dhanda, A., *et al.* (2001). C. elegans EGL-9 and mammalian homologs define a family of dioxygenases that regulate HIF by prolyl hydroxylation. Cell *107*, 43-54.

Gilles-Gonzalez, M. A., Ditta, G. S., and Helinski, D. R. (1991). A haemoprotein with kinase activity encoded by the oxygen sensor of Rhizobium meliloti. Nature *350*, 170-172.

Gray, J. M., Karow, D. S., Lu, H., Chang, A. J., Chang, J. S., Ellis, R. E., Marletta, M. A., and Bargmann, C. I. (2004). Oxygen sensation and social feeding mediated by a C. elegans guanylate cyclase homologue. Nature *430*, 317-322.

Hermes-Lima, M., and Zenteno-Savin, T. (2002). Animal response to drastic changes in oxygen availability and physiological oxidative stress. Comp Biochem Physiol C *133*, 537-556.

Honda, Y., and Honda, S. (1999). The daf-2 gene network for longevity regulates oxidative stress resistance and Mn-superoxide dismutase gene expression in Caenorhabditis elegans. Faseb J *13*, 1385-1393.

Horvitz, H. R., Chalfie, M., Trent, C., Sulston, J. E., and Evans, P. D. (1982). Serotonin and octopamine in the nematode Caenorhabditis elegans. Science *216*, 1012-1014.

Jiang, H., Guo, R., and Powell-Coffman, J. A. (2001). The Caenorhabditis elegans hif-1 gene encodes a bHLH-PAS protein that is required for adaptation to hypoxia. Proc Natl Acad Sci U S A *98*, 7916-7921.

Kaelin, W. G., Jr. (2005). Proline hydroxylation and gene expression. Annu Rev Biochem *74*, 115-128.

Kemp, P. J. (2006). Detecting acute changes in oxygen: will the real sensor please stand up? Exp Physiol *91*, 829-834.

Langlais, K. K., Stewart, J. A., and Morton, D. B. (2004). Preliminary characterization of two atypical soluble guanylyl cyclases in the central and peripheral nervous system of Drosophila melanogaster. J Exp Biol *207*, 2323-2338.

Lin, K., Hsin, H., Libina, N., and Kenyon, C. (2001). Regulation of the Caenorhabditis elegans longevity protein DAF-16 by insulin/IGF-1 and germline signaling. Nat Genet *28*, 139-145.

Lopez-Barneo, J. (2003). Oxygen and glucose sensing by carotid body glomus cells. Curr Opin Neurobiol *13*, 493-499.

Morton, D. B. (2004). Atypical soluble guanylyl cyclases in Drosophila can function as molecular oxygen sensors. J Biol Chem *279*, 50651-50653.

Morton, D. B., Langlais, K. K., Stewart, J. A., and Vermehren, A. (2005). Comparison of the properties of the five soluble guanylyl cyclase subunits in Drosophila melanogaster. J Insect Sci *5*, 12.

Nuttley, W. M., Atkinson-Leadbeater, K. P., and Van Der Kooy, D. (2002). Serotonin mediates food-odor associative learning in the nematode Caenorhabditiselegans. Proc Natl Acad Sci U S A *99*, 12449-12454.

Ortega-Saenz, P., Pascual, A., Gomez-Diaz, R., and Lopez-Barneo, J. (2006). Acute oxygen sensing in heme oxygenase-2 null mice. J Gen Physiol *128*, 405-411.

Ren, P., Lim, C. S., Johnsen, R., Albert, P. S., Pilgrim, D., and Riddle, D. L. (1996). Control of C. elegans larval development by neuronal expression of a TGF-beta homolog. Science *274*, 1389-1391.

Rogers, C., Reale, V., Kim, K., Chatwin, H., Li, C., Evans, P., and de Bono, M. (2003). Inhibition of *Caenorhabditis elegans* social feeding by FMRFamide-related peptide activation of NPR-1. Nat Neurosci *6*, 1178-1185.

Sawin, E. R., Ranganathan, R., and Horvitz, H. R. (2000). C. elegans locomotory rate is modulated by the environment through a dopaminergic pathway and by experience through a serotonergic pathway. Neuron *26*, 619-631.

Schackwitz, W. S., Inoue, T., and Thomas, J. H. (1996). Chemosensory neurons function in parallel to mediate a pheromone response in C. elegans. Neuron *17*, 719-728.

Semenza, G. L. (2001). HIF-1, O(2), and the 3 PHDs: how animal cells signal hypoxia to the nucleus. Cell *107*, 1-3.

Shen, C., Nettleton, D., Jiang, M., Kim, S. K., and Powell-Coffman, J. A. (2005). Roles of the HIF-1 hypoxia-inducible factor during hypoxia response in Caenorhabditis elegans. J Biol Chem *280*, 20580-20588.

Sylvia, D. M., Fuhrmann, J. J., Hartel, P. G., and Zuberer, D. A. (1998). Principles and Applications of Soil Microbiology (Upper Saddle River, New Jersey, Prentice Hall).

Sze, J. Y., Victor, M., Loer, C., Shi, Y., and Ruvkun, G. (2000). Food and metabolic signalling defects in a Caenorhabditis elegans serotonin-synthesis mutant. Nature *403*, 560-564.

Sze, J. Y., Zhang, S., Li, J., and Ruvkun, G. (2002). The C. elegans POU-domain transcription factor UNC-86 regulates the tph-1 tryptophan hydroxylase gene and neurite outgrowth in specific serotonergic neurons. Development *129*, 3901-3911.

Thomas, J., Birnby, D., and Vowels, J. (1993). Evidence for parallel processing of sensory information controlling dauer formation in Caenorhabditis elegans. Genetics *134*, 1105-1117.

Van Voorhies, W. A., and Ward, S. (2000). Broad oxygen tolerance in the nematode Caenorhabditis elegans. J Exp Biol *203 Pt 16*, 2467-2478.

Wannamaker, C. M., and Rice, J. A. (2000). Effects of hypoxia on movements and behavior of selected estuarine organisms from the southeastern United States. J Exp Mar Biol Ecol *249*, 145-163.

White, J. G., Southgate, E., Thomson, J. N., and Brenner, S. (1986). The structure of the nervous system of the nematode *Caenorhabditis elegans*. Phil Transact R Soc Lond B *314*, 1-340.

Williams, S. E., Wootton, P., Mason, H. S., Bould, J., Iles, D. E., Riccardi, D., Peers, C., and Kemp, P. J. (2004). Hemoxygenase-2 is an oxygen sensor for a calcium-sensitive potassium channel. Science *306*, 2093-2097.

Wu, R. S. (2002). Hypoxia: from molecular responses to ecosystem responses. Mar Pollut Bull *45*, 35-45.

Zhang, S., Sokolchik, I., Blanco, G., and Sze, J. Y. (2004). Caenorhabditis elegans TRPV ion channel regulates 5HT biosynthesis in chemosensory neurons. Development *131*, 1629-1638.

Zhang, Y., Lu, H., and Bargmann, C. I. (2005). Pathogenic bacteria induce aversive olfactory learning in Caenorhabditis elegans. Nature *438*, 179-184.

Table 3-1. Distributions of different genotypes and conditions in aerotaxis assays in a 0-21% oxygen gradient.

Bins are equally spaced along the gradient as depicted in Figure 2-1A. Values are the fractions of animals in each bin. n, number of assays. Each assay represents 80-100 animals.

Genotype	Food	n	1	2	3	4	5	6	7	8	9
N2	off	28	0.039	0.057	0.094	0.163	0.280	0.214	0.104	0.039	0.011
egl-9	off	7	0.023	0.046	0.090	0.142	0.177	0.256	0.186	0.066	0.013
hif-1	off	6	0.035	0.061	0.113	0.196	0.245	0.220	0.106	0.019	0.005
egl-9 hif-1	off	5	0.035	0.084	0.127	0.159	0.228	0.207	0.105	0.040	0.015
egl-9; qaIs2241	off	6	0.042	0.116	0.144	0.108	0.132	0.176	0.141	0.097	0.044
egl-9; qcy-36	off	3	0.048	0.130	0.156	0.143	0.146	0.158	0.155	0.056	0.009
qcy-35; egl-9	off	6	0.031	0.093	0.120	0.139	0.144	0.196	0.187	0.081	0.009
osm-9; egl-9	off	3	0.023	0.033	0.119	0.136	0.215	0.275	0.165	0.030	0.004
ocr-2; egl-9	off	3	0.020	0.041	0.080	0.157	0.247	0.268	0.138	0.038	0.010
osm-9 ocr-2; egl-9	off	3	0.015	0.052	0.097	0.187	0.209	0.266	0.134	0.035	0.005
egl-9; npr-1	off	3	0.015	0.053	0.049	0.084	0.117	0.248	0.302	0.087	0.045
hif-1; npr-1	off	3	0.014	0.024	0.075	0.161	0.252	0.245	0.133	0.072	0.024
daf-7; egl-9	off	3	0.042	0.041	0.070	0.106	0.175	0.269	0.187	0.095	0.016
egl-9; daf-3	off	4	0.039	0.066	0.082	0.157	0.186	0.212	0.168	0.078	0.012
tph-1; egl-9	off	6	0.087	0.119	0.114	0.186	0.138	0.147	0.123	0.078	0.009
tph-1; egl-9; ADF:tph-1	off	3	0.075	0.130	0.131	0.163	0.131	0.126	0.128	0.081	0.036
tph-1; egl-9; NSM::tph-1	off	3	0.049	0.107	0.104	0.143	0.152	0.213	0.128	0.094	0.009
tph-1; egl-9; NSM+ADF::tph-1	off	3	0.036	0.079	0.082	0.131	0.167	0.213	0.187	0.089	0.016
egl-9; egl-9::egl-9 #1	off	5	0.043	0.072	0.115	0.134	0.161	0.207	0.166	0.085	0.017
egl-9; egl-9::egl-9 #2	off	3	0.028	0.068	0.128	0.153	0.202	0.199	0.173	0.042	0.007
egl-9; H20::egl-9	off	3	0.034	0.075	0.084	0.171	0.214	0.242	0.131	0.037	0.012
egl-9; tph-1::egl-9	off	3	0.029	0.066	0.094	0.096	0.237	0.238	0.190	0.047	0.003
egl-9; myo-3::egl-9	off	3	0.035	0.076	0.107	0.132	0.137	0.184	0.206	0.107	0.017
egl-9; myo-2::egl-9	off	3	0.029	0.058	0.097	0.152	0.172	0.176	0.205	0.098	0.013
npr-1	off	6	0.016	0.036	0.078	0.201	0.269	0.207	0.114	0.047	0.033
npr-1 1% 6 hrs	off	3	0.034	0.034	0.026	0.083	0.112	0.241	0.303	0.129	0.037
hif-1; npr-1 1% 6hrs	off	3	0.043	0.032	0.062	0.121	0.101	0.196	0.278	0.124	0.043
N2	on	15	0.151	0.113	0.122	0.143	0.146	0.125	0.090	0.071	0.040
egl-9	on	6	0.062	0.028	0.084	0.105	0.180	0.243	0.175	0.080	0.042
hif-1	on	6	0.187	0.107	0.138	0.084	0.122	0.135	0.092	0.085	0.051
egl-9 hif-1	on	3	0.135	0.115	0.107	0.135	0.171	0.161	0.085	0.054	0.036
egl-9; qaIs2241	on	4	0.101	0.067	0.101	0.121	0.136	0.214	0.124	0.088	0.047
egl-9; qcy-36	on	3	0.045	0.102	0.114	0.138	0.128	0.187	0.159	0.086	0.042
qcy-35; egl-9	on	3	0.082	0.089	0.072	0.161	0.121	0.196	0.139	0.090	0.049
osm-9; egl-9	on	3	0.036	0.080	0.124	0.141	0.242	0.203	0.123	0.035	0.017
ocr-2; egl-9	on	3	0.057	0.050	0.125	0.137	0.201	0.251	0.129	0.043	0.008
osm-9 ocr-2; egl-9	on	3	0.035	0.021	0.067	0.173	0.247	0.246	0.158	0.045	0.008
egl-9; npr-1	on	3	0.030	0.038	0.052	0.051	0.133	0.290	0.208	0.128	0.071
hif-1; npr-1	on	3	0.049	0.047	0.086	0.109	0.225	0.211	0.139	0.084	0.051
daf-7; egl-9	on	3	0.060	0.047	0.052	0.127	0.169	0.263	0.167	0.082	0.032
egl-9; daf-3	on	4	0.065	0.044	0.084	0.107	0.154	0.262	0.172	0.086	0.027
tph-1; egl-9	on	3	0.120	0.083	0.106	0.149	0.163	0.137	0.116	0.081	0.046
tph-1; egl-9; NSM+ADF::tph-1	on	3	0.099	0.094	0.162	0.152	0.156	0.126	0.138	0.058	0.016
egl-9; egl-9::egl-9 #1	on	3	0.129	0.088	0.091	0.107	0.174	0.173	0.129	0.066	0.042
egl-9; egl-9::egl-9 #2	on	3	0.101	0.090	0.119	0.106	0.136	0.173	0.147	0.062	0.066
egl-9; H20::egl-9	on	3	0.067	0.083	0.073	0.145	0.194	0.211	0.141	0.055	0.031
egl-9; tph-1::egl-9	on	3	0.071	0.061	0.061	0.105	0.152	0.246	0.188	0.079	0.037
egl-9; myo-3::egl-9	on	3	0.049	0.086	0.086	0.129	0.195	0.178	0.189	0.059	0.030
egl-9; myo-2::egl-9	on	4	0.080	0.064	0.064	0.081	0.119	0.245	0.184	0.121	0.044
N2 1% 6 hrs	on	4	0.065	0.081	0.092	0.061	0.093	0.208	0.251	0.116	0.034
hif-1 1% 6 hrs	on	4	0.127	0.125	0.133	0.135	0.132	0.108	0.107	0.081	0.052
N2 1% 2 days	on	3	0.068	0.075	0.068	0.072	0.146	0.217	0.214	0.095	0.045
hif-1 1% 2 days	on	4	0.088	0.101	0.112	0.072	0.122	0.165	0.226	0.072	0.042

Table 3-2 (p. 1). Chi-square comparisons.

n, total number of animals tested for a given genotype and condition.

* $P < 0.01$
** $P < 0.001$

Group 1			Group 2			Chi-square	
Genotype	Food	n	Genotype	Food	n		
N2	off	2774	*egl-9*	off	710	75	**
N2	off	2774	*hif-1*	off	536	16	
N2	off	2774	*egl-9 hif-1*	off	523	15	
egl-9	off	710	*hif-1*	off	536	45	**
egl-9 hif-1	off	523	*egl-9*	off	710	41	**
egl-9 hif-1	off	523	*hif-1*	off	536	9	
egl-9; qaIs2241	off	613	*egl-9*	off	710	64	**
egl-9; qaIs2241	off	613	*qaIs2241*	off	801	59	**
egl-9; qcy-36	off	355	*egl-9*	off	710	49	**
egl-9; qcy-36	off	355	*qcy-36*	off	553	58	**
qcy-35; egl-9	off	652	*egl-9*	off	710	23	*
qcy-35; egl-9	off	652	*qcy-35*	off	823	36	**
osm-9; egl-9	off	346	*egl-9*	off	710	13	
osm-9; egl-9	off	346	*osm-9*	off	601	91	**
ocr-2; egl-9	off	399	*egl-9*	off	710	14	
ocr-2; egl-9	off	399	*ocr-2*	off	203	80	**
osm-9 ocr-2; egl-9	off	348	*egl-9*	off	710	13	
osm-9 ocr-2; egl-9	off	348	*osm-9 ocr-2*	off	598	32	**
egl-9; npr-1	off	287	*egl-9*	off	710	37	**
egl-9; npr-1	off	287	*npr-1*	off	414	102	**
hif-1; npr-1	off	293	*hif-1*	off	536	33	**
hif-1; npr-1	off	293	*npr-1*	off	594	6	
daf-7; egl-9	off	304	*egl-9*	off	710	9	
daf-7; egl-9	off	304	*daf-7*	off	403	49	**
egl-9; daf-3	off	427	*egl-9*	off	710	7	
egl-9; daf-3	off	427	*daf-3*	off	289	12	
tph-1; egl-9	off	648	*egl-9*	off	710	84	**
tph-1; egl-9	off	648	*tph-1*	off	1076	37	**
tph-1; egl-9; ADF:tph-1	off	297	*tph-1; egl-9*	off	648	9	
tph-1; egl-9; ADF:tph-1	off	297	*egl-9*	off	710	67	**
tph-1; egl-9; NSM::tph-1	off	328	*tph-1; egl-9*	off	648	13	
tph-1; egl-9; NSM::tph-1	off	328	*egl-9*	off	710	27	**
tph-1; egl-9; NSM+ADF::tph-1	off	305	*tph-1; egl-9*	off	648	30	**
tph-1; egl-9; NSM+ADF::tph-1	off	305	*egl-9*	off	710	9	
egl-9; egl-9::egl-9 Line 1	off	523	*egl-9*	off	710	15	
egl-9; egl-9::egl-9 Line 2	off	292	*egl-9*	off	710	12	
egl-9; H20::egl-9	off	322	*egl-9*	off	710	15	
egl-9; tph-1::egl-9	off	320	*egl-9*	off	710	14	
egl-9; myo-3::egl-9	off	309	*egl-9*	off	710	16	
egl-9; myo-2::egl-9	off	309	*egl-9*	off	710	10	
npr-1	off	594	*npr-1* 1% 6hrs	off	268	102	**
hif-1; npr-1	off	293	*hif-1; npr-1* 1% 6hrs	off	306	49	**
hif-1; npr-1	off	293	*npr-1*	off	594	6	
npr-1 1% 6hrs	off	268	*hif-1; npr-1* 1% 6hrs	off	306	8	

Table 3-2 (p. 2). Chi-square comparisons.

n, total number of animals tested for a given genotype and condition.

* $P < 0.01$
** $P < 0.001$

Group 1			Group 2				
Genotype	Food	n	Genotype	Food	n	Chi-square	
N2	off	2774	N2	on	1161	315	**
egl-9	off	710	*egl-9*	on	588	30	**
hif-1	off	536	*hif-1*	on	364	142	**
egl-9 hif-1	off	523	*egl-9 hif-1*	on	179	82	**
egl-9; qaIs2241	off	613	*egl-9; qaIs2241*	on	334	21	*
egl-9; gcy-36	off	355	*egl-9; gcy-36*	on	312	14	
gcy-35; egl-9	off	652	*gcy-35; egl-9*	on	358	38	**
osm-9; egl-9	off	346	*osm-9; egl-9*	on	365	18	
ocr-2; egl-9	off	399	*ocr-2; egl-9*	on	387	13	
osm-9 ocr-2; egl-9	off	348	*osm-9 ocr-2; egl-9*	on	352	11	
egl-9; npr-1	off	287	*egl-9; npr-1*	on	291	15	
hif-1; npr-1	off	293	*hif-1; npr-1*	on	245	13	
daf-7; egl-9	off	304	*daf-7; egl-9*	on	320	5	
egl-9; daf-3	off	427	*egl-9; daf-3*	on	373	14	
tph-1; egl-9	off	648	*tph-1; egl-9*	on	294	21	*
tph-1; egl-9; NSM+ADF::tph-1	off	305	*tph-1; egl-9; NSM+ADF::tph-1*	on	300	28	**
egl-9; egl-9::egl-9 Line 1	off	523	*egl-9; egl-9::egl-9 Line 1*	on	249	28	**
egl-9; egl-9::egl-9 Line 2	off	292	*egl-9; egl-9::egl-9 Line 2*	on	261	34	**
egl-9; H20::egl-9	off	322	*egl-9; H20::egl-9*	on	255	8	
egl-9; tph-1::egl-9	off	320	*egl-9; tph-1::egl-9*	on	296	25	*
egl-9; myo-3::egl-9	off	309	*egl-9; myo-3::egl-9*	on	270	9	
egl-9; myo-2::egl-9	off	309	*egl-9; myo-2::egl-9*	on	365	29	**
N2	on	1161	*egl-9*	on	588	126	**
N2	on	1161	*hif-1*	on	364	16	
N2	on	1161	*egl-9 hif-1*	on	179	2	
egl-9 hif-1	on	179	*egl-9*	on	588	49	**
egl-9 hif-1	on	179	*hif-1*	on	364	11	
egl-9; qaIs2241	on	334	*egl-9*	on	588	22	*
egl-9; qaIs2241	on	334	*qaIs2241*	on	346	16	
egl-9; gcy-36	on	312	*egl-9*	on	588	34	**
egl-9; gcy-36	on	312	*gcy-36*	on	237	48	**
gcy-35; egl-9	on	358	*egl-9*	on	588	33	**
gcy-35; egl-9	on	358	*gcy-35*	on	240	51	**
osm-9; egl-9	on	365	*egl-9*	on	588	43	**
osm-9; egl-9	on	365	*osm-9*	on	249	61	**
ocr-2; egl-9	on	387	*egl-9*	on	588	27	**
ocr-2; egl-9	on	387	*ocr-2*	on	254	32	**
osm-9 ocr-2; egl-9	on	352	*egl-9*	on	588	30	**
osm-9 ocr-2; egl-9	on	352	*osm-9 ocr-2*	on	259	83	**
egl-9; npr-1	on	291	*egl-9*	on	588	27	**
egl-9; npr-1	on	291	*npr-1*	on	627	53	**
hif-1; npr-1	on	245	*hif-1*	on	364	50	**
hif-1; npr-1	on	245	*npr-1*	on	627	6	
daf-7; egl-9	on	320	*egl-9*	on	588	7	
daf-7; egl-9	on	320	*daf-7*	on	589	11	
egl-9; daf-3	on	373	*egl-9*	on	588	4	
egl-9; daf-3	on	373	*daf-3*	on	197	27	**
tph-1; egl-9	on	294	*egl-9*	on	588	42	**
tph-1; egl-9	on	294	*tph-1*	on	436	14	
tph-1; egl-9; NSM+ADF::tph-1	on	300	*egl-9*	on	588	58	**
tph-1; egl-9; NSM+ADF::tph-1	on	300	*tph-1; egl-9*	on	294	10	
egl-9; egl-9::egl-9 Line 1	on	249	*egl-9*	on	588	32	**
egl-9; egl-9::egl-9 Line 2	on	261	*egl-9*	on	588	33	**
egl-9; H20::egl-9	on	255	*egl-9*	on	588	20	
egl-9; tph-1::egl-9	on	296	*egl-9*	on	588	9	
egl-9; myo-3::egl-9	on	270	*egl-9*	on	588	22	*
egl-9; myo-2::egl-9	on	365	*egl-9*	on	588	19	
N2 1% 2 days	on	449	N2	on	1161	133	**
hif-1 1% 2 days	on	372	*hif-1*	on	364	11	
N2 1% 2 days	on	449	*hif-1* 1% 2 days	on	372	69	**
N2 1% 6 hrs	on	271	N2	on	1161	69	**
hif-1 1% 6 hrs	on	376	*hif-1*	on	364	37	**
N2 1% 6 hrs	on	271	*hif-1* 1% 6 hrs	on	376	9	
N2 1% 6 hrs	on	271	N2 1% 2 days	on	449	10	
hif-1 1% 6 hrs	on	376	*hif-1* 1% 2 days	on	372	32	**

Table 3-3. Median preferred oxygen concentrations in a 0-21% oxygen gradient.

n, number of assays. Each assay represents 80-100 animals.
p values are from Dunnett test against either N2 or *egl-9* control at the same food condition.
Blue indicates values less than control. Yellow indicates values greater than control.
SEM is standard error of the mean.

Genotype	Food	n	Median Preferred Oxygen Concentration (%)	SEM	vs. N2	vs. *egl-9*
N2	off	28	10.420	0.117		<0.01
egl-9	off	7	9.110	0.201	<0.01	
hif-1	off	6	10.676	0.434		<0.01
egl-9 hif-1	off	5	10.450	0.441		<0.05
egl-9; qaIs2241	off	6	10.335	0.708		<0.05
egl-9; gcy-36	off	3	11.303	0.352		<0.01
gcy-35; egl-9	off	6	9.788	0.244		
osm-9; egl-9	off	3	9.693	0.368		
ocr-2; egl-9	off	3	9.731	0.193		
osm-9 ocr-2; egl-9	off	3	10.018	0.304		
egl-9; npr-1	off	3	7.540	0.696	<0.01	<0.05
hif-1; npr-1	off	3	9.542	0.363		
daf-7; egl-9	off	3	8.715	0.598	<0.01	
egl-9; daf-3	off	4	9.654	0.204		
tph-1; egl-9	off	6	11.673	0.201	<0.01	<0.01
tph-1; egl-9; ADF:tph-1	off	3	11.620	0.142	<0.05	<0.01
tph-1; egl-9; NSM::tph-1	off	3	10.146	0.442		
tph-1; egl-9; NSM+ADF::tph-1	off	3	9.270	0.101		
egl-9; egl-9::egl-9 #1	off	5	9.753	0.391		
egl-9; egl-9::egl-9 #2	off	3	10.108	0.266		
egl-9; H20::egl-9	off	3	10.174	0.069		
egl-9; tph-1::egl-9	off	3	9.517	0.075		
egl-9; myo-3::egl-9	off	3	9.111	0.985	<0.05	
egl-9; myo-2::egl-9	off	3	9.542	0.331		
npr-1	off	6	10.111	0.400		
npr-1 1% 6 hrs	off	3	7.349	0.264	<0.01	<0.01
hif-1; npr-1 1% 6 hrs	off	3	7.660	0.254	<0.01	<0.05
N2	on	15	12.019	0.319		<0.01
egl-9	on	6	8.919	0.281	<0.01	
hif-1	on	6	12.200	0.706		<0.01
egl-9 hif-1	on	3	11.508	0.523		<0.01
egl-9; qaIs2241	on	4	9.763	0.226	<0.01	
egl-9; gcy-36	on	3	9.841	0.671	<0.01	
gcy-35; egl-9	on	3	9.755	0.327	<0.01	
osm-9; egl-9	on	3	10.437	0.227	<0.05	
ocr-2; egl-9	on	3	10.118	0.266	<0.05	
osm-9 ocr-2; egl-9	on	3	9.735	0.122	<0.01	
egl-9; npr-1	on	3	7.682	0.365	<0.01	
hif-1; npr-1	on	3	9.462	0.201	<0.01	
daf-7; egl-9	on	3	8.916	0.290	<0.01	
egl-9; daf-3	on	4	8.899	0.118	<0.01	
tph-1; egl-9	on	3	11.093	0.241		<0.05
tph-1; egl-9; NSM+ADF::tph-1	on	3	11.789	0.270		<0.01
egl-9; egl-9::egl-9 #1	on	3	10.441	0.410		
egl-9; egl-9::egl-9 #2	on	3	10.083	0.684		
egl-9; H20::egl-9	on	3	10.016	0.598	<0.01	
egl-9; tph-1::egl-9	on	3	8.817	0.115	<0.01	
egl-9; myo-3::egl-9	on	3	9.833	0.143	<0.01	
egl-9; myo-2::egl-9	on	4	8.421	0.311	<0.01	
N2 1% 6 hrs	on	3	8.507	0.413	<0.01	
hif-1 1% 6 hrs	on	4	9.244	0.183	<0.01	
N2 1% 2 days	on	4	8.039	0.157	<0.01	
hif-1 1% 2 days	on	4	11.683	0.492		<0.01

Figure 3-1. Upregulation of the HIF-1 pathway alters oxygen preference and sensory requirements for hyperoxia avoidance.

(A) Aerotaxis of wild-type N2 animals and *egl-9* mutants in a 0-21% oxygen gradient. The preferred oxygen range for *egl-9* mutants is shifted to lower oxygen (5-14%) vs. wild-type N2 animals (7-14%).

(B) Aerotaxis of *egl-9*, *hif-1*, and *egl-9 hif-1* mutants in a 0-21% oxygen gradient.

(C) Aerotaxis of wild-type N2 animals and *egl-9* mutants in a 0-10% oxygen gradient.

(D) Aerotaxis of *egl-9*, *hif-1*, and *egl-9 hif-1* mutants in a 0-10% oxygen gradient.

(E) Aerotaxis of *egl-9; qaIs2241* strain a 0-21% oxygen gradient. *qaIs2241* carries a transgene that kills the URX, AQR, and PQR neurons (Chang et al., 2006).

(F) Aerotaxis of *egl-9; gcy-36* mutants in a 0-21% oxygen gradient.

(G) Aerotaxis of *gcy-35; egl-9* mutants in a 0-21% oxygen gradient.

(H) Aerotaxis of *osm-9; egl-9* mutants in a 0-21% oxygen gradient.

(I) Aerotaxis of *ocr-2; egl-9* mutants in a 0-21% oxygen gradient.

(J) Aerotaxis of *osm-9 ocr-2; egl-9* mutants in a 0-21% oxygen gradient.

In B-J, asterisks denote distributions different by Chi-square analysis at $p < 0.01$ from the first distribution in the panel, unless otherwise noted. $n \geq 3$ assays per genotype, 80-100 animals/assay. Error bars are standard error of the mean (SEM).

(K) The hyperoxia avoidance index is defined as [average(fraction of animals in 5-14% O_2) - average(fraction of animals in 14-21% O_2)] / [average(fraction of animals in 5-14% O_2) + average(fraction of animals in 14-21% O_2)].

In K, asterisks denote values different from *egl-9* controls at $p < 0.01$ by Dunnett test. Error bars denote SEM.

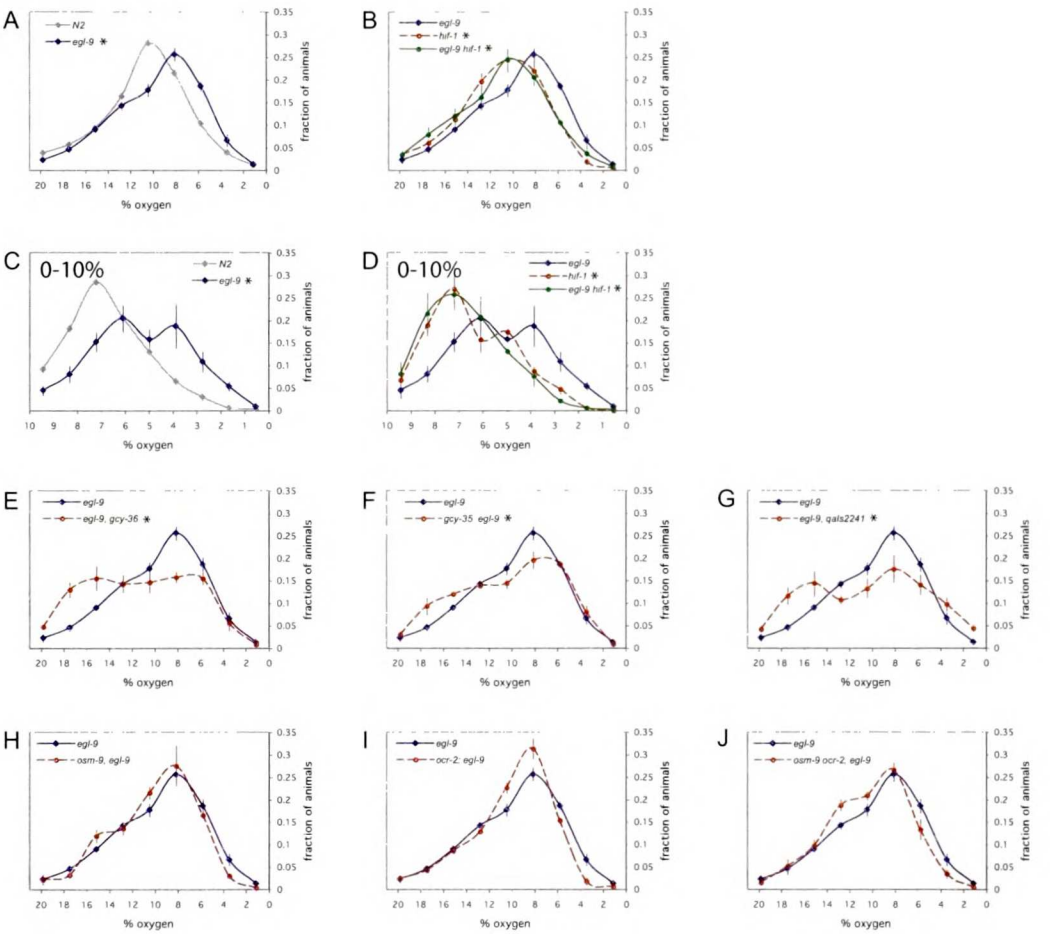
A
N2
egl-9 *
fraction of animals
% oxygen
B
egl-9
hif-1 *
egl-9 hif-1 *
C
0-10%
D
0-10%
E
egl-9
egl-9; gcy-36 *
F
egl-9
gcy-35 egl-9 *
G
egl-9
egl-9; qals2241 *
H
egl-9
osm-9; egl-9
I
egl-9
ocr-2; egl-9
J
egl-9
osm-9 ocr-2; egl-9

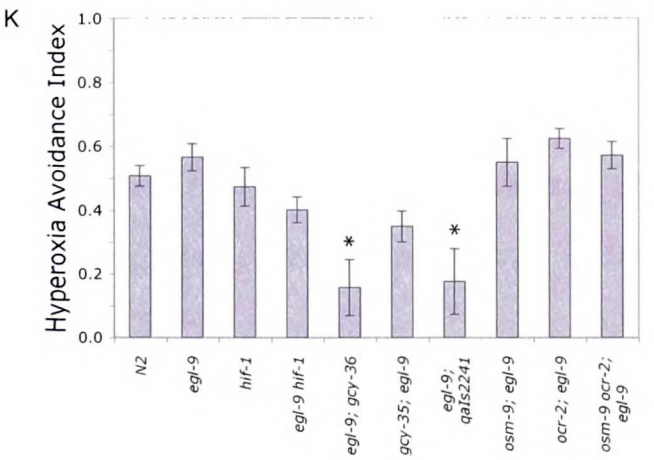
K
Hyperoxia Avoidance Index
N2
egl-9
hif-1
egl-9 hif-1
egl-9; gcy-36
gcy-35; egl-9
egl-9; qals2241
osm-9; egl-9
ocr-2; egl-9
osm-9 ocr-2; egl-9

Figure 3-2. Hyperoxia avoidance of *egl-9* mutants requires serotonin in multiple neurons.

(A) Aerotaxis of *tph-1; egl-9* double mutants

(B) Aerotaxis of *tph-1; egl-9* mutants rescued for *tph-1* in ADF neurons using a *srh-142::tph-1::gfp* transgene (Zhang et al., 2005).

(C) Aerotaxis of *tph-1; egl-9* mutants rescued for *tph-1* in NSM neurons using a *ceh-2::tph-1::gfp* transgene (Zhang et al., 2005).

(D) Aerotaxis of *tph-1; egl-9* mutants rescued for *tph-1* in NSM and ADF neurons using a transgenic array with both *ceh-2::tph-1::gfp* and *srh-142::tph-1::gfp* (Zhang et al., 2005).

For A-D, asterisks denote distributions different by Chi-square analysis at $p < 0.01$ from the first distribution in the panel, unless otherwise noted. NS, not significant. $n \geq 3$ assays per genotype, 80-100 animals/assay. Error bars denote SEM.

(E) Hyperoxia avoidance index as defined in Figure 3-1K. Asterisks, values different from *egl-9* controls at $p < 0.01$ by Dunnett test. Single cross, value different from *tph-1; egl-9* at $p < 0.05$ by Bonferroni *t* test with *egl-9* and *tph-1; egl-9*. Error bars denote SEM.

(F) Quantitation of *tph-1::GFP* fluorescence in ADF neurons. Asterisks, values different from *egl-9* controls at $p < 0.01$ by Dunnett test. $n \geq 15$ animals per genotype. Error bars denote SEM.

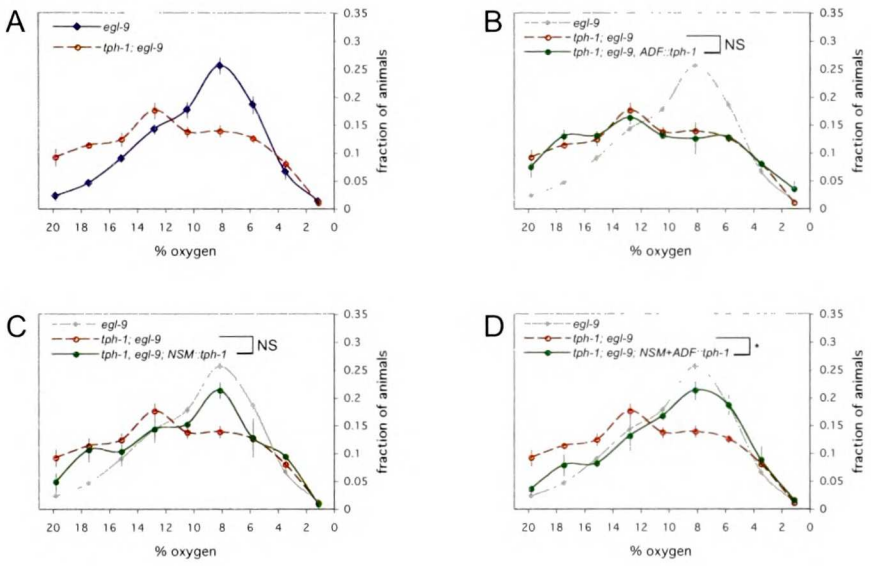
A
egl-9
tph-1; egl-9
fraction of animals
% oxygen
B
egl-9
tph-1; egl-9
tph-1; egl-9; ADF::tph-1
NS
fraction of animals
% oxygen
C
egl-9
tph-1; egl-9
tph-1, egl-9; NSM::tph-1
NS
fraction of animals
% oxygen
D
egl-9
tph-1; egl-9
tph-1; egl-9; NSM+ADF::tph-1
*
fraction of animals
% oxygen

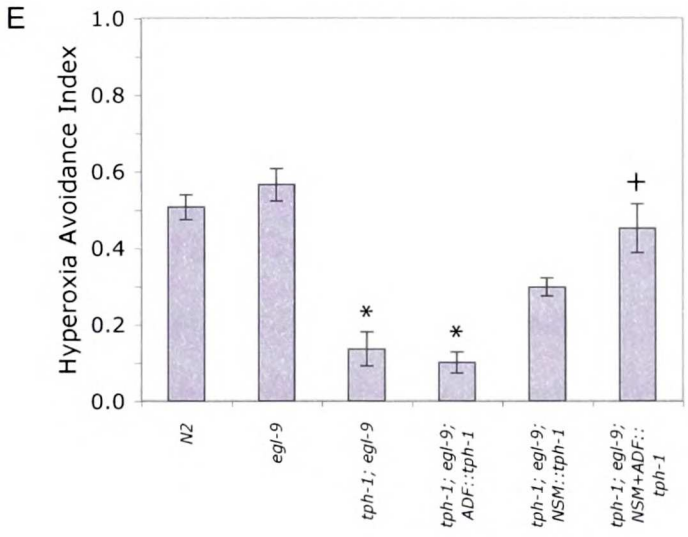
E
Hyperoxia Avoidance Index
N2
egl-9
tph-1; egl-9
tph-1; egl-9; ADF::tph-1
tph-1; egl-9; NSM::tph-1
tph-1; egl-9; NSM+ADF::tph-1

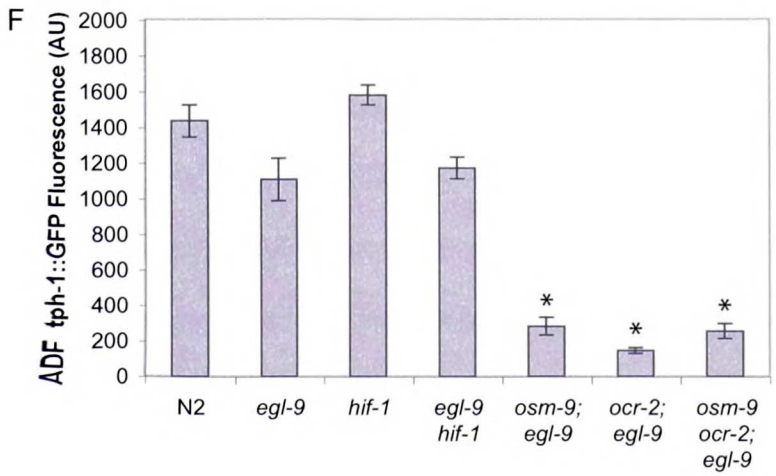
F
ADF tph-1::GFP Fluorescence (AU)
N2
egl-9
hif-1
egl-9 hif-1
osm-9; egl-9
ocr-2; egl-9
osm-9 ocr-2; egl-9

Figure 3-3. *egl-9* mutants avoid hyperoxia in the presence of food.

(A-J) In all panels, dotted lines indicate aerotaxis in the presence of a small amount of bacterial food.

(A) Aerotaxis of wild-type N2 animals.

(B) Aerotaxis of *egl-9* mutants.

(C) Aerotaxis of *hif-1* mutants.

(D) Aerotaxis of *egl-9 hif-1* double mutants.

(E) Aerotaxis of *egl-9; qaIs2241* strain. *qaIs2241* carries a transgene that kills the URX, AQR, and PQR neurons (Chang et al., 2006).

(F) Aerotaxis of *egl-9; gcy-36* double mutants.

(G) Aerotaxis of *gcy-35; egl-9* double mutants.

(H) Aerotaxis of *osm-9; egl-9* double mutants.

(I) Aerotaxis of *ocr-2; egl-9* double mutants.

(J) Aerotaxis of *osm-9 ocr-2; egl-9* triple mutants.

For A-J, asterisks denote distributions different by Chi-square analysis at $p < 0.01$ from the same genotype without food. $n \geq 3$ assays per genotype and condition, 80-100 animals/assay. Error bars denote SEM.

(K) Hyperoxia avoidance index as defined in Figure 3-1K. Asterisks denote values significantly different from the same genotype without food at $p < 0.05$ by t test. *ocr-2; egl-9* mutants did show a significantly difference in hyperoxia avoidance indices off and on food by t test ($p < 0.05$), but the distributions of these animals off and on food were not significant by Chi-square analysis ($p > 0.05$) (Table 3-2). Error bars denote SEM.

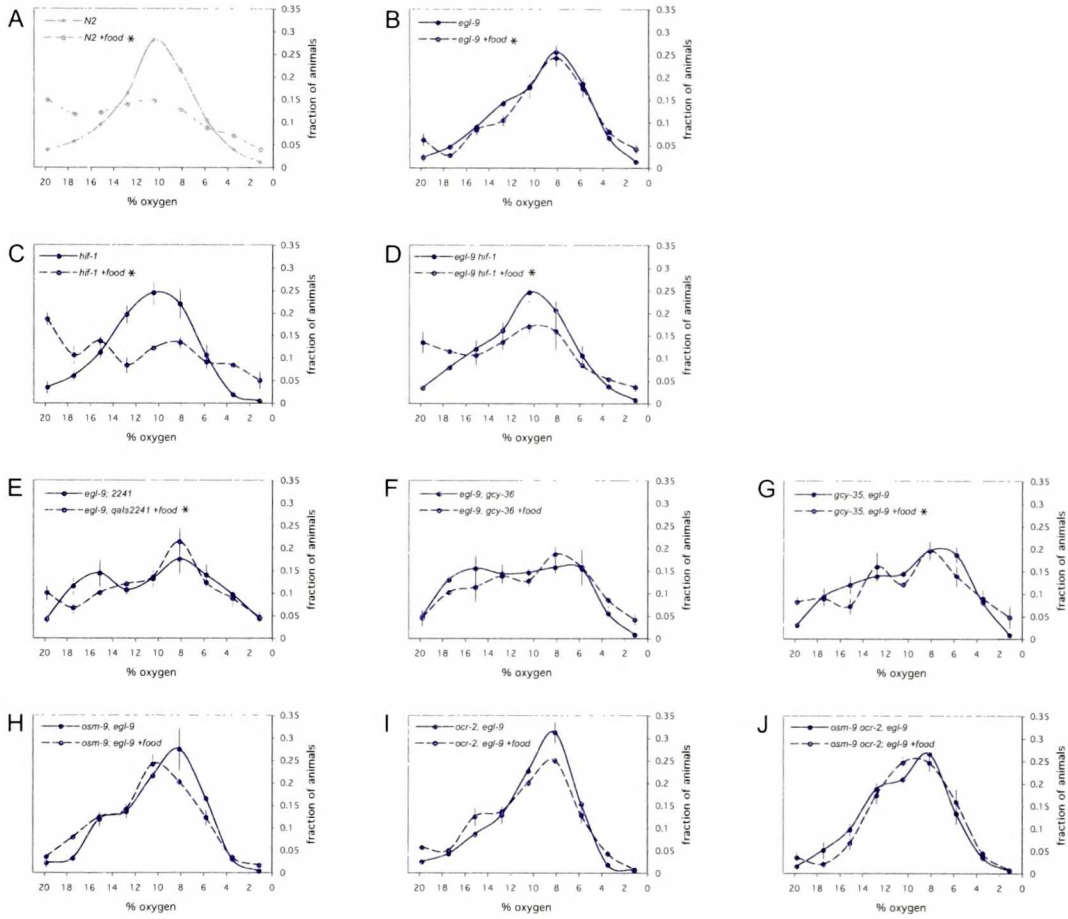
A
N2
N2 +food *
B
egl-9
egl-9 +food *
C
hif-1
hif-1 +food *
D
egl-9 hif-1
egl-9 hif-1 +food *
E
egl-9; 2241
egl-9, qals2241 +food *
F
egl-9; gcy-36
egl-9, gcy-36 +food
G
gcy-35; egl-9
gcy-35; egl-9 +food *
H
osm-9; egl-9
osm-9; egl-9 +food
I
ocr-2; egl-9
ocr-2; egl-9 +food
J
osm-9 ocr-2; egl-9
osm-9 ocr-2; egl-9 +food
fraction of animals
% oxygen

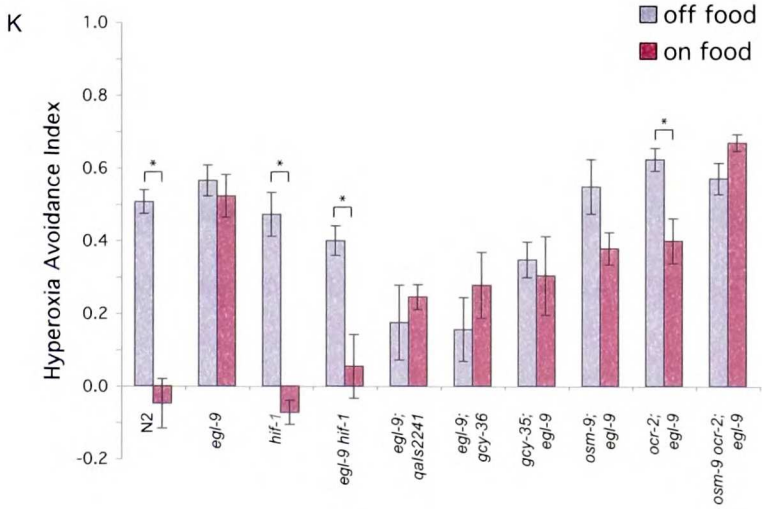
K
off food
on food
Hyperoxia Avoidance Index
N2
egl-9
hif-1
egl-9 hif-1
egl-9; qals2241
egl-9; gcy-36
gcy-35; egl-9
osm-9; egl-9
ocr-2; egl-9
osm-9 ocr-2; egl-9

Figure 3-4. The HIF-1 pathway acts in parallel to the NPR-1 and DAF-7 pathways for food regulation of hyperoxia avoidance.

(A-H) In all panels, dotted lines indicate aerotaxis in the presence of a small amount of bacterial food.

(A) Aerotaxis of wild-type N2 animals.

(B) Aerotaxis of *egl-9* mutants.

(C) Aerotaxis of *egl-9; npr-1* double mutants.

(D) Aerotaxis of *hif-1; npr-1* double mutants.

(E) Aerotaxis of *daf-7; egl-9* double mutants.

(F) Aerotaxis of *egl-9; daf-3* double mutants.

(G) Aerotaxis of *tph-1; egl-9* double mutants.

(H) Aerotaxis of *tph-1; egl-9* mutants rescued for *tph-1* in NSM and ADF neurons using a transgenic array with both *ceh-2::tph-1::gfp* and *srh-142::tph-1::gfp* (Zhang et al., 2005).

For A-H, asterisks denote distributions different by Chi-square analysis at $p < 0.01$ from the same genotype without food. $n \geq 3$ assays per genotype and condition, 80-100 animals/assay. Error bars denote SEM.

(I) Hyperoxia avoidance index as defined in Figure 3-1K. Asterisks, values significantly different from the same genotype without food at $p < 0.05$ by t test. Error bars denote SEM.

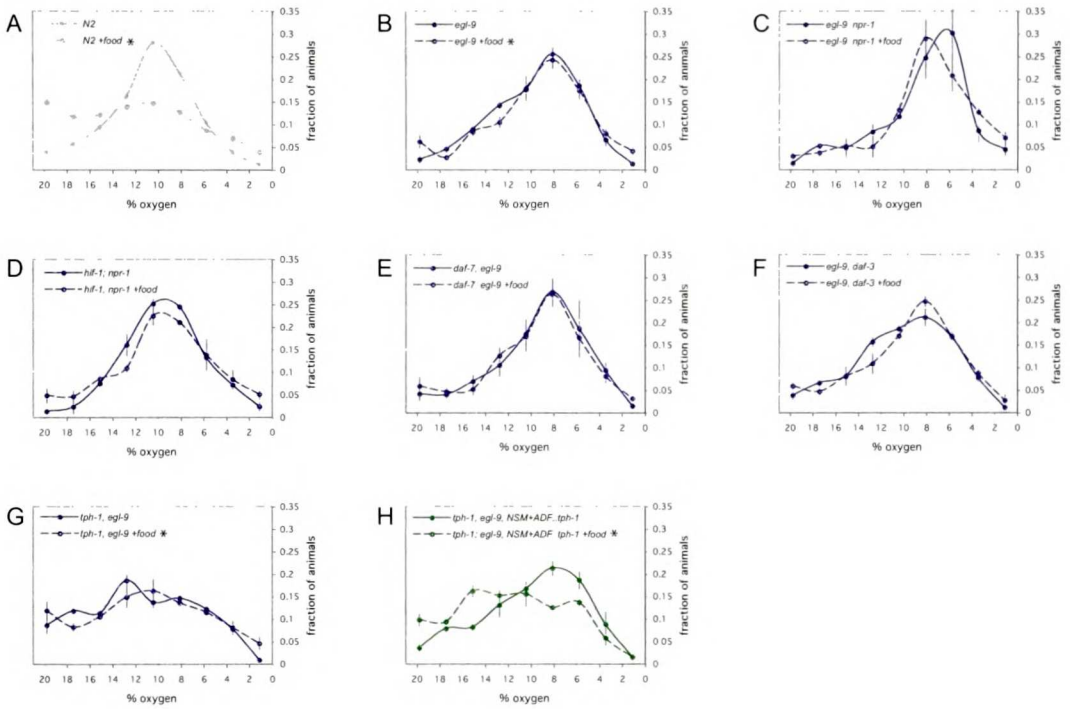
A
N2
N2 +food *
B
egl-9
egl-9 +food *
C
egl-9 npr-1
egl-9 npr-1 +food
D
hif-1; npr-1
hif-1; npr-1 +food
E
daf-7; egl-9
daf-7 egl-9 +food
F
egl-9; daf-3
egl-9; daf-3 +food
G
tph-1; egl-9
tph-1; egl-9 +food *
H
tph-1; egl-9; NSM+ADF::tph-1
tph-1; egl-9; NSM+ADF::tph-1 +food *
fraction of animals
% oxygen

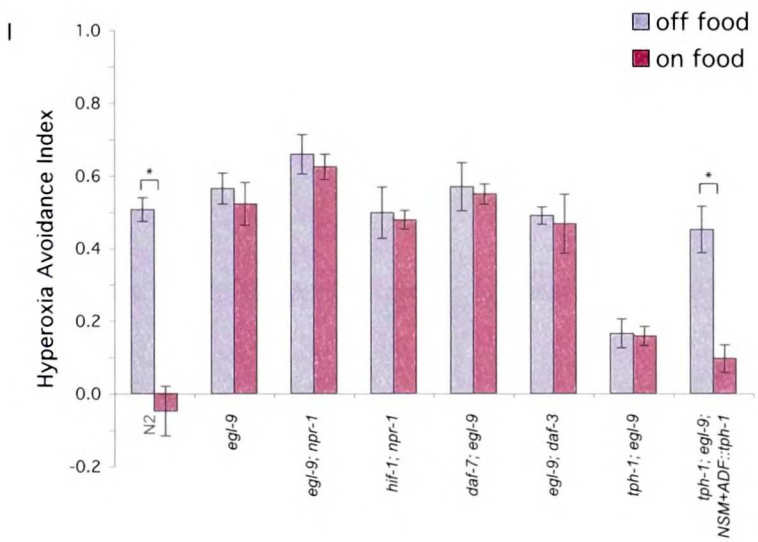
I
off food
on food
Hyperoxia Avoidance Index
N2
egl-9
egl-9; npr-1
hif-1; npr-1
daf-7; egl-9
egl-9; daf-3
tph-1; egl-9
tph-1; egl-9; NSM+ADF::tph-1

Figure 3-5. Cell-specific rescue of food regulation defect in *egl-9* mutants.

(A-H) In all panels, dotted lines indicate aerotaxis in the presence of a small amount of bacterial food.

(A) Aerotaxis of wild-type N2 animals.

(B) Aerotaxis of *egl-9* mutants.

(C) Aerotaxis of *egl-9* mutants rescued in *egl-9*-expressing cells using an *egl-9::egl-9::gfp* transgene. Line #1.

(D) Aerotaxis of *egl-9* mutants rescued in *egl-9*-expressing cells using an *egl-9::egl-9::gfp* transgene. Line #2.

(E) Aerotaxis of *egl-9* mutants rescued in most neurons using an *H20::egl-9::gfp* transgene.

(F) Aerotaxis of *egl-9* mutants rescued in NSM, ADF, and HSN neurons and gut using a *tph-1::egl-9::gfp* transgene.

(G) Aerotaxis of *egl-9* mutants rescued in body wall muscle using a *myo-3::egl-9::gfp* transgene.

(H) Aerotaxis of *egl-9* mutants rescued in pharyngeal muscle using a *myo-2::egl-9::gfp* transgene.

For A-H, asterisks denote distributions different by Chi-square analysis at $p < 0.01$ from the same genotype without food. $n \geq 3$ assays per genotype and condition, 80-100 animals/assay. Error bars denote SEM.

(I) Hyperoxia avoidance index as defined in Figure 3-1K. Asterisks, values significantly different from the same genotype without food at $p < 0.05$ by t test. Error bars denote SEM.

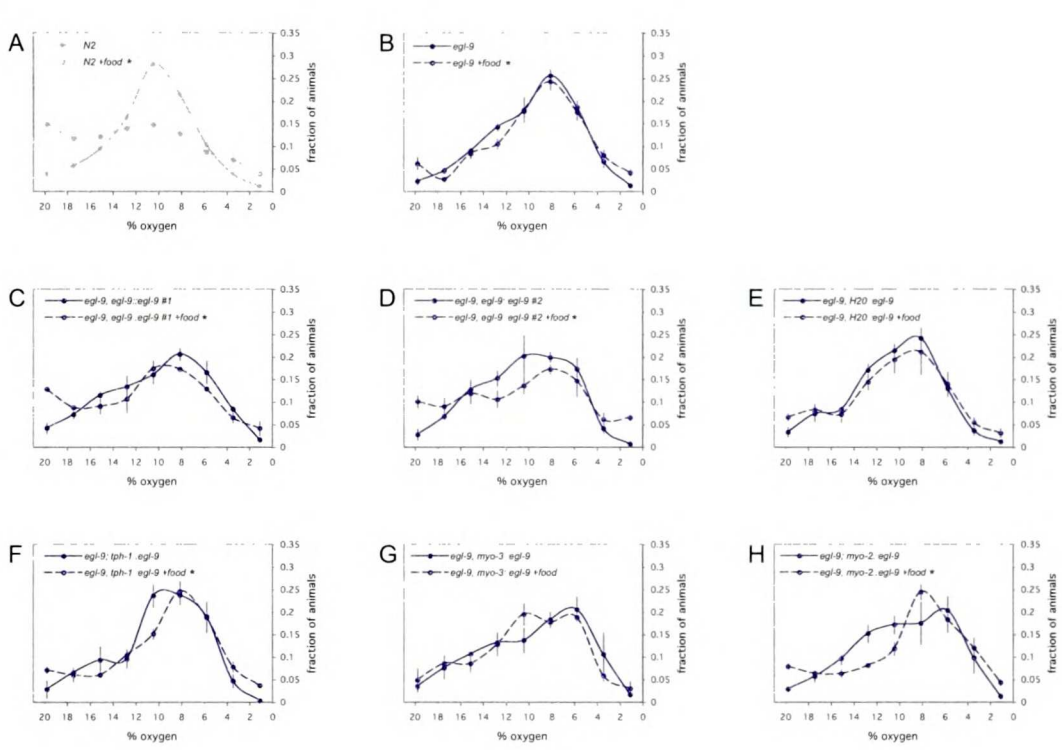
A
N2
N2 +food *
B
egl-9
egl-9 +food *
C
egl-9; egl-9::egl-9 #1
egl-9; egl-9::egl-9 #1 +food *
D
egl-9; egl-9::egl-9 #2
egl-9; egl-9::egl-9 #2 +food *
E
egl-9; H20::egl-9
egl-9; H20::egl-9 +food
F
egl-9; tph-1::egl-9
egl-9; tph-1::egl-9 +food *
G
egl-9; myo-3::egl-9
egl-9; myo-3::egl-9 +food
H
egl-9; myo-2::egl-9
egl-9; myo-2::egl-9 +food *
fraction of animals
% oxygen

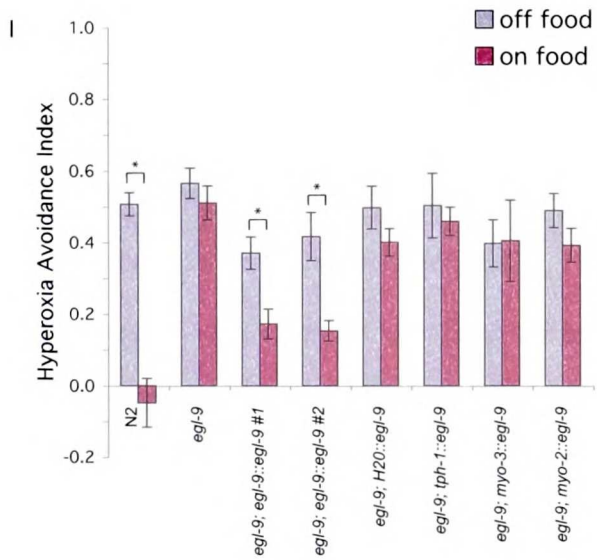
I
off food
on food
Hyperoxia Avoidance Index
N2
egl-9
egl-9; egl-9::egl-9 #1
egl-9; egl-9::egl-9 #2
egl-9; H20::egl-9
egl-9; tph-1::egl-9
egl-9; myo-3::egl-9
egl-9; myo-2::egl-9

Figure 3-6. NPR-1 and HIF-1 pathways modulate different aspects of hyperoxia avoidance.

(A) Aerotaxis of *npr-1* mutants grown in normal culture conditions and 1% oxygen for 6 hours as adults.

(B) Aerotaxis of *hif-1; npr-1* double mutants grown in normal culture conditions and 1% oxygen for 6 hours as adults.

(C) Aerotaxis of *npr-1* and *hif-1; npr-1* mutants grown in normal culture conditions.

(D) Aerotaxis of *npr-1* and *hif-1; npr-1* mutants grown in 1% oxygen for 6 hours as adults.

(E) Aerotaxis on food of wild-type N2 and *hif-1* mutants grown in 1% oxygen for 6 hours as adults.

(F) Aerotaxis on food of wild-type N2 and *hif-1* mutants grown in 1% oxygen for 2 days before adult.

For A-F, asterisks denote distributions different by Chi-square analysis at $p < 0.01$ from the first distribution in the panel, unless otherwise noted. $n \geq 3$ assays per genotype, 80-100 animals/assay. Error bars denote SEM.

(G) Hyperoxia avoidance index as defined in Figure 3-1K. Asterisks, values different from N2 or *hif-1* on food in normal culture conditions at $p < 0.01$ by Dunnett test. By t test, *hif-1* grown at 1% for 2 days was significantly different from N2 grown at 1% for 2 days ($p = 0.001$), but *hif-1* grown at 1% for 6 hours was not different from N2 grown at 1% for 6 hours ($p = 0.084$). Error bars denote SEM.

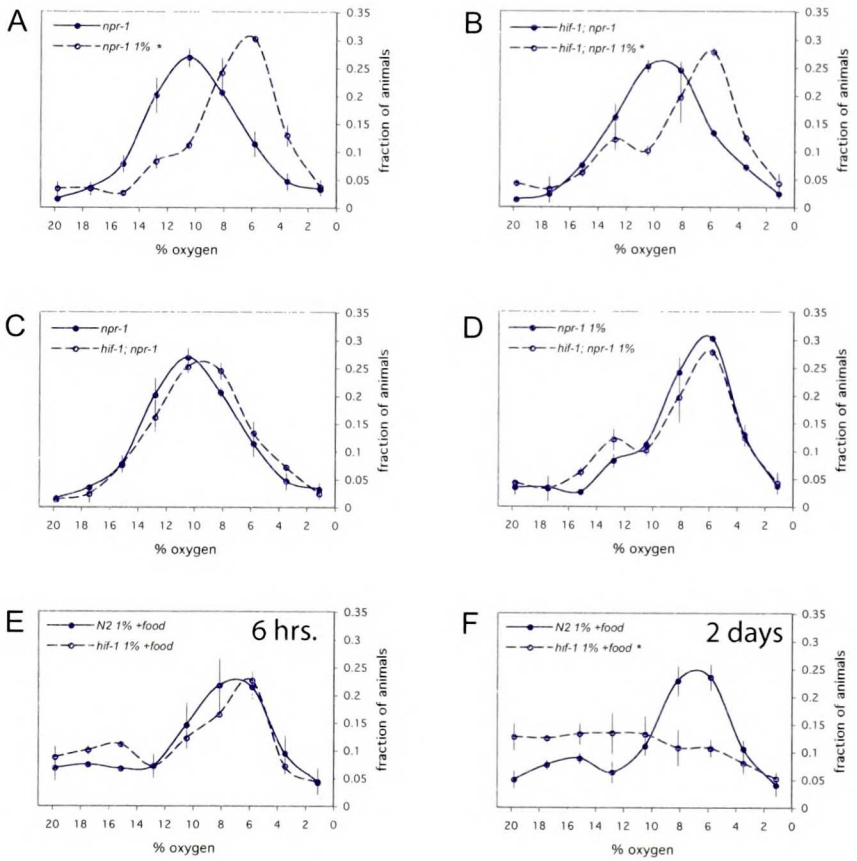
A
npr-1
npr-1 1% *
fraction of animals
% oxygen
B
hif-1; npr-1
hif-1; npr-1 1% *
C
hif-1; npr-1
D
npr-1 1%
hif-1; npr-1 1%
E
N2 1% +food
hif-1 1% +food
6 hrs.
F
2 days

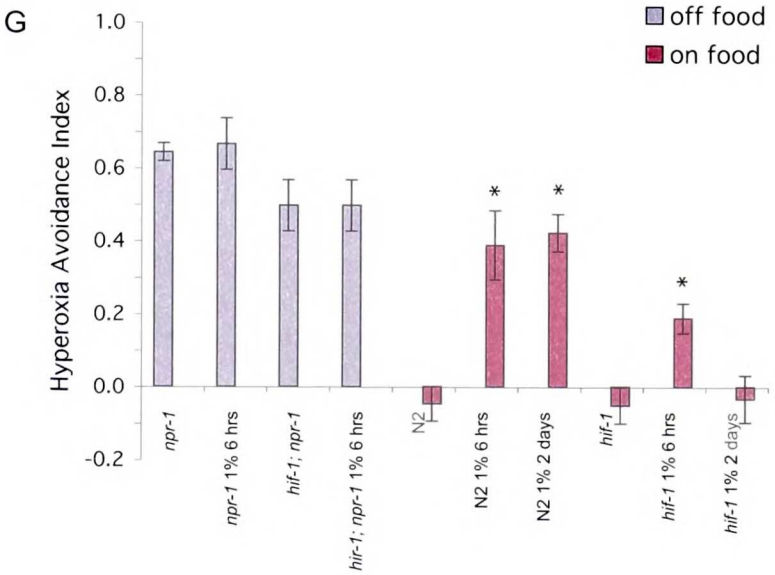
G
off food
on food
Hyperoxia Avoidance Index
npr-1
npr-1 1% 6 hrs
hif-1; npr-1
hif-1; npr-1 1% 6 hrs
N2
N2 1% 6 hrs
N2 1% 2 days
hif-1
hif-1 1% 6 hrs
hif-1 1% 2 days

Figure 3-7. An altered circuit for oxygen preference in *egl-9* mutants.

In the absence of food, a network of sensory neurons generates hyperoxia avoidance in *egl-9* mutants. Triangles denote sensory neurons; hexagons denote interneurons. URX, AQR, and PQR, and SDQ, ALN, and BDU neurons (abbreviated as "SDQ" for simplicity) express sGCs; these neurons are likely oxygen sensors. Unlike N2 and *npr-1* animals, *egl-9* mutants require the activity of URX, AQR, and PQR, and not TRPV channel-expressing neurons (ASH and ADF), for hyperoxia avoidance. In *egl-9* mutants, NSM instead of ADF neurons promote hyperoxia avoidance by producing serotonin. Synaptic connections to the AUA interneurons and AVA backward command neurons are shown; additional synapses are omitted. The NSM neurons receives inputs from multiple pharyngeal neurons and form *en passant* connections to the ventral nerve cord, but do not connect to other neurons in this circuit via chemical synapses (White et al., 1986). The larger, distributed network of neurons observed in N2 and *npr-1* animals for hyperoxia avoidance is reduced to a smaller, fixed network in *egl-9* mutants.

egl-9 mutants off food

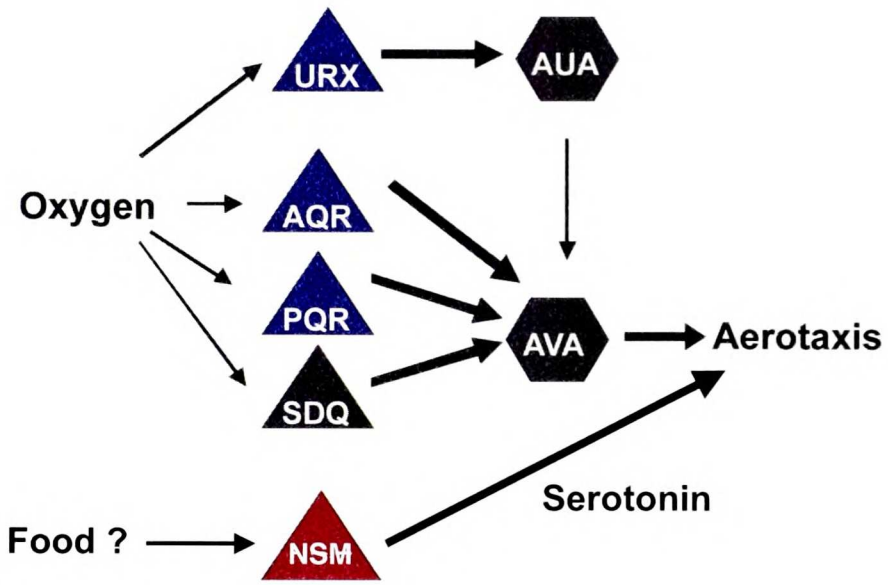

Chapter 4:

Hypoxia avoidance and feeding behavior

Introduction

For aerobic organisms, oxygen is critical for life. This is mainly due to the role of oxygen in the energy-producing process of cellular respiration, in which oxygen is the final electron acceptor in a series of chemical reactions that generate adenosine triphosphate (ATP) from organic molecules. The chemical energy in ATP is then used for all kinds of work inside the cell.

Hypoxia presents a challenging condition for aerobic organisms, yet many organisms can adapt to acute and chronic hypoxia. As mentioned in Chapter 3, the carotid body is an acute hypoxia-sensing cluster of cells in mammals (Lopez-Barneo, 2003), and the HIF-1 pathway is a highly conserved transcriptional pathway for oxygen homeostasis in response to hypoxia (Kaelin, 2005). While the term hypoxia refers generally to a shortage of environmental oxygen, ischemia refers specifically to the inadequate supply of oxygen to an organ, which can be caused by hypoxia as well as problems in the circulatory system. Organs such as the heart, brain, and kidneys are particularly sensitive to changes in oxygen supply. In the brain, ischemia caused by stroke or head injury leads to the ischemic cascade, a complex set of processes triggered by a drop in ATP levels that ultimately lead to excitotoxicity and cell death. These damaging effects can continue for days after ischemia (Fisher and Schaebitz, 2000). The return of oxygen supply after ischemia can lead to even more damage in a process called reperfusion injury that is partly caused by an inflammatory response (Rock and Yao, 2002). Interestingly, local ischemia in the brain can have effects different from anoxia throughout the entire body. Experiments in dogs and pigs show that these animals can be

resuscitated after prolonged exsanguination, or removal of blood, with minimal impact on brain function (Alam et al., 2002; Safar et al., 2000), in contrast with the toxicity of ischemia.

The effects of hypoxia and anoxia on physiology have been studied in the experimental animal *Caenorhabditis elegans*. In hypoxia (1% oxygen), the *hif-1* signaling pathway is required for normal reproductive growth of *C. elegans* (Jiang et al., 2001). In anoxia, the survival of larvae and adults decreases significantly after 72 hours, but embryos can survive longer by entering suspended animation, during which all microscopically observable movement ceases (Padilla et al., 2002). Suspended animation in anoxia is also observed in fruit fly, brine shrimp, killifish, and zebrafish embryos (Clegg, 1997; Foe and Alberts, 1985; Padilla and Roth, 2001; Podrabsky and Hand, 1999). Anoxic *C. elegans* embryos arrest in all phases of the cell cycle, except for anaphase, and resume cell cycle progression when oxygen levels increase again. Cell cycle arrest and survival in anoxia require spindle checkpoint components called *san-1* and *mdf-2*. While *san-1* and *mdf-2* are required for survival in anoxia, they are not required for survival in hypoxia (Nystul et al., 2003); conversely, *hif-1* is required for survival in hypoxia, but not required for survival in anoxia (Padilla et al., 2002). These results suggest that physiological adaptation to hypoxia and anoxia utilize distinct pathways.

Most animals living in aqueous environments avoid regions of hypoxia and anoxia, probably by modifying their behavior to find preferred oxygen concentrations (Wannamaker and Rice, 2000; Wu, 2002). In this chapter, I examine avoidance responses of *C. elegans* to hypoxia in a simple oxygen gradient assay as well as in a

complex feeding assay where bacterial food is presented in hypoxic conditions. My studies uncover two signaling pathways required for hypoxia avoidance: sensory signaling through the TAX-4/TAX-2 cyclic nucleotide-gated channel and hypoxia sensing through the canonical HIF-1 pathway.

Results

Hypoxia avoidance requires the TAX-4 cyclic nucleotide-gated channel in a subset of sensory neurons.

In a 0-21% oxygen gradient, the distribution of wild-type N2 animals suggests that *C. elegans* avoids both hyperoxia and hypoxia to accumulate at 7-14% oxygen (Chang et al., 2006; Gray et al., 2004). Studies that focused on hyperoxia avoidance were described in Chapters 2 and 3. To study hypoxia avoidance, I tested various candidate mutants in a 0-10% oxygen gradient using the same microfluidic device that has been described (Gray et al., 2004). In a 0-10% oxygen gradient, wild-type N2 accumulated at 4.4-9% oxygen, with a peak at 7% oxygen (Fig. 4-1). Because the fraction of animals/bin drops below random non-preference of any oxygen concentration (1.0 / 9 bins = 0.11/bin) at 4.4% oxygen (bin 6), I will consider 0-4.4% oxygen (bins 6-9) as the hypoxic range for these assays. In this chapter, "aerotaxis" will refer to distributions of animals, analyzed by Chi-square analysis (Tables 4-1 and 4-2), and "hypoxia avoidance" will refer to the fraction of animals in hypoxia (bins 6-9, 0-4.4% O_2).

Hyperoxia avoidance of wild-type N2 animals depends on the cyclic nucleotide gated-channel *tax-4* and the soluble guanylate cyclase homologs (sGCs) *gcy-36, gcy-35,*

and *gcy-34* in URX, AQR, and PQR neurons (Chang et al., 2006; Gray et al., 2004). I first tested if these sensory components were also used for hypoxia avoidance. Five sGCs, *gcy-32, gcy-34, gcy-35, gcy-36,* and *gcy-37,* are co-expressed in the URX, AQR, and PQR sensory neurons; *gcy-35* is also expressed in additional neurons (Gray et al., 2004). Available mutants of these sGCs did not have any defect in hypoxia avoidance (Fig. 4-1A, B, I); *gcy-37* could not be tested because no mutant was available. The two remaining sGCs in *C. elegans* are *gcy-31* and *gcy-33*, which are co-expressed in the BAG neurons ((Yu et al., 1997); J. Gray, personal communication). *gcy-33; gcy-31* double mutants were proficient in hypoxia avoidance (Fig. 4-1C, I). These results suggest that these sGCs are not individually required for hypoxia avoidance, although redundant functions are possible.

Mutants in the cGMP-gated channel TAX-4 were strongly defective for hypoxia avoidance compared to N2 animals (Fig. 4-1D, I). This hypoxia avoidance defect was not rescued by *tax-4* expression in URX, AQR, and PQR neurons using the *gcy-32* promoter (Fig. 4-1E, I), a transgene that can rescue the hyperoxia avoidance defect of *tax-4* mutants (Gray et al., 2004). Besides URX, AQR, and PQR, *tax-4* is expressed in numerous other sensory neurons (Komatsu et al., 1996). Expression of *tax-4* in sensory neurons that express the receptor chaperone gene *odr-4* rescued the *tax-4* hypoxia avoidance defect (Fig. 4-1F, I). *tax-4* and *odr-4* overlap in expression in AWB, AWC, ASG, ASI, ASJ, and ASK head sensory neurons (Dwyer et al., 1998; Komatsu et al., 1996). Chemotaxis towards benzaldehyde, a behavior mediated by TAX-4 signaling in AWC neurons (Bargmann et al., 1993; Komatsu et al., 1996), was also rescued by this *tax-4; odr-4::tax-4* strain, and not by *tax-4; gcy-32::tax-4* strains (data not shown).

These results suggest that *tax-4* activity promotes hypoxia avoidance through *odr-4*-expressing sensory neurons, a different set from those implicated in hyperoxia avoidance. The residual hypoxia avoidance in *tax-4* mutants further suggests that additional sensory pathways also contribute to hypoxia sensation.

Mutants in the TRPV channels *osm-9* and *ocr-2* are defective for hyperoxia avoidance (Chang et al., 2006). However, single mutants in these genes and the *osm-9 ocr-2* double mutant were proficient in hypoxia avoidance (Fig. 4-1G-I), further demonstrating that hypoxia avoidance may use a distinct circuit from hyperoxia avoidance.

Hypoxia avoidance is regulated by the HIF-1 pathway.

The prolyl hydroxylase EGL-9 is an oxygen-sensitive enzyme whose activity is inhibited by hypoxia (Epstein et al., 2001). In Chapter 3, I showed that mutants in *egl-9*, which have constitutively high activity of the HIF-1 transcriptional pathway (Epstein et al., 2001), prefer lower oxygen than wild-type N2 animals in 0-21% and 0-10% oxygen gradients (Fig. 3-1). In a 0-10% oxygen gradient, more *egl-9* mutants accumulated in hypoxia than N2 animals, a defect that was suppressed by loss of *hif-1* activity (Fig. 4-2A, B, E). Thus, under normal conditions, *egl-9* inhibits *hif-1* to promote hypoxia avoidance.

Aerotaxis in *tax-4; egl-9* double mutants was intermediate between *tax-4* and *egl-9* single mutants, (Fig. 4-2C, E), suggesting that these genes do not function in a simple epistasis relationship. One possible explanation is that *egl-9* affects both *tax-4*-dependent and *tax-4*-independent hypoxia sensing neurons. *gcy-35; egl-9* double mutants resembled

egl-9 single mutants (Fig. 4-2D, E); other sGCs were not examined in the *egl-9* background.

Feeding patterns on bacterial lawns are modified by hypoxic conditions.

In its natural soil environment, *C. elegans* may encounter situations where bacterial food is present in only in hypoxic conditions, due to high metabolism of bacteria in soil particles and the slow rate of oxygen diffusion in non-turbulent environments. To simulate this condition, we developed a simple assay we call the "agar plug assay," in which bacterial food is presented in a hypoxic context (Fig. 4-3A). In this assay, four *E. coli* bacterial lawns were grown overnight on NGM agar plates. The next day, two lawns were covered by NGM agar plugs, so that the lawns were sandwiched between two pieces of agar. Animals were transferred to the middle of the assay plate, and their distribution among the four lawns was scored shortly thereafter.

In chemotaxis assays, wild-type N2 animals are strongly attracted to *E. coli* lawns. In the agar plug assay, most N2 animals found both uncovered and covered lawn within 1 hour. Wild-type N2 animals distributed throughout bacterial lawns to feed, slightly favoring the edge of the lawn (de Bono and Bargmann, 1998; Gray et al., 2004) (data not shown). However, they avoided entering covered lawns: instead, they fed from the edge of these lawns, constantly moving around the lawn in a circular pattern. If no bacteria were present, animals moved freely under agar plugs (data not shown). Thus, it was the presence of bacteria in covered lawns that repelled N2 animals.

Was avoidance behavior in covered lawns due to hypoxia or other repellents produced by bacteria? An hour after application of the agar plug, the edge and center of

covered lawns corresponded to 4% and 3% oxygen, respectively (Fig. 4-3C), confirming that we had generated a hypoxic state at the edge of the lawn. These oxygen concentrations were much lower than those reported for the edge and center of uncovered bacterial lawns, which were 17% and 12%, respectively (Gray et al., 2004). Covered lawns had a linear oxygen gradient from 21% at the edge of the plug to 2-3% in the center of covered lawns (data not shown). Linear chemical gradients are generated by a constant source and sink, suggesting the diffusion of oxygen through aqueous agar is slow and that the bacterial lawn is a constant consumer of oxygen.

E. coli consumes oxygen during respiration; to slow down this metabolic process, I irradiated bacterial lawns with shortwave ultraviolet light (UV) and tested animals' response to the covered, irradiated lawns. UV light induces DNA damage, and UV treatment for 3 minutes was sufficient to prevent *E. coli* cells from subsequent growth when streaked out on LB agar (data not shown). However, these bactera were still metabolically active, as measured by their ability to consume oxygen. Oxygen concentrations in covered, irradiated lawns and the behavior of *C. elegans* towards the lawns varied in a dose-dependent manner from 3-9 minutes UV irradiation. Increasing the duration of UV treatment increased the concentration of oxygen at the edge and center of covered lawns (Fig. 4-3C), presumably by damaging *E. coli* cells severely enough to decrease rates of respiration. Correspondingly, more N2 animals accumulated in the center of covered lawns at higher oxygen (Fig. 4-3B). Thus, hypoxia is likely to be an important repulsive cue generated by covered lawns. I suggest that the agar plug assay represents a complex environment where attraction to bacterial food is countered by repulsion from hypoxia and possibly other chemical repellents generated by bacterial

metabolism. I will call this avoidance behavior in the agar plug assay "hypoxic lawn avoidance."

I tested a variety of mutants to see what mechanisms were important for hypoxic lawn avoidance. Mechanosensation did not appear to be important for hypoxic lawn avoidance, because *mec* mutants defective in body touch sensation did not show any alteration in the behavior (Chalfie and Sulston, 1981) (Table 4-3).

If the head or tail of an animal ever entered the covered lawn, the animals would immediately reverse or move forward as appropriate to exit the lawn. This behavior could arise from sensory integration by head and tail neurons. Several sensory neurons descended from Q cells are dispersed along the length of the animal. In larval development, one Q cell migrates to the anterior and the other to the posterior part of the animal; these cells then divide and differentiate into various cells along the body axis. *mab-5* mutants defective in Q cell migration, and thus the distribution of sensory neurons to the head or tail, were normal for hypoxic lawn avoidance (Harris et al., 1996) (Table 4-3). This result suggests that integration of signals between head and tail neurons derived from the Q cells was not necessary for lawn avoidance.

The cyclic nucleotide-gated channel TAX-4/TAX-2 is required for avoidance of covered lawns.

Because activity of the cyclic nucleotide-gated channel subunit TAX-4 was required for hypoxia avoidance in a 0-10% oxygen gradient (Fig. 4-1A, I), I tested mutants in subunits of the TAX-4/TAX-2 cyclic nucleotide-gated channel in the agar plug assay. In *C. elegans*, the *tax-4* and *tax-2* genes encode α and β subunits of a cyclic

nucleotide-gated channel (Coburn and Bargmann, 1996; Komatsu et al., 1996). Functional cation channels sensitive to cyclic guanosine monophosphate (cGMP) are formed by TAX-4 alone or TAX-4 and TAX-2 together, but not by TAX-2 alone (Komatsu et al., 1999; Komatsu et al., 1996). *tax-4* and *tax-2* are co-expressed in many sensory neurons, and mutants in *tax-4* and *tax-2* display defects in behaviors such as chemotaxis and thermotaxis (Coburn and Bargmann, 1996; Komatsu et al., 1996). Two point mutants in *tax-4* affecting highly conserved residues of α subunits, *ks11* and *ks28*, were defective in avoiding covering lawns, but an early stop mutant in *tax-4*, *p678*, was normal for lawn avoidance (Komatsu et al., 1996) (Fig. 4-4). *tax-2 (p694)* mutants, which may have reduced *tax-2* expression in only the AQR, AFD, ASE, and BAG neurons, were weakly defective for lawn avoidance while a strong behavioral mutant, *tax-2 (p691)*, was normal for lawn avoidance (Fig. 4-4). The *tax-4 (p691); tax-4 (p678)* double mutant was strongly defective in avoiding covered lawns, in contrast to the behavior of either single mutant (Fig. 4-4).

These results are consistent with a model in which TAX-4 and TAX-2 function together to promote avoidance of covered lawns and hypoxia. Because these subunits can form heteromeric TAX-4/TAX-2 channels as well as homomeric channels, assembly of channels with a defective α subunit, as in *tax-4 (ks11)* and *tax-4 (ks28)* mutants, may have a greater impact on sensory activity than channels lacking an α subunit, as in *tax-4 (p678)* mutants. In the absence of the TAX-4 α subunit, there are three other α subunits that might associate with the TAX-2 β subunit to form functional heteromeric channels. Two of these other α subunits, *cng-1* and *cng-3*, are expressed in subsets of sensory neurons that express *tax-2*. Mutants for these genes do not have behavioral defects (Cho

et al., 2005; Cho et al., 2004), but double mutants between *tax-4 (p678)* and *cng-1* or *cng-3* could be tested for lawn avoidance to address the hypothesis that these *cngs* play a hidden role in hypoxic lawn avoidance. The difference between *tax-2 (p694)* and *tax-2 (p691)* may result from complex effects of subsets of *tax-2*-expression neurons on feeding behavior in covered lawns. Because *tax-2 (p694)* affects only four sets of neurons, this mutation may affect only neurons that promote avoidance, while *tax-2 (p691)* may affect neurons that promote avoidance as well as those that mediate attraction to the lawn. Alternatively, the specific nature of the *p691* and *p694* mutations may be important.

To identify further components of hypoxic lawn avoidance, other signaling pathways in the *C. elegans* sensory system were tested in avoidance of covered lawns. Some of these signaling pathways overlap with TAX-4/TAX-2 function. Of the sGC-expressing neurons, URX, AQR, PQR, and BAG express *tax-4* and/or *tax-2* (Coburn and Bargmann, 1996; Komatsu et al., 1996), and *tax-4* activity in URX, AQR, and PQR is implicated in hyperoxia sensing (Gray et al., 2004). Single and combination mutants in sGCs and a transgenic strain that killed URX, AQR, and PQR (*qaIs2241*) were all normal (Table 4-3), suggesting that cGMP signaling through TAX-4/TAX-2 channels act in cells besides URX, AQR, PQR, and BAG to promote avoidance of covered lawns. These results are consistent with the failure to rescue the *tax-4* hypoxia avoidance defect in URX, AQR, and PQR (Fig. 4-1A, B, I) and the normal hypoxia avoidance of double mutants of *gcy-33* and *gcy-31*, which are co-expressed in BAG (Fig. 4-1F, I).

tax-4 and *tax-2* are also co-expressed in AWB and AWC neurons, which sense volatile repellents and attractants, respectively (Bargmann et al., 1993; Coburn and

Bargmann, 1996; Komatsu et al., 1996; Troemel et al., 1997). *lim-4* mutants affecting AWB cell fate and *odr-1* mutants defective in cGMP signaling in AWB and AWC were both normal in hypoxic lawn avoidance (L'Etoile and Bargmann, 2000; Sagasti et al., 1999) (Table 4-3). These results suggest that *tax-4* and *tax-2* may function in the different neurons (AFD, ASE, ASI, ASJ, ASK) to promote avoidance of covered lawns.

Signaling pathways that do not use the TAX-4/TAX-2 channels were also examined. Mutants in the TRPV channel subunits *osm-9* and *ocr-2* were proficient in hypoxic lawn avoidance, and in fact probably avoided more strongly than wild-type animals (Colbert et al., 1997; Tobin et al., 2002) (Table 4-3). Mutants in *osm-6*, which have defective cilium structure in all ciliated neurons, were also normal in avoidance (Collet et al., 1998) (Table 4-3). Thus, it is likely that oxygen sensation can occur in the absence of intact cilia.

Surprisingly, mutants in *odr-7*, which have an AWA cell fate defect, have a significant defect in hypoxic lawn avoidance (Sengupta et al., 1994) (Table 4-3). AWA neurons are known to promote attraction to volatile chemicals, but not known to mediate repulsive behaviors; it would be interesting if AWA can promote both attractive and repulsive behaviors. Alternatively, *odr-7* may affect another cell besides AWA for lawn avoidance behavior.

Neuromodulatory pathways linked to food regulation of behavior were examined. Even though *npr-1* neuropeptide signaling mutants prefer lower oxygen than N2 animals on food (Chang et al., 2006; Gray et al., 2004), they were normal for avoidance of covered lawns (Table 4-3), suggesting that they do not have hypoxia avoidance defects. *npr-1* mutants bordered and aggregated in social groups on uncovered lawns, but they did

not aggregate in social groups under agar plugs. Aggregation is suppressed at low oxygen concentrations (Gray et al., 2004); oxygen concentrations under agar plugs may be too low to induce aggregation behavior (data not shown).

Dopamine and serotonin signaling have been linked to food-regulated behaviors (Chao et al., 2004; Horvitz et al., 1982; Nuttley et al., 2002; Sawin et al., 2000; Zhang et al., 2005). Mutants that affect dopamine and serotonin signaling (*cat-1*, *cat-2*, and *tph-1*) (Duerr et al., 1999; Lints and Emmons, 1999; Sze et al., 2000) did not show any defects in hypoxic lawn avoidance (Table 4-3), suggesting that these modulatory pathways are not required for this behavior.

Upregulation of the HIF-1 pathway decreases avoidance of covered lawns.

HIF-1 signaling promotes survival in hypoxia and regulates hypoxia avoidance (Jiang et al., 2001) (Fig. 4-2). Mutants with constitutively high levels of HIF-1 protein, such as *egl-9* and *vhl-1*, may be better adapted for feeding in hypoxic conditions (Epstein et al., 2001). Two mutants in *egl-9*, *sa307* and *n571*, showed defects in avoiding covered lawns (Fig. 4-5), consistent with the *egl-9* hypoxia avoidance defect (Fig. 4-2). The defect in *egl-9 (sa307)* mutants was suppressed by a mutation in *hif-1* (Fig. 4-5), suggesting that *egl-9* acts through *hif-1* for its lawn avoidance phenotype.

Similarly, *vhl-1* mutants were defective for lawn avoidance in a *hif-1* dependent manner (Fig. 4-5). The *vhl-1* lawn avoidance defect was attenuated in sensitized conditions where lawns were treated with 3 minutes of UV irradiation (Fig. 4-5B). *vhl-1* mutants had a weaker defect than *egl-9 (sa307)* and *egl-9 (n571)* mutants (Fig. 4-5), even though *egl-9* and *vhl-1* mutants have similarly high levels of HIF-1 protein (Shen et al.,

2006). *egl-9* mutants have higher expression of *hif-1*-dependent transcriptional targets than *vhl-1* mutants; thus, EGL-9 may affect both HIF-1 stability and activity to exert a stronger effect on HIF-1 signaling than VHL-1 (Shen et al., 2006).

To examine the interaction between the *tax-4/tax-2* and *egl-9/hif-1* pathways, I tested *tax-4 (ks28); egl-9 (sa307)* double mutants in hypoxic lawn avoidance. The defect of the double mutant was not enhanced compared to either single mutant (Fig. 4-5), similar to the result from hypoxia avoidance (Fig. 4-1 and 4-2). With no UV treatment, *tax-4 (ks28); egl-9 (sa307)* double mutants resembled *egl-9 (sa307)* single mutants rather than *tax-4 (ks28)* single mutants, suggesting a complex interaction between these pathways. With 3 minutes UV treatments, these mutants were indistinguishable. These results suggest a complex interaction between the *tax-4/tax-2* and *egl-9/hif-1* pathways under different conditions.

Interestingly, one mutant in *egl-9*, *sa330*, was not defective in hypoxic lawn avoidance (Fig. 4-5). For *egl-9* mutants, the lawn avoidance defect correlated with defects in bordering and egg-laying behavior on food: *sa307* and *n571* mutants bordered strongly and were egg-laying defective while *sa330* mutants did not border and had normal egg-laying behavior (Darby et al., 1999; Trent et al., 1983). *sa307* and *n571* mutants also have higher constitutive levels of HIF-1 protein than *sa330* mutants (Epstein et al., 2001). This suggests that very high levels of HIF-1 protein may be required to generate behavioral defects. The *sa330* mutation is an early stop codon, and *sa307* and *n571* mutations lie further downstream in the *egl-9* sequence (Darby et al., 1999). There are multiple isoforms of *egl-9*, two of which start downstream of the *sa330* stop codon and may not be affected by the *sa330* mutation. Perhaps these shorter *egl-9* isoforms are

sufficiently produced and active in *sa330* mutants to regulate normal behavior. Nevertheless, all three *egl-9* mutants exhibit similar levels of resistance to fast-killing toxins made by the pathogenic bacterium *Pseudomonas aeruginosa* (Darby et al., 1999), suggesting that the N-terminus of EGL-9 may be required for some phenotypes and not others.

Discussion

In this chapter, I used a simple oxygen gradient assay and a complex agar plug assay to study hypoxia avoidance in *C. elegans*. Using a candidate approach, these assays identified two pathways that promote hypoxia avoidance: sensory signaling through the cyclic nucleotide-gated channel TAX-4/TAX-2 and hypoxia sensing through the HIF-1 pathway. Unlike hyperoxia avoidance, hypoxia avoidance does not require the activity of soluble guanylate homologs or URX, AQR, and PQR neurons. Instead, hypoxia avoidance requires *tax-4* activity in a subset of sensory neurons in the head, a set of neurons in which no acute oxygen sensor has been identified to date.

EGL-9 is unlikely to be the direct oxygen sensor for rapid hypoxia avoidance because EGL-9 acts through a transcription factor, HIF-1. Downregulation of EGL-9 activity by hypoxia results in accumulation of HIF-1 protein over hours, and HIF-1 acts through transcriptional regulation (Epstein et al., 2001). Nevertheless, constitutive upregulation of the HIF-1 pathway by mutations in *egl-9* and *vhl-1* may set a different oxygen preference for animals by regulating downstream targets with oxygen-sensing functions (Epstein et al., 2001). Because *egl-9* and *vhl-1* mutants have high HIF-1 levels

comparable to wild-type animals grown in hypoxia, they may be behaviorally adapted to prefer lower oxygen and suppress hypoxia avoidance.

The agar plug assay is a complex configuration in which bacterial food generates both attractive and repulsive cues to *C. elegans*. When lawns are presented under agar plugs, *C. elegans* must balance its attraction to food with dangerously low oxygen conditions in these lawns. Animals successfully solve this problem by feeding only from the edge of covered lawns, thereby minimizing their exposure to low oxygen while gaining sustenance.

Under agar plugs, animals adopt a locomotory strategy of maintaining a circular path around covered lawns that resembles isothermal tracking in a radial temperature gradient (Mori and Ohshima, 1995). How this deterministic behavior is maintained would be interesting to elucidate, as other *C. elegans* behaviors, such as chemotaxis, can be explained simply by a stochastic, biased random walk model (Pierce-Shimomura et al., 1999). In addition, the rapid withdrawal of animals that enter a covered lawn suggests that integration of signals between head and tail cells may be crucial for hypoxia avoidance.

Materials and Methods

Strains

Strains were cultured under standard conditions (Brenner, 1974) and fed *E. coli* HB101. Wild-type animals were *C. elegans* Bristol strain N2. Other strains used in this work include: FK103 *tax-4 (ks28)* III, CX6743 *tax-4 (ks28)* III; *kyEx745 [gcy-32::tax-4::gfp, unc-122::gfp]*, CX6752 *tax-4 (ks28)* III; *kyEx748 [odr-4::tax-4::gfp, unc-122::gfp]*, FK129 *tax-4 (ks11)* III, PR678 *tax-4 (p678)* III, PR694 *tax-2 (p694)* I, PR691 *tax-2 (p691)* I, CX2989 *tax-2 (p691)* I; *tax-4 (p678)* III, AX1297 *gcy-36 (db66)* X, CX6448 *gcy-35 (ok769)* I, RB1062 *gcy-34 (ok1012)* V, CX6804 *gcy-32 (ok995)* V, CZ3805 *gcy-33 (ok232)* V; *gcy-31 (ok296)* X, CX7102 *lin-15 (n765) qaIs2241 [gcy-36::egl-1, gcy-35::gfp, lin-15(+)]* X, XA2262 *gcy-33 (ok232)* V; *gcy-31 (ok296) qaIs2241* X, CX6422 *gcy-35 (ok769)* I; *gcy-33 (ok232)* V; *gcy-31 (ok296) qaIs2241* X, JT307 *egl-9 (sa307)* V, ZG31 *hif-1 (ia4)* V, CX6571 *egl-9 (sa307) hif-1 (ia4)* V, CX6745 *gcy-35 (ok769)* I; *egl-9 (sa307)* V, CX6608 *tax-4 (ks28)* III; *egl-9 (sa307)* V, MT1201 *egl-9 (n571)* V, JT330 *egl-9 (sa330)* V, CB5602 *vhl-1 (ok161)* X, CX6562 *hif-1 (ia4)* V; *vhl-1 (ok161)* X, DA609 *npr-1 (ad609)* X, CX4057 *npr-1 (g320)* X, CX4991 *lim-4 (ky403)* X, CX2065 *odr-1 (n1936)* X, CX4 *odr-7 (ky4)* X, CX4537 *osm-9 (ky10)* IV, CX4544 *ocr-2 (ak47)* IV, CX4651 *osm-9 (ky10) ocr-2 (ak47)* IV, PR811 *osm-6 (p811)* V, CB75 *mec-2 (e75)* X, CB1338 *mec-3 (e1338)* IV, CB1339 *mec-4 (e1339)* X, CB1111 *cat-1 (e1111)* X, CB1112 *cat-2 (e1112)* II, GR1321 *tph-1 (mg280)* II, CB1239 *mab-5 (e1239)* III, CF911 *mab-5 (e2008)* III, CB3256 *mab-5 (e1751gf)* III. Unless indicated, null alleles or strong loss-of-function alleles were used.

Behavioral Assays

Aerotaxis assays were performed by placing animals on nematode growth medium (NGM) agar in custom-made microfluidic devices fabricated from polydimethylsiloxane with a gas-phase linear gradient from 0-10% oxygen, and monitoring animals' accumulation in nine bins across the gradient (Gray et al., 2004). Gradients were generated by delivering gases under laminar flow to source and drain chambers immediately outside the behavioral arena, using a syringe pump; diffusion of the gases established the gradient in the small assay chamber. For 0-10% gradients, 100% nitrogen and 10% oxygen/90% nitrogen gases were used. Gases were obtained from Airgas (Radnor, Pennsylvania), Matheson (Montgomeryville, Pennsylvania), and TW Smith (Brooklyn, New York). Animals were prepared for assays as described (Chang et al., 2006). Results from two devices were binned for one assay (~80-100 animals per assay). At least three independent assays on three different days for each genotype were used to generate the results. Data presented represent distributions 25 minutes from start of the assay.

For the agar plug assay (Fig. 4-3A), the assay plate contained 4 lawns of 15 μl *E. coli* HB101 seeded on NGM agar and grown overnight. When indicated, lawns were irradiated by shortwave UV after overnight growth. Before transfer of animals, two lawns were covered by circular plugs of NGM agar that were larger than these lawns, such that these lawns were sandwiched between two layers of agar. 100-200 adult animals were transferred to the middle of the plate by washing. The fraction of animals in the center of covered lawns equals the total number of animals inside covered lawns divided by the total number of animals under agar plugs on one assay plate. At least

three assay plates were used to generate the results. The fraction of animals was scored at 1 and 4 hours from start of the assay.

Direct oxygen measurements of oxygen concentrations in the agar plug were performed using a Clark-style microelectrode (Diamond Microsensors, Ann Arbor, Michigan), calibrated with standards before use.

Statistical Analysis

Statistical analysis of aerotaxis was conducted in multiple steps. The nine individual points in the aerotaxis assay are not independent – accumulation of animals in one bin necessarily affects all other bins – so they cannot be analyzed individually. A first test to assess the overall distribution of animals in the aerotaxis assay was a comparison of experimental strains to controls by Chi-square analysis (nine bins per aerotaxis assay x 2 strains = 8 degrees of freedom). Chi-square analysis takes into account the non-Gaussian nature of the aerotaxis distributions as well as the total number of animals tested. It is overly conservative, because it combines all animals tested into a single contingency table and does not take into account the fact that each assay was repeated multiple times. Therefore, assays that are not statistically different by this criterion may actually be different. With this issue in mind, we have emphasized positive findings in this chapter. For controls such as N2 that were compared to multiple mutants, $p < 0.01$ was used as the level of significance for the Chi-square test. All results discussed explicitly in the text of this chapter were significant at $p < 0.001$ (Table 4-2). In the text, any stated differences in fraction of animals in low oxygen (bins 6-9, 0-4.4% O_2) had also passed this first test using Chi-square analysis of the entire distribution ($p <$

0.01). Each strain or condition was tested in at least 3 assays with ~80-100 animals each, and the mean fraction of animals in low oxygen across all assays was used to test significance.

For all data described in this chapter, *t* tests were used to compare between two data points. Analysis of variance (ANOVA) plus Bonferroni *t* tests or Dunnett tests were conducted for multiple comparisons of data points (Statview, Cary, North Carolina). For controls such as N2 that were compared to multiple mutants, $p < 0.01$ was used as the level of significance.

References

Alam, H. B., Bowyer, M. W., Koustova, E., Gushchin, V., Anderson, D., Stanton, K., Kreishman, P., Cryer, C. M., Hancock, T., and Rhee, P. (2002). Learning and memory is preserved after induced asanguineous hyperkalemic hypothermic arrest in a swine model of traumatic exsanguination. Surgery *132*, 278-288.

Bargmann, C. I., Hartwieg, E., and Horvitz, H. R. (1993). Odorant-selective genes and neurons mediate olfaction in C. elegans. Cell *74*, 515-527.

Brenner, S. (1974). The genetics of Caenorhabditis elegans. Genetics *77*, 71-94.

Chalfie, M., and Sulston, J. (1981). Developmental genetics of the mechanosensory neurons of Caenorhabditis elegans. Dev Biol *82*, 358-370.

Chang, A. J., Chronis, N., Karow, D. S., Marletta, M. A., and Bargmann, C. I. (2006). A distributed chemosensory circuit for oxygen preference in C. elegans. PLoS Biol *4*, e274.

Chao, M. Y., Komatsu, H., Fukuto, H. S., Dionne, H. M., and Hart, A. C. (2004). Feeding status and serotonin rapidly and reversibly modulate a Caenorhabditis elegans chemosensory circuit. Proc Natl Acad Sci U S A *101*, 15512-15517.

Cho, S. W., Cho, J. H., Song, H. O., and Park, C. S. (2005). Identification and characterization of a putative cyclic nucleotide-gated channel, CNG-1, in C. elegans. Mol Cells *19*, 149-154.

Cho, S. W., Choi, K. Y., and Park, C. S. (2004). A new putative cyclic nucleotide-gated channel gene, cng-3, is critical for thermotolerance in Caenorhabditis elegans. Biochem Biophys Res Commun *325*, 525-531.

Clegg, J. (1997). Embryos of Artemia franciscana survive four years of continuous anoxia: the case for complete metabolic rate depression. J Exp Biol *200*, 467-475.

Coburn, C. M., and Bargmann, C. I. (1996). A putative cyclic nucleotide-gated channel is required for sensory development and function in C. elegans. Neuron *17*, 695-706.

Colbert, H. A., Smith, T. L., and Bargmann, C. I. (1997). OSM-9, a novel protein with structural similarity to channels, is required for olfaction, mechanosensation, and olfactory adaptation in Caenorhabditis elegans. J Neurosci *17*, 8259-8269.

Collet, J., Spike, C. A., Lundquist, E. A., Shaw, J. E., and Herman, R. K. (1998). Analysis of osm-6, a gene that affects sensory cilium structure and sensory neuron function in Caenorhabditis elegans. Genetics *148*, 187-200.

Darby, C., Cosma, C. L., Thomas, J. H., and Manoil, C. (1999). Lethal paralysis of Caenorhabditis elegans by Pseudomonas aeruginosa. Proc Natl Acad Sci U S A *96*, 15202-15207.

de Bono, M., and Bargmann, C. I. (1998). Natural variation in a neuropeptide Y receptor homolog modifies social behavior and food response in C. elegans. Cell *94*, 679-689.

Duerr, J. S., Frisby, D. L., Gaskin, J., Duke, A., Asermely, K., Huddleston, D., Eiden, L. E., and Rand, J. B. (1999). The cat-1 gene of Caenorhabditis elegans encodes a vesicular monoamine transporter required for specific monoamine-dependent behaviors. J Neurosci *19*, 72-84.

Dwyer, N. D., Troemel, E. R., Sengupta, P., and Bargmann, C. I. (1998). Odorant receptor localization to olfactory cilia is mediated by ODR-4, a novel membrane-associated protein. Cell *93*, 455-466.

Epstein, A. C., Gleadle, J. M., McNeill, L. A., Hewitson, K. S., O'Rourke, J., Mole, D. R., Mukherji, M., Metzen, E., Wilson, M. I., Dhanda, A., *et al.* (2001). C. elegans EGL-9

and mammalian homologs define a family of dioxygenases that regulate HIF by prolyl hydroxylation. Cell *107*, 43-54.

Fisher, M., and Schaebitz, W. (2000). An overview of acute stroke therapy: past, present, and future. Arch Intern Med *160*, 3196-3206.

Foe, V. E., and Alberts, B. M. (1985). Reversible chromosome condensation induced in Drosophila embryos by anoxia: visualization of interphase nuclear organization. J Cell Biol *100*, 1623-1636.

Gray, J. M., Karow, D. S., Lu, H., Chang, A. J., Chang, J. S., Ellis, R. E., Marletta, M. A., and Bargmann, C. I. (2004). Oxygen sensation and social feeding mediated by a C. elegans guanylate cyclase homologue. Nature *430*, 317-322.

Harris, J., Honigberg, L., Robinson, N., and Kenyon, C. (1996). Neuronal cell migration in C. elegans: regulation of Hox gene expression and cell position. Development *122*, 3117-3131.

Horvitz, H. R., Chalfie, M., Trent, C., Sulston, J. E., and Evans, P. D. (1982). Serotonin and octopamine in the nematode Caenorhabditis elegans. Science *216*, 1012-1014.

Jiang, H., Guo, R., and Powell-Coffman, J. A. (2001). The Caenorhabditis elegans hif-1 gene encodes a bHLH-PAS protein that is required for adaptation to hypoxia. Proc Natl Acad Sci U S A *98*, 7916-7921.

Kaelin, W. G., Jr. (2005). Proline hydroxylation and gene expression. Annu Rev Biochem *74*, 115-128.

Komatsu, H., Jin, Y. H., L'Etoile, N., Mori, I., Bargmann, C. I., Akaike, N., and Ohshima, Y. (1999). Functional reconstitution of a heteromeric cyclic nucleotide-gated channel of Caenorhabditis elegans in cultured cells. Brain Res *821*, 160-168.

Komatsu, H., Mori, I., Rhee, J. S., Aiakie, N., and Ohshima, Y. (1996). Mutations in a cyclic nucleotide-gated channel lead to abnormal thermosensation and chemosensation in *C. elegans.* Neuron *17*, 707-718.

L'Etoile, N. D., and Bargmann, C. I. (2000). Olfaction and odor discrimination are mediated by the C. elegans guanylyl cyclase ODR-1. Neuron *25*, 575-586.

Lints, R., and Emmons, S. W. (1999). Patterning of dopaminergic neurotransmitter identity among Caenorhabditis elegans ray sensory neurons by a TGFbeta family signaling pathway and a Hox gene. Development *126*, 5819-5831.

Lopez-Barneo, J. (2003). Oxygen and glucose sensing by carotid body glomus cells. Curr Opin Neurobiol *13*, 493-499.

Mori, I., and Ohshima, Y. (1995). Neural regulation of thermotaxis in Caenorhabditis elegans. Nature *376*, 344-348.

Nuttley, W. M., Atkinson-Leadbeater, K. P., and Van Der Kooy, D. (2002). Serotonin mediates food-odor associative learning in the nematode Caenorhabditiselegans. Proc Natl Acad Sci U S A *99*, 12449-12454.

Nystul, T. G., Goldmark, J. P., Padilla, P. A., and Roth, M. B. (2003). Suspended animation in C. elegans requires the spindle checkpoint. Science *302*, 1038-1041.

Padilla, P. A., Nystul, T. G., Zager, R. A., Johnson, A. C., and Roth, M. B. (2002). Dephosphorylation of cell cycle-regulated proteins correlates with anoxia-induced suspended animation in Caenorhabditis elegans. Mol Biol Cell *13*, 1473-1483.

Padilla, P. A., and Roth, M. B. (2001). Oxygen deprivation causes suspended animation in the zebrafish embryo. Proc Natl Acad Sci U S A *98*, 7331-7335.

Pierce-Shimomura, J. T., Morse, T. M., and Lockery, S. R. (1999). The fundamental role of pirouettes in Caenorhabditis elegans chemotaxis. J Neurosci *19*, 9557-9569.

Podrabsky, J. E., and Hand, S. C. (1999). The bioenergetics of embryonic diapause in an annual killifish, austrofundulus limnaeus. J Exp Biol *202 (Pt 19)*, 2567-2580.

Rock, P., and Yao, Z. (2002). Ischemia reperfusion injury, preconditioning and critical illness. Curr Opin Anaesthesiol *15*, 139-146.

Safar, P., Tisherman, S. A., Behringer, W., Capone, A., Prueckner, S., Radovsky, A., Stezoski, W. S., and Woods, R. J. (2000). Suspended animation for delayed resuscitation from prolonged cardiac arrest that is unresuscitable by standard cardiopulmonary-cerebral resuscitation. Crit Care Med *28*, N214-218.

Sagasti, A., Hobert, O., Troemel, E. R., Ruvkun, G., and Bargmann, C. I. (1999). Alternative olfactory neuron fates are specified by the LIM homeobox gene lim-4. Genes Dev *13*, 1794-1806.

Sawin, E. R., Ranganathan, R., and Horvitz, H. R. (2000). C. elegans locomotory rate is modulated by the environment through a dopaminergic pathway and by experience through a serotonergic pathway. Neuron *26*, 619-631.

Sengupta, P., Colbert, H. A., and Bargmann, C. I. (1994). The C. elegans gene odr-7 encodes an olfactory-specific member of the nuclear receptor superfamily. Cell *79*, 971-980.

Shen, C., Shao, Z., and Powell-Coffman, J. A. (2006). The Caenorhabditis elegans rhy-1 Gene Inhibits HIF-1 Hypoxia-Inducible Factor Activity in a Negative Feedback Loop That Does Not Include vhl-1. Genetics *174*, 1205-1214.

Sze, J. Y., Victor, M., Loer, C., Shi, Y., and Ruvkun, G. (2000). Food and metabolic signalling defects in a Caenorhabditis elegans serotonin-synthesis mutant. Nature *403*, 560-564.

Tobin, D., Madsen, D., Kahn-Kirby, A., Peckol, E., Moulder, G., Barstead, R., Maricq, A., and Bargmann, C. (2002). Combinatorial expression of TRPV channel proteins defines their sensory functions and subcellular localization in C. elegans neurons. Neuron *35*, 307-318.

Trent, C., Tsuing, N., and Horvitz, H. R. (1983). Egg-laying defective mutants of the nematode Caenorhabditis elegans. Genetics *104*, 619-647.

Troemel, E. R., Kimmel, B. E., and Bargmann, C. I. (1997). Reprogramming chemotaxis responses: sensory neurons define olfactory preferences in C. elegans. Cell *91*, 161-169.

Wannamaker, C. M., and Rice, J. A. (2000). Effects of hypoxia on movements and behavior of selected estuarine organisms from the southeastern United States. J Exp Mar Biol Ecol *249*, 145-163.

Wu, R. S. (2002). Hypoxia: from molecular responses to ecosystem responses. Mar Pollut Bull *45*, 35-45.

Yu, S., Avery, L., Baude, E., and Garbers, D. L. (1997). Guanylyl cyclase expression in specific sensory neurons: a new family of chemosensory receptors. Proc Natl Acad Sci U S A *94*, 3384-3387.

Zhang, Y., Lu, H., and Bargmann, C. I. (2005). Pathogenic bacteria induce aversive olfactory learning in Caenorhabditis elegans. Nature *438*, 179-184.

Table 4-1. Distributions of different genotypes in aerotaxis assays in a 0-10% oxygen gradient.

All assays are in the absence of food.
Bins are equally spaced along the gradient. Bins 1-9 correspond to decreasing oxygen concentrations from 10% to 0% oxygen. Values are the fractions of animals in each bin.
n, number of assays. Each assay represents 80-100 animals.

Genotype	Food	n	1	2	3	4	5	6	7	8	9
N2	off	11	0.092	0.182	0.284	0.206	0.130	0.065	0.030	0.006	0.003
qcy-36	off	3	0.116	0.202	0.171	0.196	0.176	0.093	0.039	0.006	0.000
qcy-35	off	4	0.128	0.185	0.276	0.220	0.125	0.038	0.015	0.005	0.007
qcy-34	off	3	0.108	0.264	0.232	0.135	0.137	0.070	0.042	0.007	0.005
qcy-32	off	3	0.170	0.260	0.188	0.127	0.073	0.098	0.056	0.024	0.003
qcy-33; qcy-31	off	4	0.061	0.147	0.189	0.217	0.196	0.101	0.051	0.023	0.014
tax-4	off	5	0.099	0.116	0.131	0.130	0.203	0.140	0.095	0.057	0.029
tax-4; qcy-32::tax-4	off	3	0.113	0.125	0.128	0.172	0.184	0.149	0.066	0.039	0.025
tax-4; odr-4::tax-4	off	3	0.103	0.203	0.224	0.147	0.148	0.103	0.034	0.025	0.013
osm-9	off	3	0.262	0.233	0.161	0.151	0.114	0.069	0.005	0.005	0.000
ocr-2	off	3	0.099	0.168	0.209	0.252	0.139	0.076	0.032	0.020	0.004
osm-9 ocr-2	off	3	0.137	0.242	0.250	0.222	0.071	0.057	0.016	0.005	0.000
egl-9	off	6	0.045	0.081	0.153	0.205	0.158	0.187	0.109	0.054	0.009
hif-1	off	3	0.067	0.189	0.269	0.158	0.175	0.088	0.047	0.006	0.000
egl-9 hif-1	off	3	0.081	0.215	0.258	0.208	0.132	0.076	0.022	0.006	0.003
tax-4; egl-9	off	3	0.068	0.096	0.141	0.191	0.254	0.129	0.089	0.019	0.013
qcy-35; egl-9	off	3	0.045	0.083	0.187	0.155	0.184	0.175	0.117	0.039	0.014

Table 4-2. Chi-square comparisons for 0-10% oxygen gradient assays.

n, total number of animals tested for a given genotype and condition.

* $P < 0.01$
** $P < 0.001$

Group 1			Group 2			Chi-square	
Genotype	Food	n	Genotype	Food	n		
N2	off	884	*qcy-36*	off	364	22	*
N2	off	884	*qcy-35*	off	381	8	
N2	off	884	*qcy-34*	off	320	20	*
N2	off	884	*qcy-32*	off	266	49	**
N2	off	884	*qcy-33; qcy-31*	off	380	47	**
N2	off	884	*tax-4*	off	412	141	**
tax-4; qcy-32::tax-4	off	248	N2	off	884	79	**
tax-4; qcy-32::tax-4	off	248	*tax-4*	off	412	5	
tax-4; odr-4::tax-4	off	231	N2	off	884	21	*
tax-4; odr-4::tax-4	off	231	*tax-4*	off	412	32	**
N2	off	884	*osm-9*	off	258	73	**
N2	off	884	*ocr-2*	off	253	9	
N2	off	884	*osm-9 ocr-2*	off	218	17	
osm-9 ocr-2	off	218	*osm-9*	off	258	23	*
osm-9 ocr-2	off	218	*ocr-2*	off	253	17	
N2	off	884	*egl-9*	off	664	176	**
N2	off	884	*hif-1*	off	320	13	
N2	off	884	*egl-9 hif-1*	off	320	5	
egl-9	off	664	*hif-1*	off	320	77	**
egl-9 hif-1	off	320	*egl-9*	off	664	100	**
egl-9 hif-1	off	320	*hif-1*	off	320	10	
qcy-35; egl-9	off	287	*egl-9*	off	664	6	
qcy-35; egl-9	off	287	*qcy-35*	off	381	104	**
tax-4; egl-9	off	304	*egl-9*	off	664	24	*
tax-4; egl-9	off	304	*tax-4*	off	412	22	*

Table 4-3. Fraction of animals in the center of covered lawns for various mutants.

Fraction of animals in the center of untreated covered lawns. Animals scored at 4 hours. *n*, number of assays. SEM denotes standard error of the mean. With the exception of *odr-7*, no strain was significantly different from N2 controls at $p < 0.05$ by Dunnett test. *odr-7* mutants were different from N2 controls at $p < 0.01$ by Dunnett test.

Genotype	*n*	Fraction of Animals	SEM	
N2	39	0.025	0.009	
mec-2 (e75)	6	0.000	0.000	
mec-3 (e1338)	3	0.000	0.000	
mec-4 (e1339)	6	0.004	0.003	body touch
mab-5 (e1239)	3	0.043	0.030	
mab-5 (e2008)	3	0.005	0.005	
mab-5 (e1751gf)	3	0.021	0.011	Q cell migration
gcy-35 (ok769)	15	0.041	0.011	
gcy-33 (ok232); gcy-31 (ok296)	6	0.030	0.030	
qals2241 (URX-AQR-PQR-)	12	0.057	0.013	
gcy-33; gcy-31 qals2241	12	0.070	0.014	
gcy-35; gcy-33; gcy-31 qals2241	6	0.031	0.010	sGC signaling
lim-4 (ky403)	12	0.083	0.031	
odr-1 (n1936)	6	0.030	0.020	
odr-7 (ky4)	6	0.175	0.033	
osm-9 (ky10)	3	0.012	0.012	
ocr-2 (ak47)	3	0.009	0.009	
osm-6 (p811)	3	0.089	0.012	sensory signaling
npr-1 (ad609)	15	0.087	0.014	neuropeptide
npr-1 (g320)	15	0.026	0.009	signaling
cat-1 (e1111)	3	0.011	0.006	
cat-2 (e1112)	3	0.066	0.034	
tph-1 (mg280)	3	0.042	0.014	food modulation

Figure 4-1. Hypoxia avoidance requires the TAX-4 cyclic nucleotide-gated channel in a subset of sensory neurons.

(A-H) Aerotaxis of animals in a 0-10% oxygen gradient.

(A) Aerotaxis of N2, *gcy-36* and *gcy-35* animals.

(B) Aerotaxis of *gcy-34* and *gcy-32* mutants.

(C) Aerotaxis of *gcy-33; gcy-31* double mutants.

(D) Aerotaxis of *tax-4* mutants.

(E) Aerotaxis of *tax-4* mutants rescued for *tax-4* in URX, AQR, and PQR neurons using a *gcy-32::tax-4::gfp* transgene (Gray et al., 2004).

(F) Aerotaxis of *tax-4* mutants rescued for *tax-4* in multiple sensory neurons using an *odr-4::tax-4::gfp* transgene.

(G) Aerotaxis of *osm-9* and *ocr-2* mutants.

(H) Aerotaxis of *osm-9 ocr-2* double mutants.

In A-H, asterisks denote distributions different by Chi-square analysis at $p < 0.01$ from the first distribution in the panel, unless otherwise noted. $n \geq 3$ assays per genotype, 80-100 animals/assay. Error bars are standard error of the mean (SEM).

(I) Fraction of animals in 0-4.4% oxygen. Asterisks, values different from N2 controls at $p < 0.01$ by Dunnett test. Cross, value different from *tax-4* mutants, and not from N2 control, at $p < 0.05$ by Bonferroni *t* test. NS, value different from N2 control, and not from *tax-4* mutants, at $p < 0.05$ by Bonferroni *t* test. Error bars denote SEM.

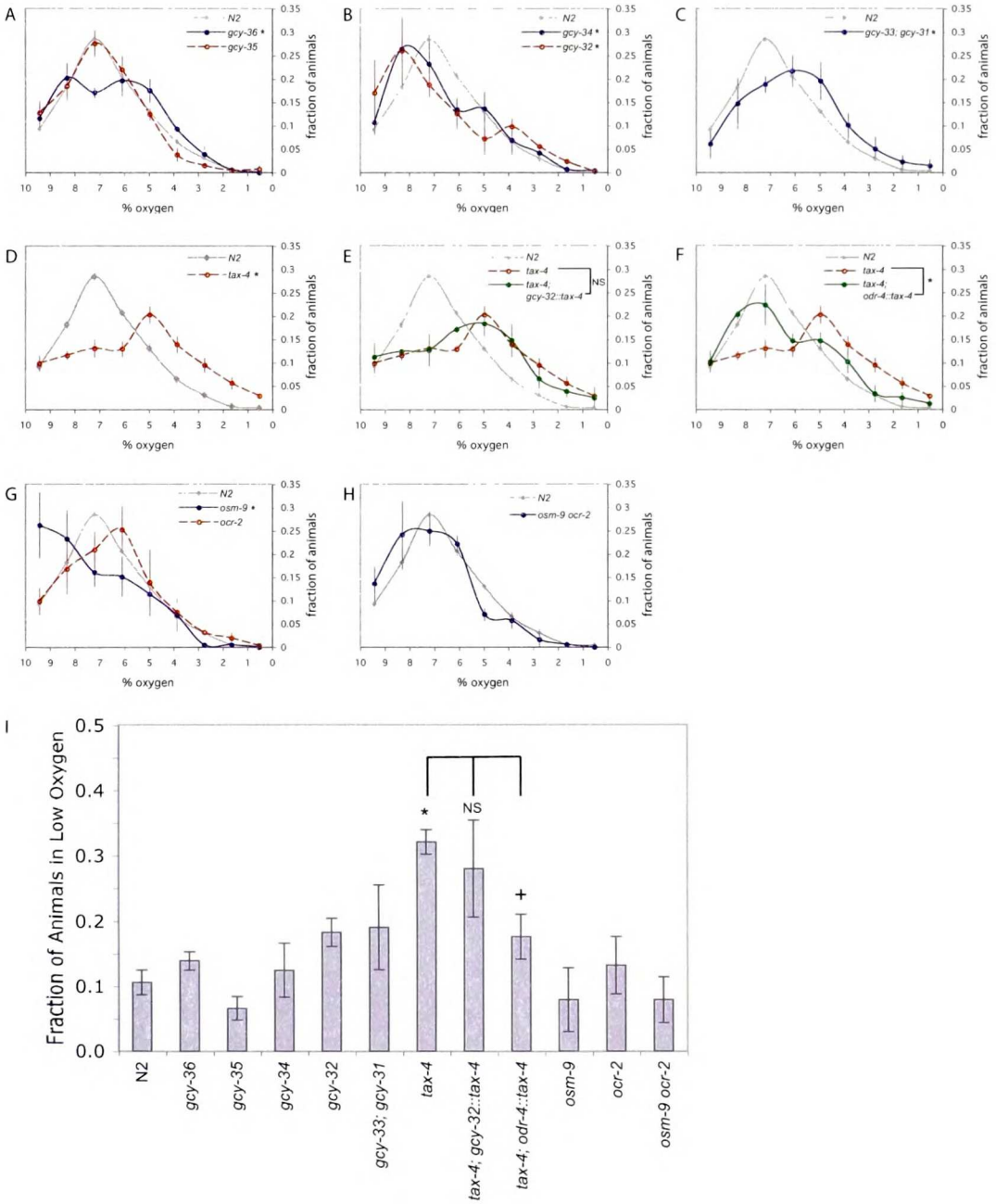
A
N2
gcy-36 *
gcy-35
B
N2
gcy-34 *
gcy-32 *
C
N2
gcy-33; gcy-31 *
D
N2
tax-4 *
E
N2
tax-4
tax-4; gcy-32::tax-4
NS
F
N2
tax-4
tax-4; odr-4::tax-4
*
G
N2
osm-9 *
ocr-2
H
N2
osm-9 ocr-2
fraction of animals
% oxygen
I
Fraction of Animals in Low Oxygen
*
NS
+
N2
gcy-36
gcy-35
gcy-34
gcy-32
gcy-33; gcy-31
tax-4
tax-4; gcy-32::tax-4
tax-4; odr-4::tax-4
osm-9
ocr-2
osm-9 ocr-2

Figure 4-2. Hypoxia avoidance is regulated by the HIF-1 pathway.

(A-D) Aerotaxis of animals in a 0-10% oxygen gradient.

(A) Aerotaxis of wild-type N2 and *egl-9* animals.

(B) Aerotaxis of *egl-9*, *hif-1*, and *egl-9 hif-1* mutants.

(C) Aerotaxis of *tax-4; egl-9* double mutants.

(D) Aerotaxis of *gcy-35; egl-9* double mutants.

In A-D, asterisks denote distributions different by Chi-square analysis at $p < 0.01$ from the first distribution in the panel. $n \geq 3$ assays per genotype, 80-100 animals/assay. Error bars are standard error of the mean (SEM).

(I) Fraction of animals in 0-4.4% oxygen. Asterisks, values different from N2 controls at $p < 0.01$ by Dunnett test. *gcy-35; egl-9* mutants are different from *gcy-35* mutants, and not from *egl-9* mutants, at $p < 0.05$ by Bonferroni *t* test. *egl-9*, *tax-4*, and *tax-4; egl-9* mutants are not different by ANOVA at $p = 0.449$. Error bars denote SEM.

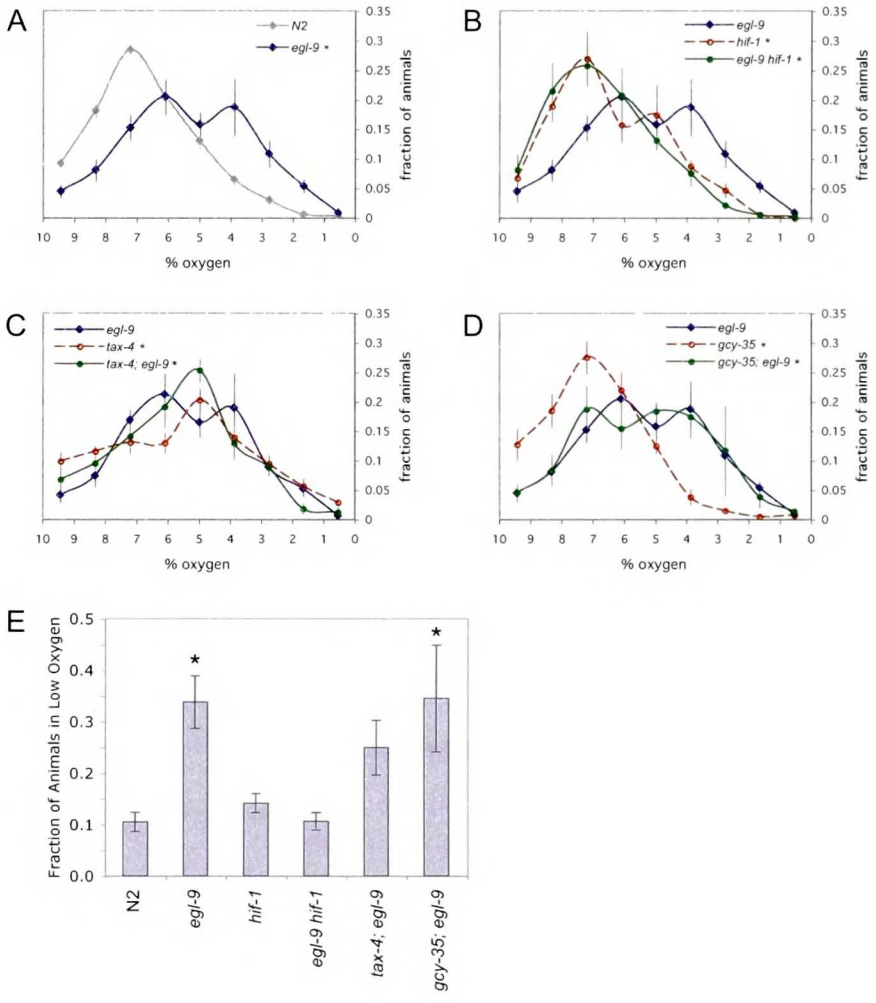
A
N2
egl-9 *
fraction of animals
% oxygen
B
egl-9
hif-1 *
egl-9 hif-1 *
fraction of animals
% oxygen
C
egl-9
tax-4 *
tax-4; egl-9 *
fraction of animals
% oxygen
D
egl-9
gcy-35 *
gcy-35; egl-9 *
fraction of animals
% oxygen
E
Fraction of Animals in Low Oxygen
N2
egl-9
hif-1
egl-9 hif-1
tax-4; egl-9
gcy-35; egl-9

Figure 4-3. Feeding patterns on bacterial lawns are modified by hypoxic conditions.

(A) Agar plug assay. The assay plate contained 4 lawns of *E. coli* HB101 seeded on NGM agar and grown overnight. When indicated, lawns were irradiated by shortwave UV after overnight growth. Before transfer of animals, two lawns were covered by circular plugs of NGM agar that were larger than these lawns, such that these lawns were sandwiched between two layers of agar. 100-200 adult animals were transferred to the middle of the plate by washing. The distribution of animals was scored at 1 and 4 hours.

(B) The fraction of animals in the center of covered lawns = (total number of animals inside covered lawns) / (total number of animals under agar plugs) on one assay plate. Without UV treatment of lawns, wild-type N2 animals avoided the center of covered lawns. Increasing time of UV irradiation resulted in greater fractions of animals accumulating in the center of covered lawns. $n \geq 3$ assays per condition and time point, 100-200 animals/assay. Error bars denote SEM.

(C) Direct measurement of oxygen concentrations at different positions in lawns after covering them with agar plugs for 1 hour. ND, not determined.

A

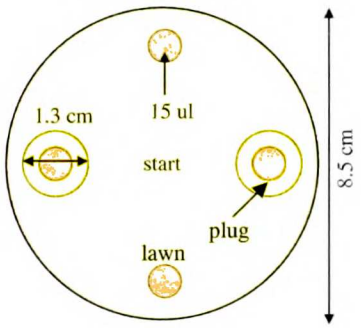

Pick 3-10 L4's.

25°C (4 days)
20°C (5 days)

Assay at growth temp.

B

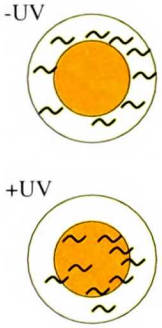

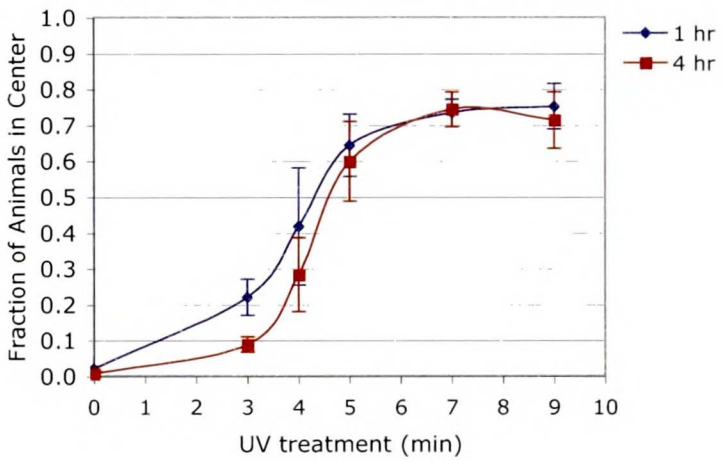

C

UV Treatment (min)	Oxygen Concentration at Agar Plug Edge (%)	Oxygen Concentration at Lawn Edge (%)	Oxygen Concentration at Lawn Center (%)
0	21	4	3
3	21	4	3
4	ND	ND	ND
5	21	14	13
7	21	16	14
9	21	18	17

Figure 4-4. The cyclic nucleotide-gated channel TAX-4/TAX-2 is required for avoidance of covered lawns.

Fraction of animals in the center of untreated covered lawns. Animals scored at 1 and 4 hours. Double asterisks, values different from N2 controls at the same time point at $p < 0.01$ by Dunnett test. $n \geq 6$ assays per genotype and time point, 100-200 animals/assay. Error bars denote SEM.

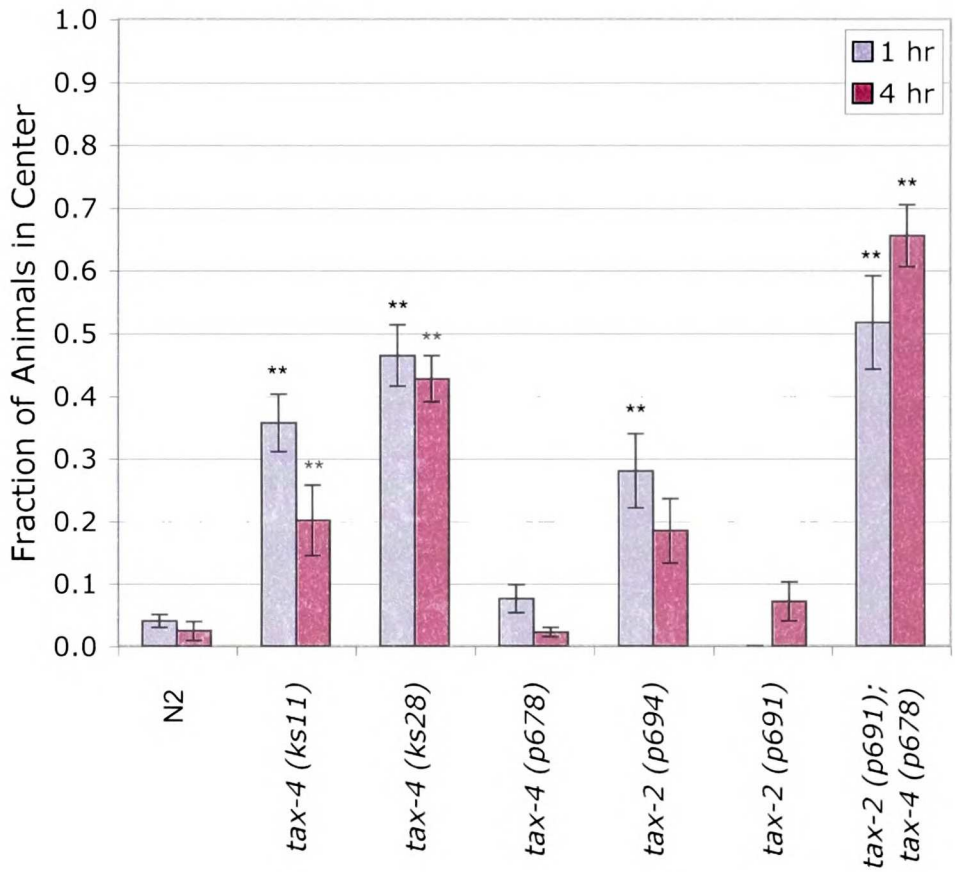
Fraction of Animals in Center
1.0
0.9
0.8
0.7
0.6
0.5
0.4
0.3
0.2
0.1
0.0
1 hr
4 hr
**
N2
tax-4 (ks11)
tax-4 (ks28)
tax-4 (p678)
tax-2 (p694)
tax-2 (p691)
tax-2 (p691); tax-4 (p678)

Figure 4-5. Upregulation of the HIF-1 pathway increases the fraction of animals in the center of covered lawns.

(A) Fraction of animals in the center of covered lawns that were not UV-irradiated.

(B) Fraction of animals in the center of covered lawns that were UV-irradiated for 3 minutes.

Animals scored at 1 and 4 hours. Asterisks and double asterisks, values different from N2 controls at the same time point at $p < 0.05$ and at $p < 0.01$, respectively, by Dunnett test. For 1 hour time point with 3 minutes UV, *tax-4; egl*-9 was not included in Dunnett test. For *t* test between N2 and *tax-4; egl*-9 at 1 hour time point, $p = 0.034$. $n \geq 3$ assays per genotype and time point, 100-200 animals/assay. Error bars denote SEM.

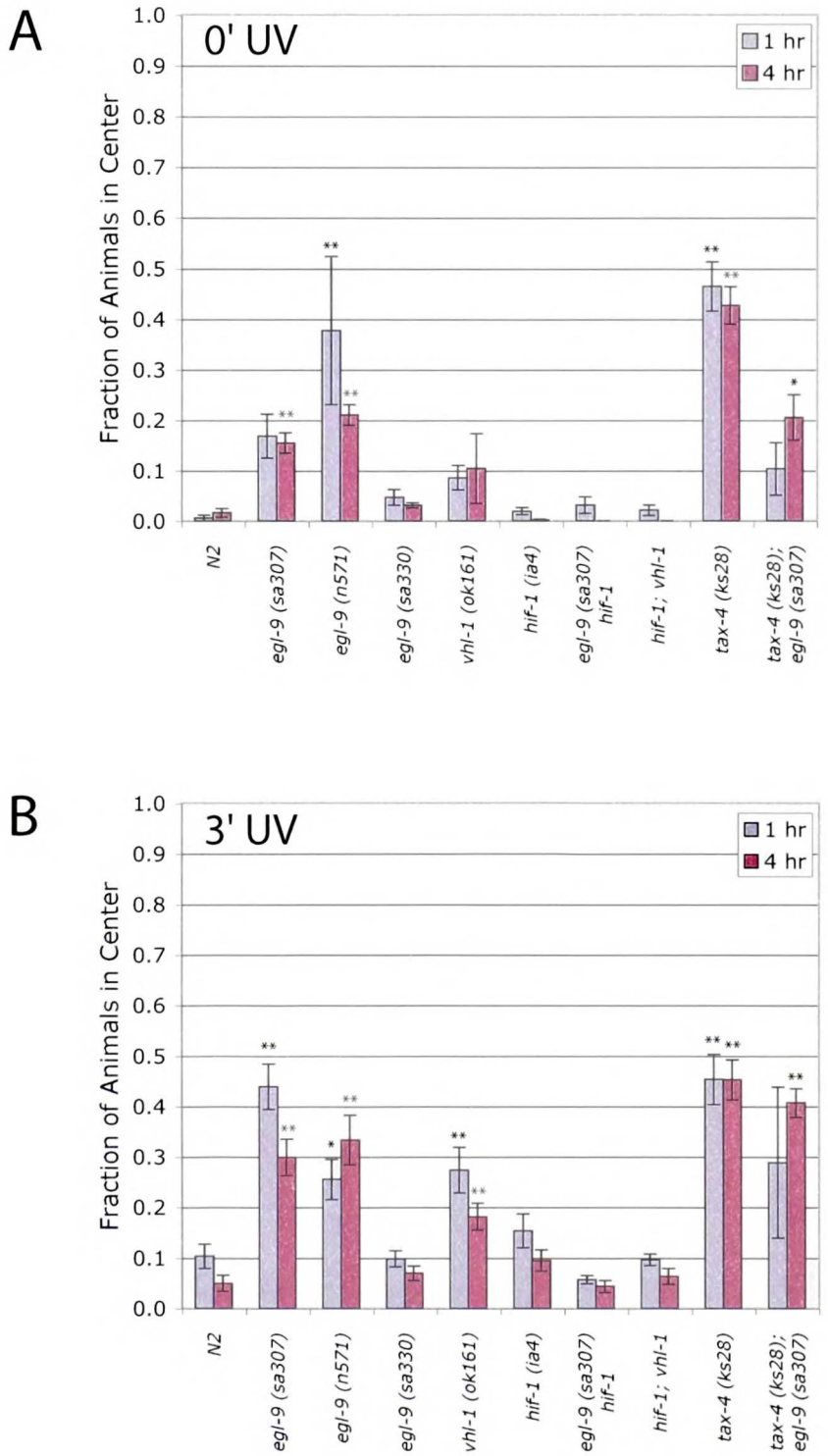
A
0' UV
1 hr
4 hr
Fraction of Animals in Center
1.0
0.9
0.8
0.7
0.6
0.5
0.4
0.3
0.2
0.1
0.0
N2
egl-9 (sa307)
egl-9 (n571)
egl-9 (sa330)
vhl-1 (ok161)
hif-1 (ia4)
egl-9 (sa307) hif-1
hif-1; vhl-1
tax-4 (ks28)
tax-4 (ks28); egl-9 (sa307)
B
3' UV
1 hr
4 hr
Fraction of Animals in Center
1.0
0.9
0.8
0.7
0.6
0.5
0.4
0.3
0.2
0.1
0.0
N2
egl-9 (sa307)
egl-9 (n571)
egl-9 (sa330)
vhl-1 (ok161)
hif-1 (ia4)
egl-9 (sa307) hif-1
hif-1; vhl-1
tax-4 (ks28)
tax-4 (ks28); egl-9 (sa307)

Chapter 5:

Future Directions

In this dissertation, my goal was to understand the neural basis for behavioral responses to one physiologically important sensory cue, oxygen, in the model organism *C. elegans*. My work suggests that *C. elegans* oxygen preference in a 0-21% oxygen range is composed of two distinct behaviors: avoidance of hyperoxia (>14%) and avoidance of hypoxia (<4%). Using a combination of genetic and neuroanatomical approaches, I uncovered a circuit for hyperoxia avoidance in which sensory and modulatory components act in a flexible, distributed manner resembling dynamic modulated networks from more complex nervous systems (Briggman et al., 2005; Nusbaum and Beenhakker, 2002; Wills et al., 2005). The discovery of ever more complex circuits for behavior in *C. elegans* validates the choice of this model for studying neural circuits and highlights the advantages of working in a genetic system with well-characterized and reproducible neuroanatomy (de Bono and Maricq, 2005).

Why would *C. elegans* devote so many sensory neurons to hyperoxia avoidance behavior? One way to think about aerotaxis off food is that animals associate oxygen concentration with food, and when they are transferred from food to the assay plate, they try to find the oxygen concentration that last corresponded with food. The preferred oxygen concentrations of wild-type N2 animals off food are similar to oxygen concentrations of bacterial lawns from which they were transferred (Chang et al., 2006; Gray et al., 2004). In *npr-1* mutants, oxygen preference can be shifted to lower oxygen if animals are incubated with food at 1% oxygen, but not if they were incubated without food at 1% oxygen (Cheung et al., 2005) (Fig. 3-6). When animals are removed from food, they may use TRPV channel-expressing neurons (ASH and ADF) to sense the food state and sGC-expressing, oxygen-sensing neurons (URX, AQR, PQR, SDQ, ALN, and

PLN) to track to preferred oxygen concentrations (Fig. 2-8). Only subsets of either food-sensing neurons or oxygen-sensing neurons are required for hyperoxia avoidance.

One reason for the apparent redundancy of function may be due to the fact that multiple locomotory strategies enable animals to accumulate at preferred oxygen concentrations in a 0-21% oxygen gradient. To accumulate at the preferred oxygen concentrations, wild-type N2 animals slow down in the preferred range and reverse when they move out of it. At a visual level, modulation of either speed or reversal frequency seems to be sufficient for accumulation at the preferred concentration. This is most evident in *osm-9* rescue experiments where either expression of *osm-9* in ASH, PHA, and PHB neurons or ADF neurons was sufficient to restore hyperoxia avoidance to *osm-9* mutants (Fig. 2-2). Mutants rescued for *osm-9* in ASH, PHA, and PHB neurons had high speed during the assay and reversed frequently when they entered hyperoxia from the preferred oxygen concentrations. On the other hand, mutants rescued for *osm-9* in ADF neurons were slow during the assay and completely stopped once they found their preferred oxygen concentrations. To determine the precise locomotory contribution of each sensory neuron to oxygen preference behavior, animals should be tracked during the gradient assay, and distinct locomotory parameters, such as speed and reversal frequency, should be quantitated over time at different positions along the gradient. Under more varied environmental conditions in nature, different locomotory strategies employing subsets of neurons in this circuit may be appropriate to find preferred oxygen levels.

The presence of food in the oxygen gradient assay suppresses hyperoxia avoidance. Multiple pathways (DAF-7, NPR-1, and HIF-1) modulate hyperoxia avoidance in the presence of food, probably by coupling environmental conditions to

behavior. DAF-7 TGF-ß signaling is downregulated by low food availability and high population (pheromone) density (Ren et al., 1996; Schackwitz et al., 1996). The NPR-1 neuropeptide pathway may be regulated by neuropeptide release from neurons and intestine (Rogers et al., 2003) and thus can potentially monitor both external and internal environments. The HIF-1 pathway senses hypoxic stress throughout the animal (Epstein et al., 2001; Jiang et al., 2001). These pathways monitor distinct stressors to affect the same output behavior, allowing the animal to respond to diverse conditions. Whereas DAF-7 and HIF-1 pathways respond to chronic states and act through transcription, NPR-1 signaling may be regulated constitutively or acutely. An important future direction would be to determine how NPR-1 signaling is regulated by its neuropeptide ligands.

While expression of *npr-1* is restricted to relatively few cells, the *daf-7/daf-3* and *egl-9/hif-1* transcriptional pathways may be used more broadly throughout the animal (Coates and de Bono, 2002; Jiang et al., 2001; Patterson et al., 1997). This makes it difficult to determine which transcriptional targets of *daf-7/daf-3* and *egl-9/hif-1* pathways specifically regulate aerotaxis. Microarray experiments that examine global changes in gene expression are likely to miss relevant targets important in only a few cells; in fact, microarray experiments on the HIF-1 pathway yielded many metabolic genes required for adaptation to hypoxia and few genes involved in sensory transduction (Bishop et al., 2004; Shen et al., 2005). One possible way to address this problem is to enrich for cells of interest by fluorescence activated cell sorting (FACS), and then perform microarray experiments on these cells (Zhang et al., 2002). Cells already implicated in hyperoxia avoidance are a good starting point for this line of experiments.

A complementary method to study the circuit for hyperoxia avoidance is functional imaging experiments using genetically encoded calcium sensors, such as cameleon or G-CaMP (Miyawaki et al., 1999; Nakai et al., 2001). *C. elegans* does not have voltage-activated sodium channels, and calcium is the major cation that is exchanged to initiate changes in membrane potential and neuronal activity. Both cameleon and G-CaMP have been successfully used to image the activity of *C. elegans* neurons and muscle (Hilliard et al., 2005; Kahn-Kirby et al., 2004; Kerr et al., 2000; Kodama et al., 2006). A microfluidic device has been developed to deliver changes in oxygen levels to animals (N. Chronis and M. Zimmer, personal communication). Neurons that express sGCs (URX, AQR, PQR, SDQ, ALN, PLN, and BAG) and other neurons implicated in hyperoxia avoidance should be tested for their sensitivity to changes in oxygen levels in wild-type and mutant backgrounds. Given the number of sGCs and neurons involved in hyperoxia avoidance, it is likely that different sGCs and neurons are sensitive to different ranges of oxygen and direction of change. Modulatory pathways (DAF-7, NPR-1, and HIF-1) are likely at some point to affect the activity of some of these neurons in response to oxygen.

Hypoxia sensing is a major question for researchers interested in acute and chronic problems associated with low oxygen conditions caused by disease states, such as stroke or heart disease. The HIF-1 pathway has been studied extensively as a transcriptional system for oxygen homeostasis; however, the identity of acute oxygen sensors remains elusive. To date, hypoxia sensing has been studied mostly in mammalian systems, where redundant pathways appear to control hypoxia sensing in organs like the carotid body.

My preliminary results suggest that *C. elegans* may be a good system in which to find an acute hypoxia sensor. *C. elegans* exhibits strong acute repulsion from hypoxia in both the 0-10% oxygen gradient assay and agar plug assay. Hypoxia avoidance requires the canonical HIF-1 hypoxia-sensing pathway and activity of sensory neurons that express the TAX-4/TAX-2 cyclic nucleotide-gated channel (Chapter 4). Sensory neurons that express *tax-4/tax-2* may sense hypoxia directly, or they may play a modulatory role in hypoxia avoidance behavior. Calcium imaging experiments can be performed on these neurons to determine their sensitivity to hypoxia.

The rapid and persistent reversal response of *C. elegans* to hypoxia is highly suitable for an unbiased genetic screen to find an acute hypoxia sensor. The agar plug assay can be used to find animals that fail to avoid the center of covered lawns, but the plug is not easy to remove without disturbing the lawn. A better screen would utilize a configuration in which preferred and hypoxic zones are spatially isolated in a microfluidic device (G. Lee, personal communication); animals that accumulate in hypoxic regions can then be further tested.

Ultimately, it would be beneficial to develop more complex behavioral assays that more closely resemble animals' experience in natural settings. Because oxygen is such an important sensory cue, it would be useful to combine oxygen with other sensory cues in complex assays. The agar plug assay is one example of complex presentation of sensory cues, balancing attraction to bacterial food with dangerous hypoxic conditions. Using the microfluidic device designed for the oxygen gradient assay, one can test animals in a complex gradient combining a gradient of oxygen with a gradient of a repulsive gas, such as carbon dioxide, to see how animals integrate multiple cues to find a

preferred location. To determine what properties of bacterial food modulate *C. elegans* aerotaxis, pure chemicals or physical substrates can be substituted for bacterial lawns to see if they can reproduce the effect of suppressing hyperoxia avoidance.

C. elegans is a remarkably versatile model system to study behavior. Its genetic tractability allows for unbiased screens for new components of sensory transduction and dissection of interactions between signaling pathways. The simplicity and reproducibility of its neuroanatomy permit physical and molecular manipulations of cellular components of neural circuits in single animals as well as populations. Recent technological advances in engineering and *in vivo* imaging give us greater access to quantitative measures of animal behavior and cell activity. As we move towards developing paradigms for more complex behaviors in *C. elegans*, the synthesis of these approaches will help us gain a more complete understanding of behavior from the molecular to system level.

References

Bishop, T., Lau, K. W., Epstein, A. C., Kim, S. K., Jiang, M., O'Rourke, D., Pugh, C. W., Gleadle, J. M., Taylor, M. S., Hodgkin, J., and Ratcliffe, P. J. (2004). Genetic analysis of pathways regulated by the von Hippel-Lindau tumor suppressor in Caenorhabditis elegans. PLoS Biol *2*, e289.

Briggman, K. L., Abarbanel, H. D., and Kristan Jr., W. B. (2005). Optical imaging of neuronal populations during decision-making. Science *307*, 896-901.

Chang, A. J., Chronis, N., Karow, D. S., Marletta, M. A., and Bargmann, C. I. (2006). A distributed chemosensory circuit for oxygen preference in C. elegans. PLoS Biol *4*, e274.

Cheung, B. H., Cohen, M., Rogers, C., Albayram, O., and de Bono, M. (2005). Experience-dependent modulation of C. elegans behavior by ambient oxygen. Curr Biol *15*, 905-917.

Coates, J. C., and de Bono, M. (2002). Antagonistic pathways in neurons exposed to body fluid regulate social feeding in Caenorhabditis elegans. Nature *419*, 925-929.

de Bono, M., and Maricq, A. V. (2005). Neuronal substrates of complex behaviors in C. elegans. Annu Rev Neurosci *28*, 451-501.

Epstein, A. C., Gleadle, J. M., McNeill, L. A., Hewitson, K. S., O'Rourke, J., Mole, D. R., Mukherji, M., Metzen, E., Wilson, M. I., Dhanda, A., *et al.* (2001). C. elegans EGL-9 and mammalian homologs define a family of dioxygenases that regulate HIF by prolyl hydroxylation. Cell *107*, 43-54.

Gray, J. M., Karow, D. S., Lu, H., Chang, A. J., Chang, J. S., Ellis, R. E., Marletta, M. A., and Bargmann, C. I. (2004). Oxygen sensation and social feeding mediated by a C. elegans guanylate cyclase homologue. Nature *430*, 317-322.

Hilliard, M. A., Apicella, A. J., Kerr, R., Suzuki, H., Bazzicalupo, P., and Schafer, W. R. (2005). In vivo imaging of C. elegans ASH neurons: cellular response and adaptation to chemical repellents. Embo J *24*, 63-72.

Jiang, H., Guo, R., and Powell-Coffman, J. A. (2001). The Caenorhabditis elegans hif-1 gene encodes a bHLH-PAS protein that is required for adaptation to hypoxia. Proc Natl Acad Sci U S A *98*, 7916-7921.

Kahn-Kirby, A. H., Dantzker, J. L., Apicellar, A. J., Schafer, W. R., Browse, J., Bargmann, C. I., and Watts, J. L. (2004). Specific polyunsaturated fatty acids drive TRPV-dependent sensory signaling in vivo. Cell *119*, 889-900.

Kerr, R., Lev-Ram, V., Baird, G., Vincent, P., Tsien, R. Y., and Schafer, W. R. (2000). Optical imaging of calcium transients in neurons and pharyngeal muscle of C. elegans. Neuron *26*, 583-594.

Kodama, E., Kuhara, A., Mohri-Shiomi, A., Kimura, K. D., Okumura, M., Tomioka, M., Iino, Y., and Mori, I. (2006). Insulin-like signaling and the neural circuit for integrative behavior in C. elegans. Genes Dev *20*, 2955-2960.

Miyawaki, A., Griesbeck, O., Heim, R., and Tsien, R. Y. (1999). Dynamic and quantitative Ca2+ measurements using improved cameleons. Proc Natl Acad Sci U S A *96*, 2135-2140.

Nakai, J., Ohkura, M., and Imoto, K. (2001). A high signal-to-noise Ca(2+) probe composed of a single green fluorescent protein. Nat Biotechnol *19*, 137-141.

Nusbaum, M. P., and Beenhakker, M. P. (2002). A small-systems approach to motor pattern generation. Nature *417*, 343-350.

Patterson, G. I., Koweek, A., Wong, A., Liu, Y., and Ruvkun, G. (1997). The DAF-3 Smad protein antagonizes TGF-beta-related receptor signaling in the Caenorhabditis elegans dauer pathway. Genes Dev *11*, 2679-2690.

Ren, P., Lim, C. S., Johnsen, R., Albert, P. S., Pilgrim, D., and Riddle, D. L. (1996). Control of C. elegans larval development by neuronal expression of a TGF-beta homolog. Science *274*, 1389-1391.

Rogers, C., Reale, V., Kim, K., Chatwin, H., Li, C., Evans, P., and de Bono, M. (2003). Inhibition of *Caenorhabditis elegans* social feeding by FMRFamide-related peptide activation of NPR-1. Nat Neurosci *6*, 1178-1185.

Schackwitz, W. S., Inoue, T., and Thomas, J. H. (1996). Chemosensory neurons function in parallel to mediate a pheromone response in C. elegans. Neuron *17*, 719-728.

Shen, C., Nettleton, D., Jiang, M., Kim, S. K., and Powell-Coffman, J. A. (2005). Roles of the HIF-1 hypoxia-inducible factor during hypoxia response in Caenorhabditis elegans. J Biol Chem *280*, 20580-20588.

Wills, T. J., Lever, C., Cacucci, F., Burgess, N., and O'Keefe, J. (2005). Attractor dynamics in the hippocampal representation of the local environment. Science *308*, 873-876.

Zhang, Y., Ma, C., Delohery, T., Nasipak, B., Foat, B. C., Bounoutas, A., Bussemaker, H. J., Kim, S. K., and Chalfie, M. (2002). Identification of genes expressed in C. elegans touch receptor neurons. Nature *418*, 331-335.

Appendix A:

Sensory integration in chemotaxis

Statement of contributions:

I performed the experiments presented in Figure A-1, Figure A-2 A and B, and Figure A-4. A rotation student, Adria LeBoeuf, conducted the experiments in Figure A-2 C and Figure A-3.

Introduction

Animals live in complex environments in which they must be able to respond appropriately to sensory cues. The soil nematode *C. elegans* exhibits behavioral responses to a variety of volatile chemical stimuli associated with bacterial food. Some chemicals, such as 2-butanone, isoamyl alcohol, diacetyl, and pyrazine, are attractive at all concentrations tested. Others, like 1-octanol and 1-nonanol, are not attractive at any concentration and repulsive at high concentrations (Bargmann et al., 1993). Volatile chemical attraction or repulsion is mediated primarily by the AWA, AWB, and AWC sensory neurons (Bargmann et al., 1993; Sengupta et al., 1994; Troemel et al., 1997). The ASH neurons also detect a variety of chemical, mechanical, and osmotic repellents (Bargmann and Mori, 1997).

In this chapter, I will describe my efforts to map out neural circuits for *C. elegans* response to two volatile chemicals, 1-hexanol and 2-nonanone. Both chemicals are repulsive at high concentrations; 1-hexanol is also attractive at lower concentrations (Bargmann et al., 1993; Troemel et al., 1997). Attraction and repulsion to these chemicals appear to be mediated by distinct sets of neurons. For chemotaxis towards 1-hexanol, sensory integration of these opposing drives regulates behavior in a temporal fashion.

Results

Attraction to 1-hexanol requires the AWC *str-2::gfp* OFF neuron.

Wild-type N2 animals are repelled from high concentrations of 1-hexanol (1 and 1:2) and attracted to lower concentrations (1:10 and 1:20) in a dose-dependent manner ((Bargmann et al., 1993); Noelle Dwyer, personal communication) (Figure A-1). Using a candidate gene approach, I tested mutants in sensory signal transduction to find sensory components and neurons that promote attraction and repulsion to 1-hexanol. Previous studies showed that *C. elegans* neurons that sense volatile chemicals promote either attractive or repulsive responses (Bargmann et al., 1993; Troemel et al., 1997), so it is likely that these functions are carried out by distinct sets of sensory neurons.

Attraction to 1-hexanol at 1:10 and 1:100 concentrations was impaired in *odr-1* mutants (Figure A-1). *odr-1* encodes a transmembrane guanylate cyclase that is required for chemotaxis mediated by the AWC and AWB neurons (L'Etoile and Bargmann, 2000). Because AWC neurons promote volatile attraction while AWB neurons mediate volatile repulsion (Bargmann et al., 1993; Troemel et al., 1997), it is likely that *odr-1* acts in AWC neurons to promote 1-hexanol attraction. To address this hypothesis, I tested mutants that specifically affect AWC cell fate. The two AWC neurons exhibit stochastic asymmetric expression of a putative chemosensory receptor, *str-2* (Troemel et al., 1999); wild-type animals express a *str-2::gfp* transgene in only one AWC neuron. Some mutants that disrupt in this asymmetry are defective in discrimination between AWC-sensed odorants (Wes and Bargmann, 2001). *nsy-1 (ky542)* and *nsy-3/slo-1 (ky389gf)* mutants with two AWC neurons that express *str-2::gfp* (Davies et al., 2003; Troemel et

al., 1999; Wes and Bargmann, 2001) showed a defect in 1-hexanol attraction (Figure A-1), suggesting that an AWC neuron that does not express *str-2::gfp* or asymmetric expression of *str-2::gfp* is needed for this behavior. To determine if asymmetric expression of *str-2::gfp* was important, I tested mutants in *nsy-4 (ky616)* and *nsy-5 (ky634)*, which have two AWC neurons that do not express *str-2::gfp* ((Vanhoven et al., 2006); M. Vanhoven, personal communication). These mutants exhibited normal, if not better, attraction to 1-hexanol than wild-type N2 animals (Figure A-1). Thus, it is the presence of an AWC *str-2::gfp* OFF neuron that is required for 1-hexanol attraction, and not asymmetric expression of *str-2::gfp* in the two AWC neurons.

TRPV channels are required for repulsion from 1-hexanol.

My candidate approach found that mutants in the TRPV channels *osm-9* and *ocr-2* were defective in repulsion from high concentrations of 1-hexanol and 1-heptanol (Figure A-2A, B). This defect was more pronounced in animals grown at 25°C versus those grown at 20°C, especially for *osm-9* mutants (Figure A-2A, B), suggesting that high temperature may further decrease repulsion from these chemicals in *osm-9* and *ocr-2* mutants. *osm-9* and *ocr-2* are important in a number of *C. elegans* behaviors, including volatile attraction and acute chemical repulsion (Colbert et al., 1997; Tobin et al., 2002). Because *ocr-2* had a stronger defect in 1-hexanol repulsion and is expressed in a smaller set of sensory neurons than *osm-9* (Colbert et al., 1997; Tobin et al., 2002), I rescued *ocr-2* in subsets of *ocr-2*-expressing neurons. Expression of *ocr-2* in ADL neurons restored 1-hexanol repulsion to *ocr-2* mutants while expression of *ocr-2* in ASH, PHA, and PHB neurons partially rescued the *ocr-2* mutant defect (Figure A-2C). These neurons are

known to mediate repulsive behaviors; in particular, ADL neurons promote repulsion from 1-octanol, another *n*-alkanol (Colbert et al., 1997; Hilliard et al., 2002; Troemel et al., 1997).

Unexpectedly, expression of *ocr-2* in ADF or AWA neurons also partially restored 1-hexanol repulsion to *ocr-2* mutants (Figure A-2C). *ocr-2* acts in ADF to promote serotonin biosynthesis via upregulation of *tph-1*, a biosynthetic enzyme (Zhang et al., 2004), and serotonin has been shown to modulate acute repulsion of animals from 30% 1-octanol (Chao et al., 2004). Thus, it is possible that *ocr-2* activity regulates serotonin levels in ADF to affect 1-hexanol repulsion. *ocr-2* activity in AWA promotes volatile attraction to diacetyl (Tobin et al., 2002). It would be surprising, but possible, that AWA neurons use *ocr-2* to promote repulsion from 1-hexanol as well. Taken together, multiple *ocr-2*-expressing neurons appear to promote repulsion from 1-hexanol at high concentrations.

1-hexanol attraction and repulsion are temporally distinct.

To better understand the behavior of animals in the chemotaxis assay, we examined the distribution of animals in assays to 1:2 1-hexanol over the course of 24 hours (Figure A-3). At 30 minutes, wild-type N2 animals were weakly attracted to 1-hexanol, and repulsion only became apparent after 60 minutes and strengthened over the next 60 minutes. *odr-1* mutants defective for attraction did not exhibit any preference until 60 minutes and were consistently more repelled than N2 at later time points. *ocr-2* mutants defective for repulsion were attracted to 1-hexanol at all time points. Three *ocr-2* rescue strains showed repulsion only at later time points compared to N2 animals,

consistent with their partial rescue effect (Figure A-2C). These results suggest that attraction to 1-hexanol occurs early, followed by repulsion at later time points.

This behavior was not due to lower, attractive concentrations of 1-hexanol experienced by animals at the start of the assay, when they were in the middle of the assay plate. In a flow chamber setup, gases can be quickly exchanged in flow over animals on an agar plate. In this assay, wild-type N2 animals did not exhibit acute responses to saturated 1-hexanol vapor in the first 15 minutes. However, if 1-hexanol vapor was replaced with air for 5 minutes and then reintroduced, animals responded very strongly to 1-hexanol by increasing reversal frequency (data not shown), a behavior characteristic of acute repulsion in *C. elegans*. Thus, the ability to generate acute repulsive behavior towards 1-hexanol even at the highest concentrations occurs at least 15 minutes after initial exposure to the chemical.

2-nonanone chemotaxis may involve multiple sensory neurons.

To determine if behavior towards other volatile chemicals also has complex sensory circuits, I examined chemotaxis to 2-nonanone, a volatile repellent sensed by the AWB neurons (Troemel et al., 1997). Wild-type N2 animals were strongly repelled by undiluted 2-nonanone, a response that decreased to no preference by a 100-fold dilution (Troemel et al., 1997) (Figure A-4). Mutants in the transmembrane guanylate cyclase *odr-1* responded only half as strongly as wild-type animals to undiluted 2-nonanone (L'Etoile and Bargmann, 2000) (Figure A-4). This could be the result of redundancy of guanylate cyclases in AWB neurons or additional neurons contributing to 2-nonanone repulsion at high concentrations. To test between these possibilities, one can test

combination mutants between *odr-1* and other guanylate cyclases expressed in AWB as well as *odr-1* and the TRPV channels *osm-9* or *ocr-2*, which mediate avoidance behaviors in other sensory neurons (Colbert et al., 1997; Tobin et al., 2002).

Interestingly, mutants in *lim-4*, which have a transformation of AWB to AWC neurons (Sagasti et al., 1999), exhibited a stronger defect in 2-nonanone repulsion than *odr-1* mutants (Figure A-4). *lim-4* mutants grown at 20°C even showed significant attraction to 1:10 2-nonanone (Figure A-4A). *odr-7* mutants, which have loss of AWA function and partial transformation of AWA to AWC (Sagasti et al., 1999; Sengupta et al., 1994), also had increased attraction to 2-nonanone at 1:10 and 1:100 concentrations (Figure A-4). Assuming that AWC neurons can promote attraction to 2-nonanone that is normally masked by strong repulsion, these results suggest that increased AWC function promotes attraction to 2-nonanone that is additive with repulsion mediated by AWB. In *lim-4* mutants, the total loss of preference to undiluted 2-nonanone could result from loss of AWB repulsion plus additional AWC attraction.

Discussion

The response of *C. elegans* to 1-hexanol is an example of a sensory cue that elicits complex dose-dependent behavioral responses, like oxygen. Consistent with previous studies of chemosensation in *C. elegans*, attraction and repulsion to 1-hexanol are regulated by distinct sets of sensory neurons. Attraction to 1-hexanol requires the AWC *str-2::gfp* off neuron while repulsion is mediated by TRPV channel-expressing neurons, some of which are known to promote chemical repulsion. A similar sensory circuit exists for behavioral reponses to benzaldehyde, for which attraction in chemotaxis is mediated

by AWC neurons and acute repulsion by TRPV channel-expressing ASH neurons (Bargmann et al., 1993; Colbert et al., 1997; L'Etoile and Bargmann, 2000).

At a visual level, attraction appears to precede repulsion to high concentrations of 1-hexanol. Assuming that attraction and repulsion are additive in their contribution to overall chemotaxis, one explanation for this behavior is that attraction adapts over time in the presence of persistent repulsion. This is unlikely to be true because *odr-1* mutants defective in 1-hexanol attraction did not exhibit any repulsion before 60 minutes in the chemotaxis assay (Figure A-3). An alternative possibility is that repulsion is upregulated over time to override a constant level of attraction. This may explain why wild-type animals can only respond repulsively to 1-hexanol after at least 15 minutes pre-exposure to the chemical in the flow assay (data not shown). 1-hexanol is a volatile anesthetic and interferes with receptor-G protein function by an unknown mechanism (Streiff et al., 2004; Yoshimura et al., 2003). Wild-type N2 animals were completely immobilized by saturated 1-hexanol vapor after 15-20 minutes, from which they recovered within a few minutes after removal of 1-hexanol (Anton et al., 1992) (data not shown). Perhaps this delayed repulsion allows animals to tolerate sub-lethal exposure to 1-hexanol in exploring their environment. Formally, a combination of these explanations above may also be possible.

The possible mechanisms for signal integration in 1-hexanol chemotaxis can be addressed by more detailed behavioral studies. The flow assay should be used to test *odr-1* and *ocr-2* mutants defective in attraction and repulsion, respectively. If attraction adapts over time in a background of constant repulsion, *odr-1* mutants should exhibit repulsion (higher reversal frequency) at earlier time points than wild-type animals. If

repulsion is upregulated over time in a background of constant attraction, then *odr-1* mutants should show repulsion at the same time as wild-type animals. Attraction is often inferred when animals slow down and decrease reversal frequency upon a change in stimulus. When 1-hexanol vapor was removed after 15 minutes of exposure, wild-type N2 animals dramatically slowed and stopped reversing (data not shown). If attraction adapts over time in a background of constant repulsion, *ocr-2* mutants should show gradual loss of attractive response to removal of 1-hexanol after different periods of exposure. If repulsion is upregulated over time in a background of constant attraction, then *ocr-2* mutants should show the same level of attraction independent of length of exposure to 1-hexanol. One limitation of these experiments is the anesthetic effect of saturated 1-hexanol vapor, so a dilution of 1-hexanol may be necessary to study prolonged exposure to the chemical.

Functional imaging experiments using genetically encoded calcium sensors can also be carried out to study the responsiveness of 1-hexanol-sensing neurons at different times after exposure to the chemical. These experiments should be performed on N2, *odr-1*, and *ocr-2* animals in similar treatments as those used in the flow assays above to draw correlations between neuronal activity and behavioral output. Interpretation of results from these functional imaging experiments will depend on understanding the naive calcium responses of these neurons to changes in 1-hexanol concentration.

In observing the behavior of wild-type N2 animals in chemotaxis assays to 1-hexanol and 2-nonanone, it was clear that volatile repulsion could be generated by distinct locomotory outputs. Repulsion from 1-hexanol was typified by a high reversal frequency, causing animals to change direction constantly as they backed away from

sources of 1-hexanol (data not shown). This behavior is consistent with the role of ASH and ADL neurons, which generate acute reversals in response to repellents (Bargmann et al., 1990; Chao et al., 2004; Colbert et al., 1997; Hilliard et al., 2002). Repulsion from 2-nonanone was seen as animals turning away from sources of 2-nonanone and moving straight down the chemical gradient to the opposite side of the assay plate, a faster response than for 1-hexanol. It would be interesting to study why certain stimuli elicit ASH vs. AWB responses; perhaps the long-range AWB response is used for more toxic chemicals. Additionally, studying how these locomotory outputs are generated at a circuit level would improve our understanding of long-range repulsion.

Finally, it has been observed that repulsion from high concentrations of 1-hexanol can be switched to attraction if animals are grown under stressful conditions. Starvation, high population density, and parafilming of the culture plate all contribute additively to this effect (Noelle Dwyer, personal communication). The effect of high population density was only partially reproduced by high concentrations of dauer pheromone at low population density (Noelle Dwyer, personal communication), suggesting that other factors contribute to the population density effect, perhaps mechanosensation. Both high population density and parafilming the plate would result in low oxygen and high carbon dioxide conditions; these factors should be considered and tested independently. Mutants that affect oxygen chemosensation have already been isolated and can be tested in this modulated behavior (Chang et al., 2006; Gray et al., 2004) (Chapter 4). It would also be interesting to determine if attraction and/or repulsion is modulated by these stress sensory experiences by testing *odr-1* and *ocr-2* mutants. Ultimately, a circuit can be

reconstructed with these modulatory inputs to understand how sensory signal integration occurs in the nervous system.

Materials and Methods

Strains

Strains were cultured under standard conditions (Brenner, 1974) and fed *E. coli* HB101. Wild-type animals were *C. elegans* Bristol strain N2. Other strains used in this work include: CX2065 *odr-1 (n1936)* X, CX4731 *nsy-1 (ky542)* II, CX6342 *nsy-3 (ky389gf)* V, CX6332 *nsy-4 (ky616)* IV, CX6161 *nsy-5 (ky634)* I, CX4537 *osm-9 (ky10)* IV, CX4544 *ocr-2 (ak47)* IV, CX6234 *ocr-2 (ak47)* IV*; kyEx685 [odr-10::ocr-2, unc-122::gfp]*, CX6236 *ocr-2 (ak47)* IV*; kyEx686 [srh-142::ocr-2, unc-122::gfp]*, CX6239 *ocr-2 (ak47)* IV*; kyEx687 [sra-6::ocr-2, unc-122::gfp]*, CX6381 *ocr-2 (ak47)* IV*; kyEx692 [srh-220::ocr-2, unc-122::gfp]*, CX4 *odr-7 (ky4)* X, CX4991 *lim-4 (ky403)* X. Unless indicated, null alleles or strong loss-of-function alleles were used.

Behavioral Assays

Chemotaxis assays were performed as described (Troemel et al., 1997), except 2% agar was used instead of 1.6% agar. The amount of odorant indicated in the Figures was the amount of undiluted chemical in each spot. Two spots of odorants and two spots of control (ethanol) were applied to each assay plate. The time course experiments in Figure A-3 were performed in the presence of sodium azide. Animals were tested at the temperature in which they were raised. With the exception of Figure A-3, at least three independent assays on two different days were used to generate the results.

Statistical Analysis

For all data described in this chapter, analysis of variance (ANOVA) plus Bonferroni *t* tests or Dunnett tests were conducted for multiple comparisons of data points (Statview, Cary, North Carolina). For controls such as N2 that were compared to multiple mutants, $p < 0.05$ was used as the level of significance.

References

Anton, A. H., Berk, A. I., and Nicholls, C. H. (1992). The "anesthetic" effect of alcohols and alkanes in Caenorhabditis elegans (C.e.). Res Commun Chem Pathol Pharmacol *78*, 69-83.

Bargmann, C. I., Hartwieg, E., and Horvitz, H. R. (1993). Odorant-selective genes and neurons mediate olfaction in C. elegans. Cell *74*, 515-527.

Bargmann, C. I., and Mori, I. (1997). Chemotaxis and thermotaxis. In C. elegans II, T. B. D.L. Riddle, B.J. Meyer, J.R. Priess, ed. (Cold Spring Harbor, New York, Cold Spring Harbor Laboratory Press), pp. 717-737.

Bargmann, C. I., Thomas, J. H., and Horvitz, H. R. (1990). Chemosensory cell function in the behavior and development of Caenorhabditis elegans. Cold Spring Harb Symp Quant Biol *55*, 529-538.

Brenner, S. (1974). The genetics of Caenorhabditis elegans. Genetics *77*, 71-94.

Chang, A. J., Chronis, N., Karow, D. S., Marletta, M. A., and Bargmann, C. I. (2006). A distributed chemosensory circuit for oxygen preference in C. elegans. PLoS Biol *4*, e274.

Chao, M. Y., Komatsu, H., Fukuto, H. S., Dionne, H. M., and Hart, A. C. (2004). Feeding status and serotonin rapidly and reversibly modulate a Caenorhabditis elegans chemosensory circuit. Proc Natl Acad Sci U S A *101*, 15512-15517.

Colbert, H. A., Smith, T. L., and Bargmann, C. I. (1997). OSM-9, a novel protein with structural similarity to channels, is required for olfaction, mechanosensation, and olfactory adaptation in Caenorhabditis elegans. J Neurosci *17*, 8259-8269.

Davies, A. G., Pierce-Shimomura, J. T., Kim, H., VanHoven, M. K., Thiele, T. R., Bonci, A., Bargmann, C. I., and McIntire, S. L. (2003). A central role of the BK potassium channel in behavioral responses to ethanol in C. elegans. Cell *115*, 655-666.

Gray, J. M., Karow, D. S., Lu, H., Chang, A. J., Chang, J. S., Ellis, R. E., Marletta, M. A., and Bargmann, C. I. (2004). Oxygen sensation and social feeding mediated by a C. elegans guanylate cyclase homologue. Nature *430*, 317-322.

Hilliard, M. A., Bargmann, C. I., and Bazzicalupo, P. (2002). C. elegans Responds to Chemical Repellents by Integrating Sensory Inputs from the Head and the Tail. Curr Biol *12*, 730-734.

L'Etoile, N. D., and Bargmann, C. I. (2000). Olfaction and odor discrimination are mediated by the C. elegans guanylyl cyclase ODR-1. Neuron *25*, 575-586.

Sagasti, A., Hobert, O., Troemel, E. R., Ruvkun, G., and Bargmann, C. I. (1999). Alternative olfactory neuron fates are specified by the LIM homeobox gene lim-4. Genes Dev *13*, 1794-1806.

Sengupta, P., Colbert, H. A., and Bargmann, C. I. (1994). The C. elegans gene odr-7 encodes an olfactory-specific member of the nuclear receptor superfamily. Cell *79*, 971-980.

Streiff, J., Warner, D. O., Klimtchuk, E., Perkins, W. J., Jones, K., and Jones, K. A. (2004). The effects of hexanol on Galpha(i) subunits of heterotrimeric G proteins. Anesth Analg *98*, 660-667.

Tobin, D., Madsen, D., Kahn-Kirby, A., Peckol, E., Moulder, G., Barstead, R., Maricq, A., and Bargmann, C. (2002). Combinatorial expression of TRPV channel proteins

defines their sensory functions and subcellular localization in C. elegans neurons. Neuron *35*, 307-318.

Troemel, E. R., Kimmel, B. E., and Bargmann, C. I. (1997). Reprogramming chemotaxis responses: sensory neurons define olfactory preferences in C. elegans. Cell *91*, 161-169.

Troemel, E. R., Sagasti, A., and Bargmann, C. I. (1999). Lateral signaling mediated by axon contact and calcium entry regulates asymmetric odorant receptor expression in C. elegans. Cell *99*, 387-398.

Vanhoven, M. K., Bauer Huang, S. L., Albin, S. D., and Bargmann, C. I. (2006). The claudin superfamily protein nsy-4 biases lateral signaling to generate left-right asymmetry in C. elegans olfactory neurons. Neuron *51*, 291-302.

Wes, P. D., and Bargmann, C. I. (2001). C. elegans odour discrimination requires asymmetric diversity in olfactory neurons. Nature *410*, 698-701.

Yoshimura, H., Jones, K. A., Perkins, W. J., and Warner, D. O. (2003). Dual effects of hexanol and halothane on the regulation of calcium sensitivity in airway smooth muscle. Anesthesiology *98*, 871-880.

Zhang, S., Sokolchik, I., Blanco, G., and Sze, J. Y. (2004). Caenorhabditis elegans TRPV ion channel regulates 5HT biosynthesis in chemosensory neurons. Development *131*, 1629-1638.

Figure A-1. Attraction to 1-hexanol requires the AWC *str-2::gfp* OFF neuron.

Wild-type N2 animals are repelled from high concentrations (1 and 1:2) of 1-hexanol and attracted to lower concentrations (1:10 and 1:20).

Mutants affecting AWC neurons were tested. *odr-1 (n1936)* mutants are defective for AWC and AWB chemotaxis (L'Etoile and Bargmann, 2000). *nsy-1 (ky542)* and *nsy-3/slo-1 (ky389gf)* have 2 AWC neurons that express *str-2::gfp* (Davies et al., 2003; Troemel et al., 1999; Wes and Bargmann, 2001). *nsy-4 (ky616)* and *nsy-5 (ky634)* have 2 AWC neurons that do not express *str-2::gfp* ((Vanhoven et al., 2006); M. Vanhoven, personal communication).

Asterisks and double asterisks, values different from N2 controls at the same condition at $p < 0.05$ and $p < 0.01$, respectively, by Dunnett test. $n \geq 4$ assays per genotype and condition, 100-200 animals/assay. Error bars denote standard error of the mean (SEM).

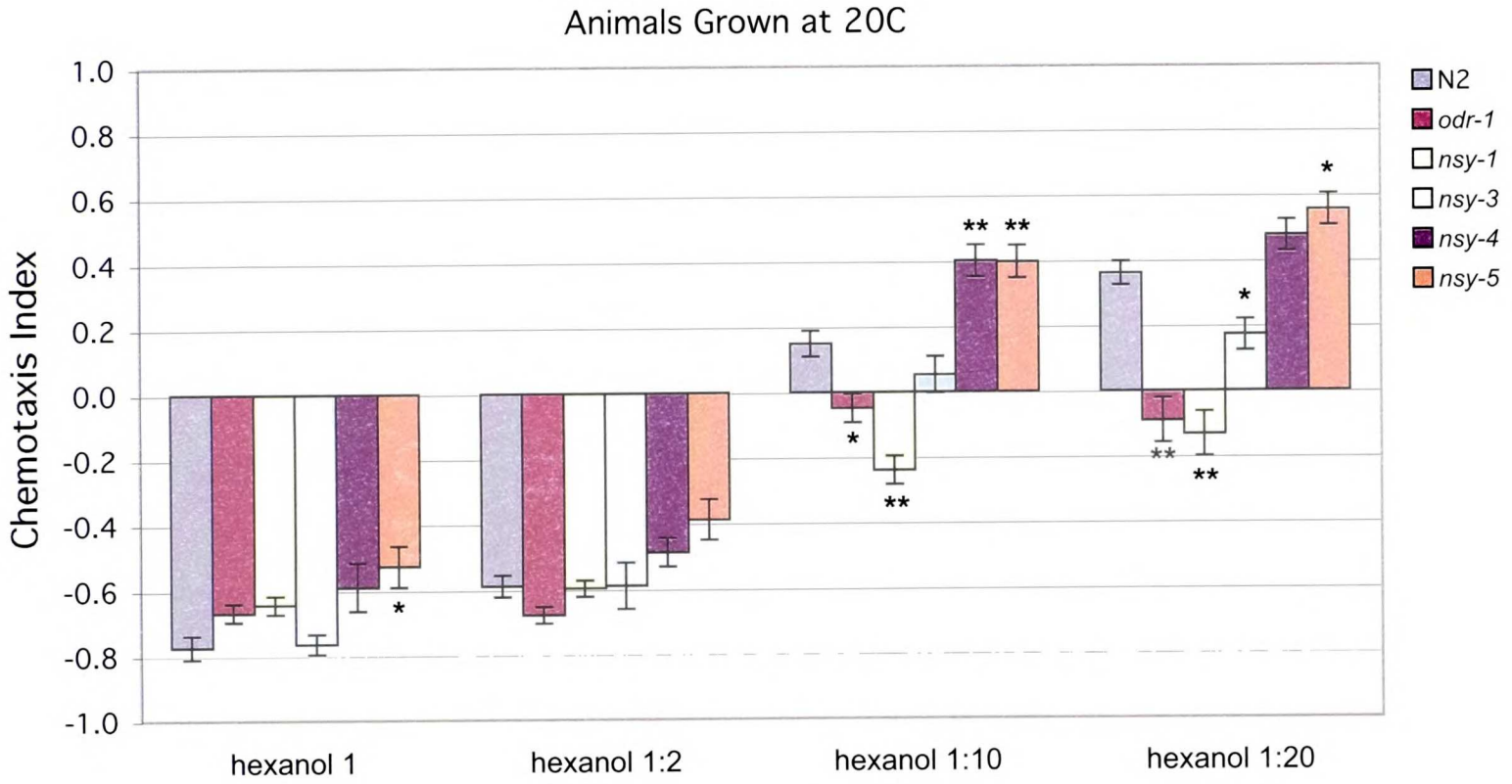
Animals Grown at 20C
Chemotaxis Index
1.0
0.8
0.6
0.4
0.2
0.0
-0.2
-0.4
-0.6
-0.8
-1.0
hexanol 1
hexanol 1:2
hexanol 1:10
hexanol 1:20
N2
odr-1
nsy-1
nsy-3
nsy-4
nsy-5

Figure A-2. TRPV channels are required for repulsion from 1-hexanol.

(A) Chemotaxis of N2, *ocr-2 (ak47)*, and *osm-9 (ky10)* animals grown at 20°C.

(B) Chemotaxis of N2, *ocr-2 (ak47)*, and *osm-9 (ky10)* animals grown at 25°C.

(C) Chemotaxis of *ocr-2 (ak47)* mutants rescued for *ocr-2* in indicated cells. In rescue strains, only animals expressing the co-injection marker were scored.

Asterisks and double asterisks, values different from N2 controls at the same condition at $p < 0.05$ and at $p < 0.01$, respectively, by Dunnett test. Single cross, value different from both N2 and *ocr-2* controls at $p < 0.05$ by Bonferroni *t* test. Double cross, value different from *ocr-2*, but not N2, at $p < 0.05$ by Bonferroni *t* test. $n \geq 6$ assays per genotype and condition, 100-200 animals/assay. Error bars denote standard error of the mean (SEM).

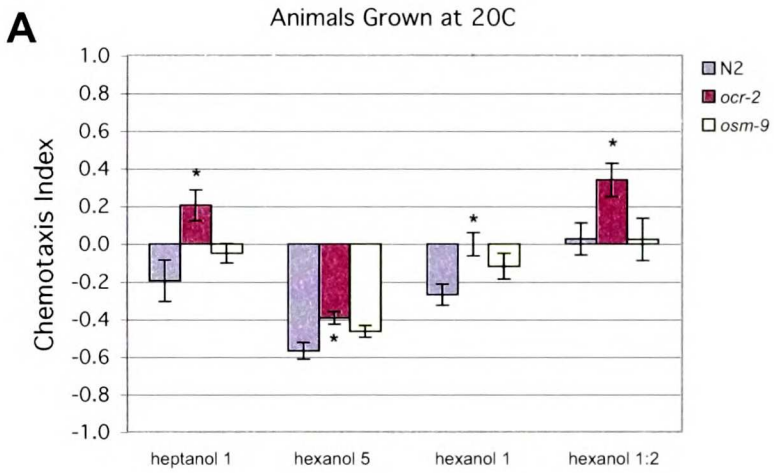
A
Animals Grown at 20C
Chemotaxis Index
1.0
0.8
0.6
0.4
0.2
0.0
-0.2
-0.4
-0.6
-0.8
-1.0
heptanol 1
hexanol 5
hexanol 1
hexanol 1:2
N2
ocr-2
osm-9

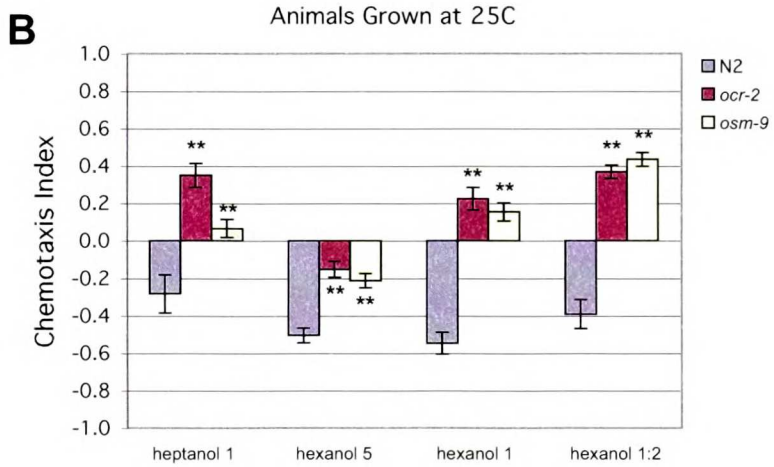
B
Animals Grown at 25C
Chemotaxis Index
1.0
0.8
0.6
0.4
0.2
0.0
-0.2
-0.4
-0.6
-0.8
-1.0
heptanol 1
hexanol 5
hexanol 1
hexanol 1:2
N2
ocr-2
osm-9

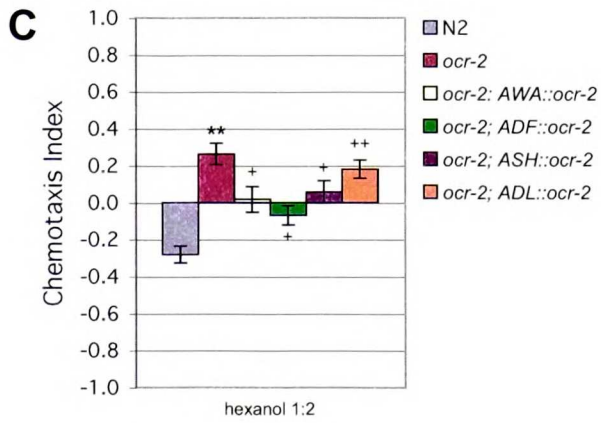
C
Chemotaxis Index
1.0
0.8
0.6
0.4
0.2
0.0
-0.2
-0.4
-0.6
-0.8
-1.0
hexanol 1:2
N2
ocr-2
ocr-2: AWA::ocr-2
ocr-2; ADF::ocr-2
ocr-2; ASH::ocr-2
ocr-2; ADL::ocr-2

Figure A-3. Time course of 1-hexanol chemotaxis.

Time course of chemotaxis of N2, *odr-1 (n1936)*, *ocr-2 (ak47)*, and *ocr-2* rescue strains to 1:2 hexanol. In rescue strains, only animals expressing the co-injection marker were scored. $n \geq 2$ assays per genotype and condition, 100-200 animals/assay. Error bars denote standard error of the mean (SEM).

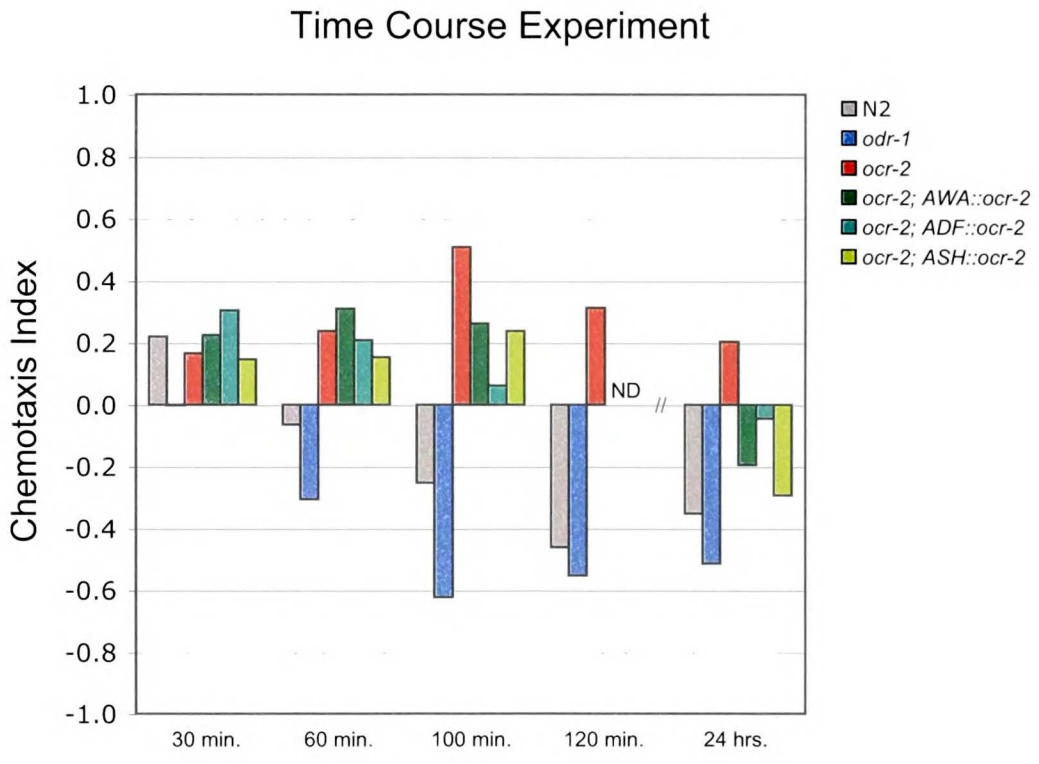
Time Course Experiment
Chemotaxis Index
1.0
0.8
0.6
0.4
0.2
0.0
-0.2
-0.4
-0.6
-0.8
-1.0
ND
30 min.
60 min.
100 min.
120 min.
24 hrs.
N2
odr-1
ocr-2
ocr-2; AWA::ocr-2
ocr-2; ADF::ocr-2
ocr-2; ASH::ocr-2

Figure A-4. 2-nonanone chemotaxis may involve multiple sensory neurons.

(A) Chemotaxis of N2, *odr-7 (ky4)*, o*dr-1 (n1936)*, and *lim-4 (ky403)* grown at 20°C.

(B) Chemotaxis of N2, *odr-7 (ky4)*, o*dr-1 (n1936)*, and *lim-4 (ky403)* grown at 25°C.

Asterisks and double asterisks, values different from N2 controls at the same condition at $p < 0.05$ and $p < 0.01$, respectively, by Dunnett test. $n \geq 3$ assays per genotype and condition, 100-200 animals/assay. Error bars denote standard error of the mean (SEM).

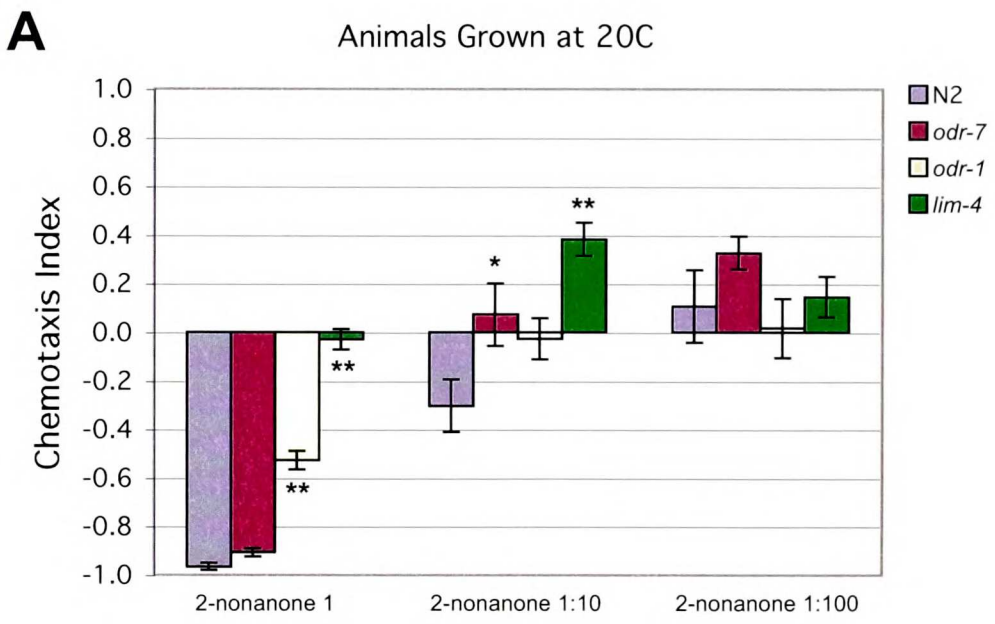
A
Animals Grown at 20C
Chemotaxis Index
1.0
0.8
0.6
0.4
0.2
0.0
-0.2
-0.4
-0.6
-0.8
-1.0
N2
odr-7
odr-1
lim-4
2-nonanone 1
2-nonanone 1:10
2-nonanone 1:100

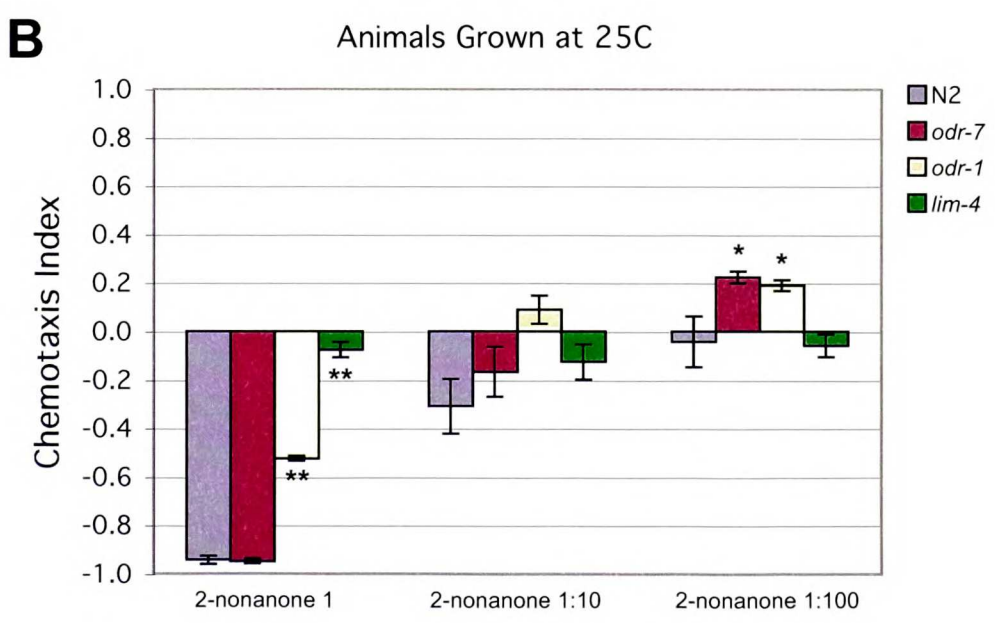
B
Animals Grown at 25C
Chemotaxis Index
1.0
0.8
0.6
0.4
0.2
0.0
-0.2
-0.4
-0.6
-0.8
-1.0
N2
odr-7
odr-1
lim-4
2-nonanone 1
2-nonanone 1:10
2-nonanone 1:100